5-1-2013

The effects of chronic calcium dysregulation on behavioral and pathological features of Alzheimer's disease

Jonathan Sabbagh
University of Nevada, Las Vegas, jjsabbagh@hotmail.com

THE EFFECTS OF CHRONIC CALCIUM DYSREGULATION ON BEHAVIORAL AND PATHOLOGICAL FEATURES OF ALZHEIMER'S DISEASE

by

Jonathan Jacob Sabbagh

Bachelor of Science in Neuroscience
Tulane University
2004

Master of Arts in Experimental Psychology
University of Nevada, Las Vegas
2010

A dissertation submitted in partial fulfillment
of the requirements for the

Doctor of Philosophy in Psychology

Department of Psychology
College of Liberal Arts
The Graduate College

University of Nevada, Las Vegas
May 2013

THE GRADUATE COLLEGE

We recommend the dissertation prepared under our supervision by

Jonathan Jacob Sabbagh

entitled

The Effects of Chronic Calcium Dysregulation on Behavioral and Pathological Features of Alzheimer's Disease

be accepted in partial fulfillment of the requirements for the degree of

Doctor of Philosophy in Psychology
Department of Psychology

Jefferson Kinney, Ph.D., Committee Chair

Laurel Pritchard, Ph.D., Committee Member

Joel Snyder, Ph.D., Committee Member

Frank van Breukelen, Ph.D., Graduate College Representative

Tom Piechota, Ph.D., Interim Vice President for Research &
Dean of the Graduate College

May 2013

ABSTRACT

Alzheimer's disease (AD) is a progressive neurodegenerative disorder whose etiology is unknown. Recent studies have implicated alterations in calcium homeostasis as a pathogenic contributor to AD. Calcium dysregulation has been observed in aged and AD brains, an event which could potentially facilitate the development of multiple pathologies observed in AD. Specifically, disrupting intracellular calcium levels *in vitro* has been demonstrated to increase amyloid-beta (Aβ) production, tau phosphorylation, and neuronal loss. However, there is a paucity of data on the behavioral and biochemical consequences of chronic *in vivo* perturbation of calcium homeostasis. In a series of experiments designed to evaluate the effects of chronic calcium dysregulation, we chronically administered different dosages of ryanodine or thapsigargin directly into the lateral ventricles at a minimal flow rate via Alzet osmotic minipumps. To investigate interactions with neuroinflammation, a common occurrence in AD, experiment 3 examined the effects of an acute inflammatory response on chronic calcium dysregulation. Learning and memory was examined in multiple paradigms including the Morris water maze and novel object recognition. Results indicate chronic alterations in calcium regulation produced deficits in the water maze and novel object recognition task following six weeks of central infusion. Analyses of protein levels revealed that there may be neurochemical changes consistent with AD following chronic calcium dysregulation. The induction of neuroinflammation combined with calcium dysregulation produced similar deficits. The data suggest that altered neural calcium handling may play a significant role in AD. Additionally, these data may shed light on the role of calcium regulation in learning and memory.

TABLE OF CONTENTS

LIST OF TABLES

LIST OF FIGURES

CHAPTER 1

INTRODUCTION

Alzheimer's disease (AD) is a neurodegenerative disorder characterized by a progressive loss of memory and a decline in cognitive function (Heese & Akatsu, 2006). It is the most common cause of age-related dementia accounting for 50-60% of age-related cases. The average age of onset for AD is 65 years, while most cases occurring before this age are referred to as early-onset familial AD, with identifiable genetic links. Dementia includes the aforementioned memory loss, confusion, disorientation, anxiety, delusions and apathy or depression (Terry & Katzman, 1983). As the disease advances, symptoms may include anger, aggression, language problems, impaired motor function, and psychoses (Souren et al., 1995; Waldemar et al., 2007).

In addition to the behavioral disruptions associated with AD, several pathological changes have been observed in the brain including amyloid-beta (Aβ) plaque deposition, neurofibrillary tangle formation, and the progressive loss of synapses and neurons, most notably cholinergic neurons (Arriagada et al., 1992; Bartus et al., 1982; Glenner & Wong, 1984; Grundke-Iqbal et al., 1986; Masters et al., 1985; Terry et al., 1991). These pathological changes are the hallmarks of the disease, and may be responsible for the cognitive and behavioral deficits exhibited in AD. However, no current widely accepted theory exists that is able to account for all the pathological changes observed. Mounting evidence suggests calcium dysregulation may play a pivotal role in AD and may represent a unifying, causative factor in the disorder.

One of the most extensively investigated hallmarks of the disorder is the senile plaques observed in post-mortem examinations. Aβ proteins form the core of senile

plaques, one of the pathological changes which may be inducing the neuronal loss seen in AD (Glenner & Wong, 1984; Masters et al., 1985). Senile plaques are extracellular structures composed mainly of aggregated Aβ, an endogenous protein of unknown function, and they are found almost exclusively in AD and AD-related pathologies like Down syndrome (Wisniewski et al., 1985). Several studies suggest that the accumulation of Aβ in the brain may initiate or lead to the pathogenesis of AD (reviewed in Selkoe, 2001). These findings and others have led to the amyloid cascade hypothesis (Hardy & Higgins, 1992), which suggests that the amyloid deposits that form plaques are the causative event in AD and the resulting neurodegeneration is a by-product of this buildup. Evidence supporting this hypothesis comes from genetic studies showing mutations in the genes associated with familial and late-onset AD lead to increased Aβ aggregation and cognitive deficits (Corder et al., 1993; Goate et al., 1991; Levy-Lahad et al., 1995; Murrell et al., 1991; Sherrington et al., 1995).

Investigators have been searching for genetic ties to AD for years in an attempt to determine the etiology of the disease but with only mild success. Although a few genes have been implicated as risk factors, none have yet provided a clear link between the pathogenesis of sporadic AD and specific genetic targets, with most promising targets tied to familial AD. Mutations in the amyloid precursor protein (APP), which is responsible for the formation of Aβ peptides and whose encoding gene is located on chromosome 21, have been linked to early-onset familial AD (Goate et al., 1991; Murrell et al., 1991). Interestingly, patients with Down syndrome, a trisomy (additional copy) of chromosome 21, show AD pathology by 40 years of age (Holtzman et al., 1996). Alternative genetic approaches have implicated mutations in genes called presenilins (PS)

which have also been tied to early-onset AD, specifically presenilin-1 (PS-1) and presenilin-2 (PS-2) located on chromosomes 14 and 1, respectively (Levy-Lahad et al., 1995; Sherrington et al., 1995). In sporadic AD, genetic investigations have implicated a specific allele of Apolipoprotein E (ApoE), whose gene is localized on chromosome 19, which has been linked to an increased likelihood of developing the disease (Corder et al., 1993). This risk factor is not linked to a mutation, but the inheritance of specific alleles. Although genetic linkage studies have provided useful insight into potential AD etiology, genetic mutations (i.e. APP or PS) related to Aβ can only account for a very small percentage of AD cases. A further limitation of the Aβ hypothesis is that many studies have indicated that there is a weak correlation between the number or size of amyloid deposits and the severity of the dementia, and that other pathologies seem to correlate better with the memory loss seen in AD (Arriagada et al., 1992; Snowdon et al., 1997; Terry et al., 1991). Therefore, additional pathologies such as the hyperphosphorylation of tau have been the focus of much research.

Neurofibrillary tangles (NFTs) are another neuropathological hallmark of AD and are composed mainly of hyperphosphorylated tau, a protein that is associated with microtubule stability and assembly. Tau hyperphosphorylation leads to the formation of paired helical filaments (PHF) which are thought to lead to microtubule disintegration and neuron death (Goedert, 1996). Because the amount of neurofibrillary tangles correlates positively with the severity of dementia in AD (Arriagada et al., 1992), it is of great interest to investigators of the disorder and those developing pharmacological treatments. In addition, the regions of the brain that appear to undergo the greatest degeneration of neurons and synapses in AD are those that project to or from areas that

have high densities of plaques and tangles, specifically the hippocampus, neocortex, and basal forebrain (for review, see Kar et al., 2004). The latter region contains large numbers of cholinergic neurons which project to the hippocampus and cortex. Acetylcholine (ACh), principally an excitatory neurotransmitter, is important for attentional processes, as well as learning and memory (Deutsch, 1971; Wenk et al., 1994; Woolf, 1996). A reduction in neurons containing ACh has been consistently observed in AD, particularly in the early stages of the disorder.

Cholinergic cell loss is a hallmark of the neurodegeneration in AD, marked by a progressive loss of ACh-containing neurons with a corresponding decline in cognitive function (Perry et al., 1981; Terry et al., 1991). The cholinergic hypothesis of AD postulates that the cognitive deficits in AD are caused by the early loss of cholinergic basal forebrain (CBF) neurons (Bartus et al., 1982). This hypothesis is supported by many post-mortem studies which demonstrate that the loss of CBF neurons occurs early in the disease progression, likely before a clinical diagnosis is reached (Bartus et al., 1982; Beach et al., 1997, 2000; Bowen et al., 1982). Also, the severity of the dementia in AD is highly correlated with the amount of cholinergic loss (Perry et al., 1981). Although CBF neurons are associated with early degeneration in AD, the pervasive nature of the cell loss throughout the course of the disorder suggests alternative mechanisms may be responsible because these cholinergic neurons are specifically localized. One such mechanism is the dysregulation of intracellular calcium, a progressive event which may account for the widespread neurodegeneration and neuropathologies in AD.

The activity of calcium ions is essential for a number of neuronal processes including transmitter release, transcriptional regulation, synaptic plasticity, and many

others (Bading et al., 1993; Borst & Sakmann, 1996; Greer & Greenberg, 2008; Hardingham et al., 1997). Many cellular resources are devoted to tightly regulating intracellular calcium levels such as calcium pumps, transporters, exchangers, and channels. The proper functioning of this machinery is necessary for maintaining calcium homeostasis and normal cellular function. Any perturbation of the mechanisms responsible for regulating calcium levels may have deleterious consequences and potentially play a role in disorders.

The calcium hypothesis of aging and neurodegenerative disease was first proposed in the 1980s (Gibson & Peterson, 1987; Khachaturian, 1987; Landfield, 1987; Landfield et al., 1989), suggesting that sustained intracellular calcium disruptions may be the cause of age-related disorders, including AD. More recently, increasing lines of evidence point to disrupted calcium homeostasis as a causative factor in AD (Bezprozvanny & Mattson, 2008; Bojarski et al., 2008; Camandola & Mattson, 2011; Thibault et al., 2007; Thibault & Landfield, 1996). Calcium dysregulation has been implicated in several pathologies of AD including Aβ and tau aggregation, and neuronal loss. Each of these pathologies has also been implicated in the cognitive impairments in AD (Arriagada et al., 1992; Cleary et al., 2005; Hsiao et al., 1996; Terry et al., 1991). In the experiments outlined below, we will examine the effects of altering intracellular calcium levels on learning and memory and AD-like neuropathological changes.

Experimental Rationale

Many studies have investigated the effects of calcium dysregulation on specific AD pathologies, such as Aβ and tau, in cell culture preparations. Sparse data exist on the

effects of *in vivo* calcium dysregulation, while to date no experiments have investigated the effects of chronic calcium perturbation. Furthermore, the behavioral consequences of altering intracellular calcium levels are unknown. The below studies sought to determine what effect chronic calcium dysregulation would have on learning and memory and histological markers consistent with AD. We examined multiple hippocampally-dependent tasks, including the Morris water maze (MWM) and novel object recognition (NOR), to assess whether chronic disruption of calcium homeostasis was sufficient to produce learning and memory impairments. We also examined protein levels of Aβ and phosphorylated tau (ptau) to determine whether chronic calcium dysregulation led to AD-like changes in these proteins. Below we have outlined a more comprehensive review of each of the aforementioned approaches and findings in AD.

CHAPTER 2

REVIEW OF RELATED LITERATURE

Amyloid β Hypothesis

The Aβ protein accumulates extracellularly in AD resulting in the formation of senile plaques, which may lead to cell damage and even cell loss. Aβ was first purified in 1984 from cerebrovascular amyloid protein by Glenner & Wong and from senile plaques the next year by Masters et al. (1985), which was when its amino acid sequence was determined. Various mechanisms have been proposed to account for the neurotoxicity of Aβ peptides and senile plaques. Several studies have discovered a disruption in calcium homeostasis following Aβ administration which could potentially lead to cell death (Mattson et al., 1992). It has also been suggested that plaques may disturb surrounding cytoskeletal elements by "squishing" nearby cells. Although the mechanism by which Aβ contributes to neurodegeneration remains to be conclusively demonstrated, how the peptide is formed has been better characterized.

Aβ is formed by the proteolytic processing of its precursor protein, APP. APP is a membrane-spanning protein encoded for on chromosome 21. Although the physiological function of APP remains unknown, it appears to be involved with synaptic transmission, axonal transport, cell adhesion and support, and cholesterol metabolism (for review, see Selkoe, 1994). Knockout (elimination of the gene product) and knockdown (reduction in the relative amount of a gene product) studies of APP have provided some information about its function. APP seems to play a role in muscle development or function, and has also been implicated in the formation of long-term potentiation (LTP), a cellular process argued to be essential for learning (Dawson et al., 1999; Douglas &

Goddard, 1975; Kauer et al., 1988; Seabrook et al., 1999; Senechal et al., 2008). Under physiological conditions, APP is degraded via a series of enzymatic events.

The proteolytic processing of APP results in Aβ fragments of varying length, depending on where APP is cleaved by specific enzymes called secretases (Shoji et al., 1992; Sisodia & Price, 1995). If APP is cleaved by alpha (α)-secretase, a soluble form of APP (sAPP) is secreted which is readily absorbed and processed by lysosomal proteolytic events. Cleavage by α-secretase occurs in the extracellular domain of APP within the Aβ sequence, thus preventing the formation of the Aβ peptide (Lannfelt et al., 1995). Several reports have demonstrated sAPP may even play a neuroprotective role (Furukawa et al., 1996; Han et al., 2005).

The senile plaques found in AD are primarily composed of the 40 and 42 amino acid Aβ peptides, with studies showing that $A\beta_{42}$ is more neurotoxic, i.e. more damaging to neurons, than the shorter variants (Roher et al., 1996). If APP is sequentially cleaved by beta (β)- and gamma (γ)-secretases, this leads to the formation of 39-43 amino acid long Aβ peptides, which are similar to the lengths of Aβ predominantly found in senile plaques in AD (Citron et al., 1996; Golde et al., 1992).

Initially, β-secretase, also referred to as β-site APP cleaving enzyme 1 (BACE-1), cleaves APP at its amino-terminus in the extracellular domain which is followed by γ-secretase cleavage within the transmembrane domain (Vassar et al., 1999). BACE-1 inhibitors have been demonstrated to inhibit β-cleavage of APP and effectively lower Aβ levels *in vitro* and *in vivo* (Hussain et al., 2007). Inhibitors of γ-secretase have also been shown to reduce Aβ levels in the brain when administered to mice that overexpress a human mutant version of APP (Dovey et al., 2001). Inhibition of either of these two

secretases theoretically leads to a reduction in the amount of Aβ because both β- and γ-secretase are necessary in order to cleave APP in a fashion that yields the 40 or 42 amino acid peptides known to aggregate and form plaques.

Considerable pharmacological research is being directed at developing β- and γ-secretase inhibitors as therapeutic targets in an effort to reduce plaque load and perhaps even halt the progression of the disease. However, recent failures of γ-secretase inhibitors in particular have raised questions about the validity of this approach (Cummings, 2010). A great deal of research has also been conducted examining the genetic underpinnings of AD with a particular focus on genes tied to the proteolytic processing of Aβ.

Genetic linkage studies have tied familial forms of AD to the gene for APP on chromosome 21 (Citron et al., 1992; Goate et al., 1991). Over twenty mutations in the gene have been identified to date that are thought to be responsible for the familial early-onset form of the disease (Chai, 2007). Individuals with any of these mutations have an increased chance, compared to the population as a whole, of developing early-onset AD because they have a greater amount of APP and thus produce more Aβ than normal individuals (Citron et al., 1992; Suzuki et al., 1994). Interestingly, almost all APP mutations are located within or adjacent to the Aβ peptide region of the precursor protein, and thus may affect the proteolytic processing of APP (Schellenberg, 1995). Related to the processing of APP are the presenilin (PS) genes which have also been implicated in autosomal dominant familial AD.

The genes coding for PS proteins have been linked to early-onset AD, specifically PS-1 on chromosome 14 and PS-2 on chromosome 1 (Levy-Lahad et al., 1995; Sherrington et al., 1995). Similar to the aforementioned mutations in APP, PS mutations

lead to increased Aβ production, especially production of $A\beta_{42}$, a species of the peptide known to be most toxic to neurons and overabundant in AD (Citron et al., 1997; Duff et al., 1996; Iwatsubo et al., 1994). Investigations into PS mutations and Aβ deposition have shown that mutations in the PS gene increase the ratio of $A\beta_{42}$ to $A\beta_{40}$ as compared to non-PS mutant cases of AD (Borchelt et al., 1996). This shift in the production of $A\beta_{42}$ can have significant consequences, as studies have suggested that $A\beta_{42}$ aggregates more readily than $A\beta_{40}$ and is deposited early in the formation of plaques (Iwatsubo et al., 1994; Jarrett et al., 1993). Furthermore, PS mutations seem to alter APP processing by increasing the amount of cleavage by γ-secretase, thus increasing the production of Aβ (DeStrooper et al., 1998; Wolfe et al., 1999). Knockout studies with animals that do not express the PS-1 and PS-2 genes show an abolishment of γ-secretase mediated cleavage of APP (Steiner et al., 1999; Yu et al., 2001).

Based on these findings and others, Wolfe et al. (1999) proposed the hypothesis that PS itself is a γ-secretase, an intramembranous protease that is responsible for γ-cleavage of APP. Despite further evidence supporting this hypothesis, it appears that PS and γ-secretase are not the same protein even though they are highly related (Takasugi et al., 2003). Although PS-knockout mice seem to exhibit a complete abolishment of γ-secretase activity, these animals still produce $A\beta_{42}$ peptide fragments, suggesting there are additional enzymes with activity similar to γ-secretase (Wilson et al., 2002).

While the discovery that these three genes (APP, PS-1, and PS-2) are linked to familial AD advanced the investigation of the disorder, it is important to recognize that they only account for a small percentage of all familial early-onset cases occurring before 65 years of age (Cruts et al., 1998). Given that more than 95% of AD cases occur after

the age of 65, it is clear that these genetic mutations contribute only minimally to the risk of developing the more common variant of the disease (Holmes, 2002). With that said, much more is known about the genetics of familial early-onset AD than about sporadic, late-onset AD.

One gene implicated in non-familial forms of AD is the gene coding for Apolipoprotein E (ApoE). ApoE is a protein critical in regulating brain Aβ peptide levels and trafficking lipids throughout the brain (for review, see Holtzman, 2001). ApoE is responsible for clearing Aβ peptides from the brain across the blood-brain barrier into the peripheral circulation (LaDu et al., 1994, 1995; Morikawa et al., 2005). Aβ peptides are normally generated at very high levels in the brain and are cleared at an equivalent rate (Bateman et al., 2006). Thus, even small reductions in the clearance of Aβ could result in elevated levels of Aβ peptides and eventual plaque formation. The lipidation status of ApoE appears to be important with regard to how well it can bind to Aβ and clear the peptide from the brain (Tokuda et al., 2000). If ApoE is in a lipidated form, it is more effective at clearing Aβ than if it is non-lipidated.

Another way that Aβ is cleared from the brain is through a proteolytic mechanism involving either neprilysin (NEP) (Iwata et al., 2000) or insulin-degrading enzyme (IDE) (Kurochkin & Goto, 1994). Inhibition of either of these proteases leads to a substantial elevation of Aβ levels in the brain and increased plaque deposition (Dolev & Michaelson, 2004). Recent research suggests that ApoE facilitates these enzymes, allowing them to degrade Aβ (Jiang et al., 2008). The ability of ApoE to clear Aβ is also dependent upon the isoform or allele of ApoE.

ApoE has three alleles: ApoE-ε2, ApoE-ε3, and ApoE-ε4, with one or two copies of the ε4 allele leading to an increased risk of developing AD (Corder et al., 1993). Studies with transgenic mice overexpressing APP have demonstrated ApoE isoform-specific effects on the ability of each allele to clear Aβ from the brain. The most effective allele at eliminating Aβ is the ε2 allele, followed by the ε3 allele, with the least effective being the ε4 allele (Holtzman, 2004). Thus, individuals with one or two ε4 alleles (two alleles being the least effective possible form) of ApoE have a less efficient mechanism for clearing Aβ from the brain, resulting in increased levels of the peptide (Saunders et al., 1993).

A genetic study done by Corder et al. (1993) showed that over 90% of subjects examined who had two copies of the ε4 allele (4/4) had AD. Almost 50% of subjects with one copy of the ε3 and one copy of the ε4 (3/4) were affected with AD. Only about 20% of subjects with no copies of the ε4 allele (2/2, 3/3, or 2/3) had the disease. These authors also examined the average age of onset in individuals with one or two copies of the ε4 allele. They found that expression of it leads to a significantly earlier age of onset, with two copies of the ε4 allele leading to an earlier onset than just one copy. While the discovery of the ApoE gene and its relation to Aβ is critical to understanding AD pathogenesis, the presence of the ε4 allele predisposes an individual to AD, but does not cause the disease.

Much of the above research eventually led to the amyloid cascade hypothesis, which suggests that abnormal Aβ production and accumulation triggers the neurodegeneration seen in AD. Hardy & Higgins (1992) proposed that deposition of Aβ protein is the causative factor in AD pathology and that the NFT, neuronal loss, and

dementia that follow are a result of this deposition. They hypothesized that neurotoxic Aβ peptides disrupt calcium homeostasis both extra- and intracellularly. This intra-neuronal increase in calcium concentration could potentially be what leads to tau proteins within the cell becoming hyperphosphorylated and forming PHFs, which are the primary component of NFT. Thus, for this interpretation of the amyloid cascade hypothesis to be correct, elevations in Aβ levels should cause hyperphosphorylation of tau and neurofibrillary pathology to develop.

This link between Aβ and tau has been verified to some extent in animal models and in cell culture, wherein Aβ causes an increase in tau phosphorylation (Gotz et al., 2001; Lewis et al., 2001; Zheng et al., 2002). Transgenic mice harboring mutations in both human APP and human Tau, as well as a mutant PS-1 allele, dubbed 3xTg-AD mice, develop both Aβ deposits and NFT-like pathology (Oddo et al., 2003a). Studies using these mice have demonstrated that Aβ accumulation precedes the development of tau pathology by several months, further suggesting Aβ may promote tau phosphorylation and aggregation (Oddo et al., 2003b). These findings with transgenic mice must be regarded carefully however due to the rarity of these mutations in humans.

Earlier studies revealed a direct relationship between Aβ and tau phosphorylation; the treatment of neurons with Aβ fibrils increased the immunoreactivity of ptau (Busciglio et al., 1995). This Aβ-induced increase in tau phosphorylation may be mediated by glycogen synthase kinase 3β (GSK-3β), one of the enzymes thought to be responsible for phosphorylating tau, as *in vitro* injection of Aβ activates this enzyme (Lovestone et al., 1996). More recently, Guo et al. (2006) observed that soluble Aβ and tau may directly interact to promote each other's aggregation. Thus, it is clear there is

some relation between Aβ and tau pathology, but more studies are necessary to clarify the connection.

Despite the amount of research supporting the amyloid cascade hypothesis, there are several gaps between the hypothesis and data collected. First, the hypothesis is inconsistent with the presence of senile plaques in normal aged brains similar to those seen in AD (Crystal et al., 1988; Katzman et al., 1988; Price et al., 1991). If Aβ deposits are the catalyst for AD neurodegeneration, then it is unlikely we would see individuals with no cognitive impairment and widespread plaque load. Furthermore, the presence of post-mortem senile plaques does not correlate well with the severity of dementia in AD (Snowdon et al., 1997; Terry et al., 1991).

Secondly, in transgenic animals that overexpress either APP or one of the PS mutations, there is no significant NFT formation or neurodegeneration despite considerable Aβ plaque load (Hsiao et al., 1996; Takeuchi et al., 2000). Because no AD-like pathology develops in these mice except for plaques, it is difficult to argue that Aβ is directly causing the significant neuronal loss seen in the disease. Another limitation of the amyloid cascade hypothesis is that neurodegeneration and dementia occur in the absence of Aβ plaques in several diseases related to the tau protein (Hutton et al., 1998; Spillantini et al., 1998). Based on these limitations and others, the amyloid cascade hypothesis has been adapted with a larger focus on soluble Aβ peptides as opposed to the insoluble aggregates which form the core of plaques (Hardy, 2006).

Although the causative nature of Aβ plaques has been debated, several lines of evidence suggest soluble Aβ peptides are neurotoxic and may be better correlates of disease severity than insoluble Aβ (McLean et al., 1999). Specifically, the aggregation of

Aβ monomers into small, soluble oligomers may be more closely tied to AD pathogenesis and cognitive deficits (Cleary et al., 2005; Walsh et al., 2002). Aβ oligomers (oAβ) inhibit LTP, impair learning and memory in animal models of AD, and have been directly linked to synapse loss and cell death (Chafekar et al., 2008; Lesné et al., 2006; Shankar et al., 2007; Townsend et al., 2006; Walsh et al., 2002). Unlike Aβ monomers, oligomers cannot be degraded and cleared by IDE (Walsh et al., 2002). These findings and others suggest the formation of oAβ in AD brains may eventually result in the aggregation of these peptides into senile plaques. However, much more research is necessary before a complete understanding of Aβ dynamics in AD can be reached.

Regardless of whether or not Aβ peptides are the causative agent in AD, it is likely that they contribute to the cognitive symptoms and pathogenesis of AD. Another pathogenic contributor to the neurodegeneration observed in AD is the tau protein which is hyperphosphorylated resulting in NFTs and neuronal loss.

Tau Hypothesis

Tau is an intracellular protein found abundantly in the central and peripheral nervous systems and is critical for microtubule stability, assembly, and flexibility (Goedert et al., 1989, 1992). Microtubules are located throughout the neuron; especially in the axon where they are essential for neurotransmission, axonal transport and axonal support (Kraemer et al., 2003; Paulson & McClure, 1974; Weingarten et al., 1975). Tau is a phosphoprotein which implies that it requires phosphorylation, or the addition of a phosphate group, in order for it to become activated (Butler & Shelanski, 1986). Tau is partially phosphorylated in the normal brain and this phosphorylation may regulate

microtubule stability and assembly (Lindwall & Cole, 1984). This microtubule regulation appears to occur by reducing tau's binding to tubulin, a protein that makes up microtubules, and reducing the promotion of microtubule assembly (Hasegawa, 2004). Thus, the phosphorylation of tau plays a pivotal role in regulating microtubule production by reducing the amount of microtubule assembly and decreasing the ability of tau to bind to tubulin.

In AD, the tau protein is hyperphosphorylated, which leads to the destruction of microtubule assemblies via the aforementioned mechanisms (Grundke-Iqbal et al., 1986). The degradation of microtubules may cause impaired axonal transport and possibly cell death (Kosik et al., 1986). Tau hyperphosphorylation renders tau unable to bind to microtubules, an event proposed to be responsible for tau aggregation and self-assembly into PHFs (Bramblett et al., 1993; Goedert et al., 1988; Yoshida & Ihara, 1993). These PHFs, which are primarily made up of hyperphosphorylated tau, correlate strongly with neuronal death in AD (Gomez-Isla et al., 1997). Also, whereas Aβ pathology is relatively specific to AD, NFT formation occurs in other diseases/disorders related to tau, collectively referred to as tauopathies.

In 1998, several mutations in the tau gene were discovered in families with frontotemporal dementia and parkinsonism linked to chromosome 17 (FTDP-17), a related but distinct neurodegenerative disease, producing genetic evidence that tau abnormalities may be sufficient to lead to neurodegeneration (Hong et al., 1998; Hutton et al., 1998; Poorkaj et al., 1998; Spillantini et al., 1998). This discovery led to the production of many different transgenic lines of mice with tau mutations. One specific line, the P301L mice, shows significant age-dependent NFT formation, memory

impairment, and neuron loss (Lewis et al., 2000; Ramsden et al., 2005). Although there is significant neurodegeneration in these animals, they do not develop any Aβ pathology, implying that tau mutation or tangle formation are not sufficient on their own to cause senile plaques in an animal model of AD. These findings provide strong evidence that tau may induce neuronal loss in the absence of Aβ, but also suggest that Aβ plaque formation may lie upstream of tau, at least for AD.

Consistent with the findings that Aβ plaque burden does not correlate well with the severity of dementia but NFT formation does, is the finding that NFTs can be differentiated into neuropathological stages in AD. Braak & Braak (1991) reported detailed pathological studies about the distribution of plaques and tangles in post-mortem brains of demented and non-demented individuals. They showed that Aβ deposition was of little significance in relation to neuropathological staging, whereas NFTs exhibited a neuroanatomical distribution pattern permitting the differentiation of six stages of disease progression in AD.

Tangles are first observed in the entorhinal cortex where neuronal loss occurs earliest, and are closely related to the initial memory impairment in AD. Conversely, Aβ deposits are not found in the hippocampal formation until the late stages of the disease (Hasegawa, 2004). Another post-mortem study showed that both NFTs and neuronal loss increased in parallel with the duration of AD, although the amount of neuronal loss was quite larger than the amount of tangle accumulation (Gomez-Isla et al., 1997). In contrast, the authors found that the amount of plaques and Aβ accumulation was not related to neuronal loss, the number of NFTs, or the duration of the disease.

Despite the recent attention the tau hypothesis has received, it has limitations similar to the Aβ hypothesis. Foremost is the finding that NFTs are extremely common and perhaps universal in the nucleus basalis of Meynert, a basal forebrain region rich in cholinergic fibers, in non-demented aged individuals (Beach et al., 1998). Secondly, because humans with, or animal models of, tauopathies fail to develop Aβ pathology or the global neuronal loss seen in AD, it is difficult to claim that tau aggregation and NFTs are causing the disease.

Recently, soluble tau proteins have been suggested to account for neurotoxicity and cognitive deficits as opposed to insoluble tau aggregates and NFTs. In an inducible transgenic mouse model carrying mutant tau, the suppression of the transgene with doxycycline in the rodents' diet led to the amelioration of learning and memory impairments. Interestingly, this improvement occurred despite the lack of reduction in NFTs observed in these mice, indicating soluble tau may have been responsible for the deficits (Santacruz et al., 2005). These results were corroborated in a drosophila (fruit fly) model of tauopathy where it was found that soluble ptau contributed to neurodegeneration (Feuillette et al., 2010).

These findings suggest that, similar to Aβ, soluble species of ptau may be especially damaging, and their sequestration into NFTs may represent an attempt at a compensatory or protective response (Alonso Adel et al., 2006; Castellani et al., 2008). More data are certainly necessary before any conclusions can be drawn about what form of tau (soluble or insoluble) contributes to the neurodegeneration and cognitive impairments observed in AD. Another possible explanation for the significant neuronal

loss and degeneration seen in AD is related to the cholinergic hypothesis and the loss of cholinergic neurons in areas important for learning and memory.

Cholinergic Hypothesis

The cholinergic deficit in AD is the earliest and most frequently reproduced finding, specifically the profound reduction in choline acetyltransferase (ChAT) activity (Bowen et al., 1982; Davies & Maloney, 1976). ChAT is the enzyme responsible for synthesizing acetylcholine (ACh), and its decreased activity leads to reduced amounts of available ACh in the brain, specifically in the hippocampus and neocortex (Davies, 1979; Perry et al., 1977). The finding that cholinergic cell loss is associated with the presence of plaques in non-demented aged individuals suggests that the loss of cholinergic neurons precedes the clinical diagnosis of AD (Beach et al., 1997). Furthermore, studies indicate that the severity of the dementia in AD correlates well with the extent of cholinergic loss and the reduction in ChAT activity in the cortex (Perry et al., 1981).

Cholinergic loss occurs first and foremost in the basal forebrain where CBF neurons deteriorate very early in the disease progression (Beach et al., 2000; Bowen et al., 1982; Whitehouse et al., 1982). ACh has been implicated in multiple cognitive functions such as learning and memory (Cox & Tye, 1973; Spencer et al., 1985; Spencer & Lal, 1983; Valentino & Dingledine, 1981; Whitehouse, 1967; Woolf, 1996). Once ACh is released, it can bind to either of two receptor subtypes: nicotinic acetylcholine receptors or muscarinic acetylcholine receptors (Role & Berg, 1996; reviewed in Ishii & Kurachi, 2003 and Wevers & Schroder, 1999).

Nicotinic receptors are ionotropic receptors (receptors that can open ion channels when ACh binds to them) while muscarinic receptors are metabotropic receptors (receptors that activate a G-protein and trigger intracellular events when ACh binds, including the opening of multiple ion channels). There appears to be a selective loss of ACh receptors in the cortex and hippocampus in AD, which seems to be more pronounced for nicotinic receptors (Flynn & Mash, 1986; Perry et al., 1995; Wevers et al., 2000).

Nicotinic receptor activation using nicotine produces a significant increase in the amount of ptau both *in vitro* and in 3xTg-AD mice (Hellstrom-Lindahl et al., 2000; Oddo et al., 2005). The exact mechanism of how this increase in phosphorylation occurs remains unclear, but it may be a result of increased calcium levels due to overactivation of the nicotinic receptors. Nicotonic receptors are one of only a few ionotropic receptors in the brain that allow an influx of calcium ions when ACh binds (McGehee et al., 1995; Role & Berg, 1996). This increase in intracellular calcium may activate different calcium-dependent kinases, such as GSK-3β, which may be responsible for phosphorylating tau (Oddo et al., 2005).

Nicotinic receptor activation also appears to have an effect on Aβ deposits in the brain. *In vitro* studies have shown that nicotine seems to inhibit Aβ fibril formation and also disrupts already formed fibrils (Ono et al., 2002; Salomon et al., 1996; Zeng et al., 2001). These findings would suggest that in the absence of ACh, the formation of fibrils is allowed to progress at a more rapid rate. Studies using Tg2576 mice, which overexpress human mutant APP, showed a dramatic decrease both in Aβ plaque burden and the levels of insoluble $A\beta_{40}$ and $A\beta_{42}$ after chronic administration of nicotine for a

period of five and a half months (Nordberg et al., 2002). It is difficult to determine what effect the loss of nicotinic receptors has on tau phosphorylation and Aβ deposits in AD, and more studies are necessary to elucidate the relationships. Furthermore, epidemiological studies linking cigarette smoking to incidence of AD have demonstrated conflicting results (Brenner et al., 1993; Cataldo et al., 2010).

Muscarinic receptors, specifically the M1 receptor subtype, are highly expressed in the cerebral cortex and hippocampus, and seem to be particularly relevant to memory function in AD (Anagnostaras et al., 2003). Activation of the M1 receptor has been shown to decrease tau phosphorylation, suggesting that decreased cholinergic activity may lead to destabilization of the microtubule network and eventual tangle formation. *In vitro* studies using cholinergic M1 agonists showed that the muscarinic-activated decrease of tau phosphorylation was both time and dose dependent (Sadot et al., 1996). *In vivo* studies using 3xTg-AD mice also showed a reduction in tau phosphorylation following administration of a muscarinic agonist and conversely showed increased tau phosphorylation after treatment with an M1 antagonist (Caccamo et al., 2006). Previous *in vitro* findings found that M1 receptor agonists decrease tau phosphorylation via reduction of GSK-3β activity (Forlenza et al., 2000), which appears to be the mechanism by which tau phosphorylation was decreased in the 3xTg-AD mice.

Muscarinic receptor activation also appears to reduce Aβ production and increase the secretion of soluble APP (Buxbaum et al., 1992). In the 3xTg-AD mice, an M1 agonist reduced Aβ deposition in the hippocampus and cortex, and ameliorated cognitive deficits in a spatial memory task (Caccamo et al., 2006). This finding that muscarinic activation regulates APP processing (Nitsch et al., 1992) formed the basis for the

hypothesis that AChE inhibitors may slow disease progression by reducing Aβ production (Inestrosa et al., 1996).

AChE inhibitors were developed as a result of the cholinergic hypothesis in order to increase cholinergic tone in individuals with AD (Bartus, 1979; Bartus et al., 1982; Davis et al., 1978). AChE is primarily responsible for the breakdown of ACh into choline and acetic acid. AChE has also been implicated in Aβ plaque formation and appears to have the ability to accelerate Aβ formation and deposition in AD (Inestrosa et al., 1996). Therefore, by inhibiting the enzymatic activity of AChE, it may be possible to reduce Aβ plaque formation and ameliorate AD symptomology. AChE inhibitors increase the amount of ACh available in the synapse as well as enhance and prolong its action on ACh receptors (Harvey & Rowan, 1990). AChE inhibitors have been approved for use in mild to moderate AD and have been shown to improve cognitive deficits (Rogers et al., 1998; Rosler et al., 1999; Tariot et al., 2000). These drugs tend to show symptomatic efficacy, but little evidence exists that they prevent or even slow the course of the disease.

Neuroinflammatory Hypothesis

Glial cells in the brain, specifically microglia and astrocytes, can serve as mediators of the inflammatory response when necessary, defending the central nervous system (CNS) from pathogens and aiding in the recovery from damage and stress (reviewed in Skaper, 2007). AD brains exhibit extensive localized activation of both microglia and astrocytes in response to neuronal and synaptic damage and Aβ accumulation (Akiyama et al., 2000). It is likely that this inflammation related to AD pathology may be both beneficial as a mechanism to promote neuronal survival and

detrimental to AD brain function and the degeneration process (Wyss-Coray & Mucke, 2002).

Studies have shown that aggregated Aβ is itself capable of activating the inflammatory response by activating microglia and enhancing the synthesis and release of proinflammatory cytokines (Combs et al., 2001; Tan et al., 1999). These proinflammatory cytokines may also accelerate tau pathology and NFT formation, perhaps linking Aβ-induced inflammation and neurofibrillary pathology (Guo et al., 2006; Quintanilla et al., 2004; Sheng et al., 2000). These findings would suggest that inflammation is actually advancing AD pathology and accelerating the neuronal loss.

Although microglial activation in AD may be caused by Aβ pathology, microglial activity correlates more closely with NFT pathology (Hayes et al., 2002). This relationship suggests that although Aβ may trigger the initial activation of microglia, the resulting inflammatory response may be more directly related to tau pathology (Blurton-Jones & LaFerla, 2006).

Calcium Hypothesis

Calcium is critical for a host of intracellular processes. For example, the release of neurotransmitter from presynaptic terminals relies on calcium influx in order to mobilize synaptic vesicles (Borst & Sakmann, 1996; Kochubey et al., 2011). In the absence of calcium, transmitter will not be released following an action potential. In the postsynaptic neuron, calcium acts as a second messenger, initiating signal transduction pathways and even regulating transcriptional events (Bading et al., 1993; Greenberg et al., 1986). Specifically, many enzymes such as calcium/calmodulin-dependent protein kinase II

(CaMKII), one of the most abundant kinases (enzyme that phosphorylates other proteins) in the brain, and cAMP-dependent protein kinase (PKA) both rely on calcium for activation (Braun & Schulman, 1995; Impey et al., 1998). These kinases then initiate signaling cascades which lead to downstream nuclear transcription. Calcium also plays a direct role in synaptic plasticity; activation of N-methyl D-aspartate (NMDA) glutamate receptors and the subsequent influx of calcium ions are necessary for the induction of LTP and many forms of learning.

Calcium influx from the extracellular fluid can occur through ligand-gated ion channels such as the NMDA receptor and several voltage-gated calcium channels (VGCC) such as L-, N-, P-, and T-type channels (reviewed by Catterall, 2011). Calcium also enters the cytoplasm from intracellular stores such as the endoplasmic reticulum (ER) through multiple channels. Although calcium is constantly entering neurons, levels of intracellular calcium are kept extremely low (~10^{-7} M) and tightly regulated by a host of mechanisms.

A variety of adenosine triphosphate (ATP)-dependent pumps removes calcium from the cytoplasm, either sequestering it into intracellular organelles or expelling it into the extracellular fluid. The plasma-membrane calcium-ATPase (PMCA) efficiently pumps calcium ions out of neurons, while the sarco/endoplasmic reticulum calcium-ATPase (SERCA) pump sequesters intracellular calcium into the ER (Gunteski-Hamblin et al., 1988; Strehler et al., 2007). These pumps require a great deal of energy expenditure from the cell in order to maintain the low levels of intracellular calcium and high sensitivity for the ion. Other membrane-bound mechanisms do not utilize ATP to extrude calcium but instead rely on its electrochemical gradient.

The sodium/calcium exchanger, an ion transporter localized primarily to the plasma membrane, removes one calcium ion from the cytoplasm for every three sodium ions that flow into the cell. However, this process is reversible and completely dependent upon the electrochemical gradient of potassium, sodium, and calcium, as well as the membrane potential of the cell (Blaustein & Lederer, 1999). This exchanger is likely the predominant mechanism for calcium efflux across the plasma membrane, especially when intracellular calcium levels are elevated due to a high rate of neuronal activity (Lytton, 2007).

High rates of activity may also lead to calcium uptake into mitochondria via mitochondrial calcium uniporters (DeLuca & Engstrom, 1961). These calcium transporters bring calcium across the mitochondrial membrane using the electrochemical gradient of calcium and the mitochondrial membrane potential (Kirichok et al., 2004). Although these uniporters are important for sequestering excess calcium, sustained elevation of calcium levels in the mitochondria can be dangerous and lead to cell death.

Additional mechanisms responsible for regulating intracellular calcium levels include calcium-binding proteins such as parvalbumin (PV) and calbindin (CB). This class of proteins plays a significant role in the buffering of intracellular calcium, thereby reducing the likelihood of excessive mitochondrial calcium uptake and subsequent apoptosis (Rintoul et al., 2001). All of the mechanisms mentioned above play a role in maintaining calcium homeostasis and preventing excessive intracellular calcium levels. When this homeostasis cannot be maintained, the consequences for both an individual neuron and the brain can be severe.

Excessive calcium influx, often mediated by NMDA receptor calcium channels, can be toxic for cells, a phenomenon known as excitotoxicity (Choi, 1985; Lucas & Newhouse, 1957). Interestingly, this phenomenon is a common occurrence in several neurodegenerative diseases including Huntington's disease, Parkinson's disease, and amyotrophic lateral sclerosis (ALS) (Beal, 1998; Cluskey & Ramsden, 2001; Taylor-Robinson et al., 1994). These consistent findings across disorders suggest excitotoxicity may play an integral role in age-related neurodegeneration. Excitotoxicity also occurs in later stages of AD (Mattson, 1994). However, a sustained, low-level calcium dysregulation may have an impact in early or preclinical AD as well.

Disruptions of calcium regulation have been consistently observed in aged and AD brains (Ito et al., 1994; Peterson et al., 1985; Peterson & Goldman, 1986; Raza et al., 2007), potentially contributing to neurodegeneration in AD. Calcium levels are increased in neurons that contain NFTs as compared with tangle-free neurons (Murray et al., 1992). The increased levels of calcium may even precede tangle formation as levels of CaMKII are increased in hippocampal neurons vulnerable to degeneration (McKee et al., 1990). Tau mutations, similar to those found in FTDP-17, lead to altered calcium channel function and increased calcium influx (Furukawa et al., 2003). Similarly, an increase in Aβ production has been observed as a result of calcium influx *in vitro* (Querfurth & Selkoe, 1994; Pierrot et al., 2004). In 3xTg-AD mice, an increased resting calcium concentration is observed (Lopez et al., 2008; Vale et al., 2010). These studies and others mentioned above implicate perturbed calcium homeostasis as a major pathogenic contributor in AD, with an emphasis on the role of calcium derived from intracellular stores such as the ER and mitochondria.

Mitochondrial dysfunction has been consistently observed in both aged and AD brains, possibly contributing to the neurological changes seen in the disorder (Leslie et al., 1985; Mancuso et al., 2006; Sheehan et al., 1997). Mitochondria are involved in maintaining calcium homeostasis and allow calcium entry through a variety of mechanisms (Beutner et al., 2005; Nicholls, 2005; Sparagna et al., 1995). Excessive calcium intake by mitochondria has been shown to increase reactive oxygen species (ROS), inhibit ATP synthesis, open the mitochondrial permeability transition pore (mPTP), and induce the release of pro-apoptotic factors (Brustovetsky et al., 2003; Jiang et al., 2001). Therefore, it is possible that increased intracellular calcium levels may lead to mitochondria-induced apoptosis which may account for some of the neuronal loss witnessed in AD. The ER, another important intracellular mediator of calcium levels, has also been implicated in AD pathological dysfunction.

The ER is a crucial organelle for the synthesis, correct folding, and transport of proteins which are integral for normal cellular function (reviewed in Paschen & Mengesdorf, 2005). The ER is also central in cellular calcium storage and signaling, as high levels of calcium are necessary for proper protein synthesis and folding (Kuznetsov et al., 1992; Pozzo-Miller et al., 1997). Disruptions of normal ER functioning, termed ER stress, have been observed in AD and may contribute to the pathological disturbances (Katayama et al., 2004; LaFerla, 2002; Verkhratsky, 2005).

Under conditions of ER stress, signaling pathways may be activated in an attempt to counteract the stress, the most notable one being the unfolded protein response (UPR). The main purpose of the UPR is to restore normal ER functioning by reducing the amount of proteins that need to be folded and processed, while also increasing the protein

folding and processing capacity in the ER (Kaufman, 1999). However, if the stress is prolonged or severe, as may be the case in AD, the ER may initiate cell death pathways (Unterberger et al., 2006). The finding that PS proteins are localized on the ER membrane (Kovacs et al., 1996), in addition to their role in the γ-secretase complex, provided a critical link between known AD genetic phenomena and intracellular calcium regulation.

As mentioned above, PS mutations lead to increased production of neurotoxic Aβ and disruption of intracellular calcium homeostasis (Duff et al., 1996). This calcium disruption associated with PS mutations has been consistently demonstrated in several different neuronal preparations, both from familial AD tissue and animal models with PS mutations (Ito et al., 1994; Herms et al., 2003; Stutzmann et al., 2004). It is clear that PS proteins play a role in calcium regulation, however only recently has this role been elucidated. Studies have demonstrated that PS mutations lead to greatly exaggerated calcium liberation from ER stores after cellular stimulation (Ito et al., 1994; Leissring et al., 1999; Mattson et al., 2000; Stutzmann et al., 2004).

Several mechanisms have been proposed to explain how PS mutations alter functioning in the ER. One proposed mechanism suggests that PS mutations alter PS leak channel activity, leading to increased calcium levels within the ER (Nelson et al., 2007; Tu et al., 2006). Another study posits that PS mutations may increase inositol 1,4,5-triphosphate receptor (IP3-R) activity, leading to increased calcium release from the ER (Cheung et al., 2008).

A third mechanism suggests that PS-mediated calcium dysregulation occurs through upregulation of the ryanodine receptor (RyR), an ER calcium channel

responsible for calcium-induced calcium release (CICR) from the ER (Smith et al., 2005; Stutzmann et al., 2006). Recently, Stutzmann and colleagues found dramatically increased RyR expression in 3xTg-AD mice at an age before any cognitive deficits or neuropathological hallmarks are exhibited (Chakroborty et al., 2009). Their findings imply that perturbed, yet functional, calcium signaling occurs before AD-like events such as plaques and tangles. Thus, it is possible altered calcium signaling may facilitate development of the pathologies seen in AD.

The RyR is widely expressed throughout the mammalian brain (McPherson & Campbell, 1993). It is an important regulator of intracellular calcium homeostasis and a critical mediator of calcium release from the ER (Mignery et al., 1989; Shmigol et al., 1995). The RyR is especially crucial for calcium-mediated presynaptic neurotransmitter release (Padua et al., 1996). AD brains display a significant impairment in RyR functioning which likely occurs early in AD pathogenesis and correlates well with the development of plaques and tangles (Kelliher et al., 1999).

Early studies by Querfurth et al. (1997) demonstrated that administration of caffeine, a potent activator of RyRs, increased Aβ production in human embryonic kidney (HEK) 293 cells. Further, caffeine-induced calcium release is enhanced in 3xTg-AD mice, likely due to the increased expression of RyRs observed in these mice (Smith et al., 2005). These findings imply a bidirectional or feed-forward relationship between RyR activation and prominent AD pathologies. It is unclear what role the RyR plays in AD pathogenesis or if abnormal function of this channel is sufficient to induce AD-like neurodegeneration and cognitive deficits. Studies using *in vivo* models to investigate RyR-mediated calcium dysregulation may be necessary to answer these questions.

Several additional mechanisms for maintaining calcium homeostasis in the cell exist, especially in the ER.

ER calcium levels in the brain are largely regulated by SERCA (Miller et al., 1991), which pumps calcium back into the ER to maintain equilibrium. Disruption of normal SERCA activity with thapsigargin, an irreversible SERCA inhibitor, leads to a sharp spike in cytosolic calcium levels using *in vitro* methods (Lytton et al., 1991). This SERCA inhibition prevents refilling of ER calcium pools which creates a sustained level of increased intracellular calcium.

Various cell culture systems have taken advantage of thapsigargin to investigate AD-like calcium dysregulation. Seminal investigations by Buxbaum et al. (1994) demonstrated that thapsigargin can dose-dependently alter APP processing and levels of Aβ in Chinese hamster ovary (CHO) cells. Additional studies have shown that thapsigargin leads to increased Aβ levels in neuronal and non-neuronal preparations (Crestini et al., 2011; Querfurth et al., 1997).

Intracellular calcium dysregulation via thapsigargin can also increase tau phosphorylation both in primary neuronal cultures (Ho et al., 2012) and following acute *in vivo* administration of the compound (Fu et al., 2010). Collectively, these studies suggest that thapsigargin-induced calcium dysregulation may produce cellular changes consistent with AD. Although calcium dysregulation is centrally implicated in AD, the calcium hypothesis has suffered from a lack of genetic evidence until recently.

A novel calcium channel, named calcium homeostasis modulator 1 (CALHM1), was discovered with polymorphisms associated with an increased risk for AD (Dreses-Werringloer et al., 2008). CALHM1 is a transmembrane protein found predominantly in

the ER and neuronal membranes and is unaffected by blockers of voltage-gated calcium channels. Interestingly, calcium influx through this channel decreases Aβ production and increases the soluble form of APP produced after cleavage by α-secretase. CALHM1 may also interfere with ER calcium handling and trigger ER stress (Gallego-Sandin et al., 2011). The polymorphism found in CALHM1 has been shown to increase Aβ production, providing direct genetic evidence of a link between calcium dysregulation and AD pathology. These findings have been somewhat controversial however, and other populations have failed to exhibit an association between the CALHM1 polymorphism and AD (Beecham et al., 2009; Bertram et al., 2008; Minster et al., 2009; Sleegers et al., 2009; Tan et al., 2011).

Experiments and Hypotheses

Current animal models of AD almost exclusively rely on genetic mutations that only occur in familial, early-onset cases of the disease. They are valuable tools for investigating specific pathologies such as Aβ and tau dysfunction, but these models do not have great utility in studying the mechanisms underlying AD pathogenesis. Most investigations of AD examine prominent pathologies (i.e. plaques and tangles) in order to observe their effect on normal functioning. An alternative approach is to examine neurochemical changes upstream, pathologically and temporally, of these gross lesions.

The amount of data generated investigating mechanistic approaches upstream of Aβ and tau is scarce. As mentioned above, calcium can directly influence the processing of APP and the phosphorylation state of tau. Alterations in the regulation of calcium may represent an upstream mechanism capable of explaining the aberrant Aβ and tau activity

observed in AD. This calcium dysregulation may then be exacerbated by the pathologies it produced in a neurodegenerative feed-forward loop. Because the effects of *in vivo* calcium dysregulation are unknown, it is unclear whether this hypothesis has validity. In the below experiments, we examined a novel approach to AD by inducing a chronic dysregulation of intracellular calcium. Current AD models typically produce robust impairments in hippocampal-dependent learning and memory using tasks such as the MWM and NOR testing, as well as pathological disturbances consistent with AD (Cleary et al., 2005; Hsiao et al., 1996). We hypothesized that our manipulations would produce behavioral and neurochemical changes similar to what is observed in other animal models of AD.

This model was the first to investigate the effects of chronic perturbation of calcium homeostasis in an *in vivo* system. In order to disrupt calcium levels, we utilized ryanodine, a dose-dependent agonist of the RyR, and thapsigargin, the aforementioned SERCA inhibitor. The chronic, steady infusion of each of these compounds should produce a sustained elevation of cytosolic calcium. The effect of this prolonged calcium dysregulation *in vivo* is unknown; to the best of our knowledge, this series of studies was the first to examine it. Three experiments were performed, each of which is outlined below and summarized in Table 1.

Experiment 1

The effects of chronic intracellular calcium dysregulation were initially examined in a pilot study using ryanodine or thapsigargin centrally administered to adult male rats. Ryanodine was administered at a dose of 250 nM while thapsigargin was administered at

10 μM. Alzet osmotic mini-pumps were implanted subcutaneously and connected to a cannula, which infused the compound directly into the lateral ventricles. The osmotic mini-pump releases solution at a rate of 0.15 μL/hour over the course of six weeks. Following four weeks of infusion, learning and memory was examined in NOR and the MWM in subsequent weeks before tissue was collected at the six week point. We examined the brains for any changes in protein levels that are consistent with those observed in AD. Tau phosphorylation, an early and consistent event in AD, was investigated at the Serine 396 epitope ($pTau_{396}$ antibody). Total tau protein levels were also examined (Tau-5 antibody) to determine if chronic calcium dysregulation altered any aspect of tau expression.

We also examined protein levels of oAβ following treatment with thapsigargin or ryanodine, as evidence suggests oAβ may best correlate with disease severity (McLean et al., 1999). Because amyloid deposits are rarely if ever found in rodent brains, likely due to the slight but significant differences in the sequence of Aβ versus humans (Otvos et al., 1993), plaque load would not be a feasible measure to evaluate. These oligomers may represent an intermediate step between the easily cleared Aβ monomers and the insoluble fibrillar plaques observed in AD, making them ideally suited to investigate in a potential model of preclinical AD.

Finally we investigated protein levels of calbindin-D28k (CB-D28k), a calcium buffering protein that also likely acts as a calcium sensor, directly affecting intracellular signaling pathways (Schwaller, 2010). If thapsigargin or ryanodine perturbed calcium regulation, this change should be reflected in CB-D28k levels. Prolonged increases in intracellular calcium concentration may lead to excessive calcium binding to calcium

buffers such as CB-D28k. In turn, this may alter the neuronal expression of CB-D28k, a change which should be reflected in its protein levels.

Experiment 2

In order to determine the optimal effective dose of each ligand to produce behavioral deficits and AD-like neurochemical changes, ryanodine and thapsigargin were each administered to adult male rats at two different doses: ryanodine at 1 or 5 μM and thapsigargin at 20 or 40 μM. All other methods and timelines were identical to experiment 1 with the exception that more subjects per group were utilized in experiment 2.

Experiment 3

Neuroinflammation has been increasingly implicated as an important aspect of AD progression and onset (Hensley, 2010). Recent genetic evidence even suggests that variants in the triggering receptor expressed on myeloid cells 2 (TREM2) gene may be a risk factor for AD (Guerreiro et al., 2013; Jonsson et al., 2013). TREM2 is a phagocytic immune receptor expressed on the cell surface of microglia and is essential for the clearance of neuronal debris (Singaraja, 2013). Coupled with many other recent studies investigating the role of inflammation in neurodegeneration, the investigation of neuroimmune interactions with AD pathology has become a hot topic.

In a follow-up study to experiment 2, we investigated the interaction between chronic calcium dysregulation and inflammation. Because thapsigargin displayed more promise as a potential inducer of AD-like calcium dysregulation in our previous studies,

it was favored in experiment 3 over ryanodine. To induce the inflammatory response, lipopolysaccharide (LPS) was systemically administered to rats two weeks following surgical implantation of the Alzet osmotic pumps. LPS is derived from gram-negative bacteria and induces a strong immune response in the brain, including robust, long-lasting activation of microglia (Herber et al., 2006) and cytokines (Murray et al., 2011). Aged rats (10-12 months of age) were utilized to better reflect how closely our model mimicked prodromal AD, while the dosage of thapsigargin chronically administered was designed to be 25 μM in this experiment. Unfortunately, due to an error in filling the osmotic pumps, a combination of 25 μM and 40 μM thapsigargin was introduced into the pumps, a mistake not realized until after the experiment was finished or any corrections could be made. This error prevented a precise knowledge of what drug concentration was in the pumps and therefore all interpretations of the data from this experiment were made with extreme caution. Pumps administered the compounds for five weeks before behavioral testing commenced and tissue was collected seven weeks following surgery. All other methods and biochemical targets were consistent with experiments 1 and 2.

CHAPTER 3

MATERIALS AND METHODS

Subjects

For experiment 1, twenty-four male Sprague-Dawley (SD) rats (n=8) approximately three months of age at arrival were purchased from Charles River Laboratories; for experiment 2, sixty male SD rats (n=12) approximately three months of age at arrival were purchased from Charles River; for experiment 3, forty (n=10) male retired breeder rats approximately nine to eleven months of age at arrival were purchased from Taconic Farms. Rats were maintained in a temperature and humidity (22 ± 1°C) controlled facility, with food and water available ad libitum, on a 12:12 light/dark cycle, lights on at 7:00 a.m. In experiments 1 and 2, animals were housed in pairs until the time of the surgery, after which they were individually housed. In experiment 3, rats were individually housed upon arrival. All procedures were approved by the University of Nevada, Las Vegas Institutional Animal Care and Use Committee and were carried out in accordance with NIH guidelines for the appropriate care and use of animals.

Surgery

Surgeries were performed under aseptic conditions and a cocktail of ketamine (80 mg/kg) and dexmedetomidine (0.2 mg/kg) anesthesia as previously described (Kinney et al., 2003; Sabbagh et al., 2012). A guide cannula was implanted into the right lateral ventricle at coordinates 0.7 mm posterior and 2 mm lateral to bregma and 3.5 mm ventral to the surface of the skull (Paxinos & Watson, 1986. Three indentations were made in the

skull to allow threading of jeweler's screws, which were placed on the skull to anchor the cannula in place.

A catheter attached to an Alzet osmotic pump was then attached to the cannula and the pump was subcutaneously implanted between the scapulae. Dental acrylic was applied to bind together the screws, the base of the cannula, and the skull. Sutures were then applied to close up the wound followed by the removal of the animal from the device. Once the rats were ambulatory they were administered an analgesic, buprenorphine (0.05 mg/kg), intraperitoneally and soon after returned to the colony room. Buprenorphine (0.05 mg/kg) was administered daily for two days following the surgery to reduce post-operative pain. Following surgery animals were individually housed and left undisturbed for a minimum of one week.

Drug Treatments

Ryanodine (Tocris Biosciences, Ellisville, MO) was dissolved in artificial cerebrospinal fluid (ACSF) to a final concentration of either 250 nM, 1 µM, or 5 µM. Thapsigargin (Sigma-Aldrich, St. Louis, MO) was diluted in ACSF to a final concentration of either 10, 20, 25 or 40 µM. LPS was dissolved in saline and injected intraperitoneally at a concentration of 1 mg/kg. Mini-pumps were filled with ryanodine, thapsigargin, or vehicle, depending on the experiment. Pumps infused the compounds into the ventricular fluid at a steady rate over the course of 6-7 weeks (0.15 µL/hour). Table 1 outlines the drug administrations for each experiment.

Table 1.

Outline of the groups for each experiment with drug dosages.

Experiment 1 (n=8)	*Experiment 2 (n=12)*	*Experiment 3 (n=11)*
Vehicle	Vehicle	Vehicle
	Ryanodine (1 μM)	LPS (1 mg/kg)
Ryanodine (250 nM)	Ryanodine (5 μM)	Thapsigargin (25-40 μM)
	Thapsigargin (20 μM)	
Thapsigargin (10 μM)	Thapsigargin (40 μM)	Thapsigargin + LPS

Behavioral Testing

One week following surgery once rats had sufficient time to recover, animals were briefly handled three times a week to ensure consistent data. Behavioral testing commenced an average of four weeks following the surgeries in experiments 1 and 2 and five weeks following surgery in experiment 3. Open field and NOR testing occurred during the first week of testing and the MWM began the following week. See figure 1 for a timeline of experiments.

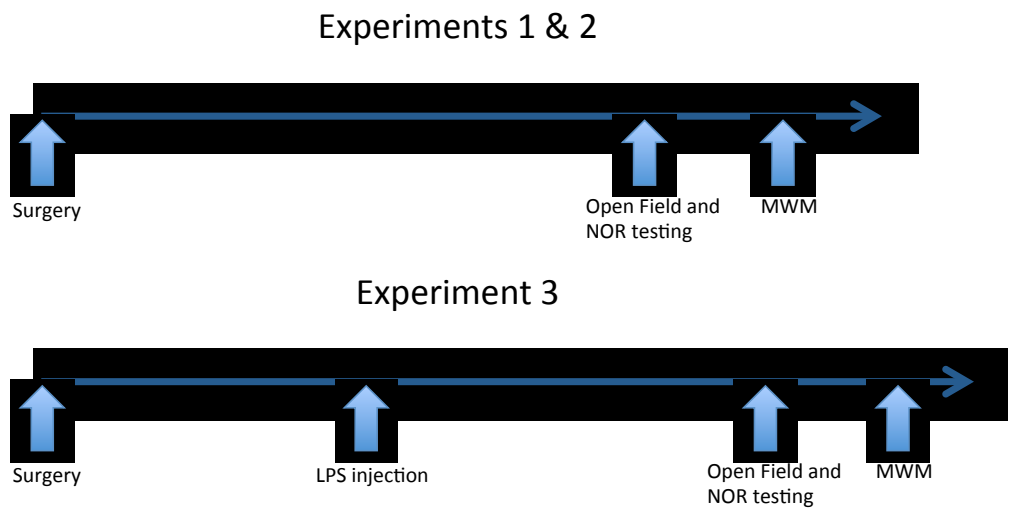

Figure 1. Timeline of experimental manipulations and testing.

Temperature and Weight Tracking

In experiment 3, animals were probed for rectal temperature before and after administration of LPS in order to verify illness. Temperatures were recorded in degrees Centigrade (°C). Weights were also tracked during this time frame to detect differences among groups.

Open Field and Novel Object Recognition Testing

The open field and NOR tasks were conducted as previously described (Bertaina-Anglade et al., 2011; Ennaceur & Delacour, 1988). For open field testing, rats were placed in a large open chamber for five minutes in order to examine anxiety-like behavior and ambulatory activity. The tracking system (Smart, San Diego Instruments, San Diego, CA) recorded a track of the animal and data were analyzed for time spent in center, time spent in the perimeter, and locomotor activity.

NOR testing began the following day. A pair of identical objects (object A) were placed in two counterbalanced corners of the chamber, and animals were allowed to freely explore the chamber for 5 minutes while time of object exploration was recorded. In experiment 1, a short-term memory (STM) test was performed 15 minutes later with a novel object (object B) paired with the original object. Conducting this STM test in experiments 2 and 3 was not feasible due to the number of subjects that needed to be run each day within the 12:12 hour light cycle. A long-term memory (LTM) test was performed 24 hours later in all experiments. In experiment 1, a novel object (object C) was paired with object B. In experiments 2 and 3, a novel object (object B) was paired with the original object (object A). Two distinct pairs of objects, previously examined to ensure no preference exists, were counterbalanced across sessions. Each session was recorded by video, and an analysis of total time spent investigating and preference for novel objects was performed by trained observers for both trials when applicable. Manual scoring was performed by multiple observers to ensure consistent data. An investigation was defined as contact with the object or sniffing of the object within 2 cm of the animal's head.

Morris Water Maze

The Morris water task was conducted in a circular tank, 1.8 m in diameter and 76 cm in height, made of white polyethylene 4.7 mm in thickness (San Diego Instruments). Tap water, 48 cm deep, was maintained at a temperature of 25°C and made opaque by the addition of white non-toxic paint (Fresco Tempera Paint, Rich Art Color Company, Northvale, NJ), and changed every other day. The escape platform, a square platform 10

cm in diameter made of clear plastic, was placed in the center of one of the four quadrants (target quadrant), 30 cm from the inside wall of the maze and 1.5 cm below the surface of the water. For visible platform training, a large black and white cover was attached to the top of the platform and protruded 2 cm above the water.

Trials were recorded and captured using the video tracking system (Smart) recorded from a Sony Handycam camera connected to a Cobalt Instruments computer. Data collected for each trial consisted of a track of the animal, which included the latency to locate the platform, speed of swimming, and thigmotaxis. On the probe trial the tracking system also recorded the amount of time subjects spent in each of the four quadrants of the maze, as well as the number of times the animal's path crossed over the previous platform location and its analogous location in each quadrant.

For the MWM procedure, subjects were taken individually from the colony room to a dedicated testing room containing the water maze, a computer desk, a table with the heating cage, and large geometric shapes positioned on each of the four walls, all serving as distal spatial cues. The rat was placed into the maze at one of three randomized locations, in the center of a quadrant that did not contain the escape platform (non-target quadrant). The rat was allowed to swim in the maze until it reached the hidden platform and placed its forepaws on the platform. If after 60 seconds the animal did not locate the hidden platform, it was guided to the platform by the experimenter. The rat was given 20 seconds on the platform to orient to distal spatial cues and was then placed under a heat lamp for a total of 30 seconds between trials.

Three additional trials were conducted in an identical fashion, for a total of four training trials per day. Following the fourth trial, the animal was dried and returned to its

home cage. The training trials for the hidden platform were conducted until control subjects reached a latency criterion of less than 15 seconds (4-trial group mean). A probe trial was conducted five hours later in experiment 1 or twenty-four hours later in experiments 2 and 3. For probe trials, the rat was placed in the maze in the same fashion as during training, but the escape platform was absent. The single probe trial was 60 seconds in duration, after which the rat was dried and returned to its home cage.

The day after completion of the probe trial, a two-day visible platform training protocol was employed. A visible platform that extends above the surface of the water (intra-maze cue) was placed into the maze instead of the hidden platform. Four trials per day were conducted for each animal in the same fashion as during the hidden platform training, with the exception that the platform location was changed on each trial. Visible platform training was conducted in order to detect any deficits in visual ability and motor function. Animals were humanely euthanized the day following completion of the MWM.

Tissue Collection

Animals were humanely euthanized via carbon dioxide asphyxiation and a secondary method of euthanasia (either decapitation or cutting of the diaphragm). Depending on the experiment, four to six rats from each group had their brains quickly removed and frontal cortex, hippocampus, and cerebellum were dissected out and flash frozen in dry ice. The dissected tissue was stored at -80° C until SDS/PAGE experiments.

The remaining rats from each group were utilized to verify that cannulae terminated in the lateral ventricle. These rats were transcardially perfused with ice-cold

phosphate-buffered saline (PBS) through the vascular system via the left ventricle of the heart followed by perfusion of 4% paraformaldehyde (PFA) to fix the tissue. Brains were then removed and placed in 4% PFA at 4° C for 48 hours followed by transfer to a 30% sucrose solution in PBS. Brains remained in this solution until they were sectioned on a cryostat to examine cannulae placement.

SDS/PAGE (Western Blots)

Tissue were homogenized in a non-denaturing lysis buffer consisting of 1X RIPA buffer (Cell Signaling; 20 mM Tris-HCL pH 7.5, 150 mM NaCL, 1 mM Na_2 EDTA, 1 mM EGTA, 1% NP-40, 1% sodium deoxycholate, 2.5 mM sodium pyrophosphate, 1 mM β-glycerophosphate, 1 mM Na_3VO_4, and 1 µg/ml leupeptin), 1 mM DTT, 1 mM phenylmethylsulfonyl fluoride (PMSF), 20 µg/ml aprotinin and 0.1% sodium dodecyl sulfate (SDS). Lysates were centrifuged at 15,000 x g for 15 minutes at 4°C, the supernatant was collected, and a protein assay to determine concentration was performed using the biciconinic acid method (BCA; Pierce, Rockford, IL). Samples (20 µg) were separated on 10 or 12% polyacryl gels, according to the method of Laemmli (1970). Proteins were then electro-transferred to nitropure 45 micron nitrocellulose membranes which were blocked in 5% milk in PBS and 0.1% sodium azide for two hours.

Individual membranes were then probed overnight at 4° C with one of the following primary antibodies diluted in 5% milk in PBS plus 0.2% Tween: rabbit polyclonal anti-$pTau_{396}$ (1:2000 dilution; Santa Cruz Biotechnology, Santa Cruz, CA), mouse monoclonal anti-Tau-5 (1:5000; Millipore, Billerica,MA), rabbit polyclonal anti-amyloid oligomer (1:1000; Millipore), mouse monoclonal anti-calbindin D-28k (1:1000;

Sigma-Aldrich), or rabbit anti-β-actin antibody as control (1:10000; Sigma-Aldrich). Detection of specific binding was performed by incubation with IRDye near-infrared secondary antibodies (1:20000 for IRDye 680 or 1:10000 for IRDye 800; LiCor Biosciences, Lincoln, NE) for one hour at room temperature. Following washes in PBS plus 0.1% Tween, membranes were imaged on an Odyssey CLx Infrared Imaging Sysytem (Li-Cor) and integrated intensity (I.I.) was obtained for each sample. Each sample was run in duplicate with β-actin or tau to normalize protein levels.

Statistical Analyses

Group differences in rectal temperature or weight were analyzed by one-way between subjects analysis of variance (ANOVA) with either treatment or group as the factor. One-way between subjects ANOVA was also used to analyze locomotor activity and time spent in the perimeter following open field testing with group as the factor. The performance index (PI) of each group for NOR testing was analyzed with paired sample t-tests. MWM hidden and visible platform training data were analyzed by repeated measures ANOVA with days as the within subjects factor and group as the between subjects factor, while probe trial data were analyzed by one-way within subjects ANOVA with percent time in quadrant or annulus crossings as the factor. Western blot integrated intensity (I.I.) data were also analyzed by one-way between subjects ANOVA with group as the factor. Tukey post-hoc comparisons of treatment groups were performed following any significant ANOVA to determine points of significance ($p<.05$).

Correlational analyses were performed to examine the relationship between water maze performance and protein level changes in the brain. Probe trial time in target

quadrant data for each subject were compared to the vehicle mean to yield a difference score. Protein levels were also equated in this fashion, with individual subject data being compared to vehicle to provide a difference score. Scatterplots were then generated to determine if any potential correlations existed between probe trial performance and protein levels for each experiment, as well as for each group within experiments. If possible correlations existed, linear regression analyses were performed to determine significance ($p<.05$).

CHAPTER 4

RESULTS

Experiment 1

Open Field Testing

Experiment 1 was a pilot study to establish if altering calcium regulation would be a tractable approach to investigate AD. In the open filed test, animals were allowed five minutes to freely explore an open box, while percent time spent in the perimeter and locomotor activity were recorded. No significant differences were observed in the amount of time spent in the perimeter among groups ($F_{2,21} = 2.050$, p=.154; see figure 2A). Similarly, neither ryanodine nor thapsigargin produced a change in the total distance travelled versus vehicle ($F_{2,21} = 1.732$, p=.201; see figure 2B).

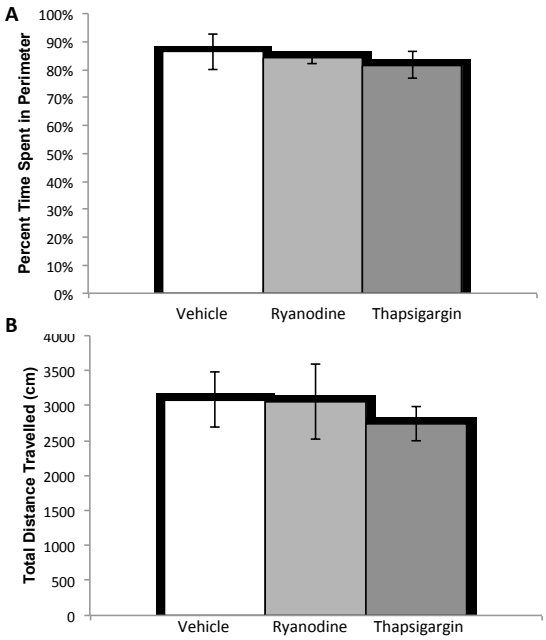

Figure 2. Open field testing in experiment 1 (n=8). (A) No significant differences were found among groups in the percent time spent in the perimeter or (B) the total distance travelled. Data are expressed as the mean ± SEM

Novel Object Recognition Testing

The day following open field testing, two identical objects (object A) were placed into the open field chamber and animals were permitted five minutes to explore. There were no significant differences among groups in the amount of time spent investigating the identical objects ($F_{2,21} = 1.733$, p=.201; see figure 3A). In the STM test fifteen minutes later (figure 3B), thapsigargin-treated animals did not spend significantly more time with the novel object (object B) than chance levels ($t_7 = 1.639$, p=.145). The groups administered vehicle or ryanodine did not display any deficits ($t_7 = 2.674$, $p<.05$ and $t_7 = 3.096$, $p<.05$, respectively). Twenty-four hours later in the LTM test (figure 3C), neither the vehicle nor thapsigargin groups spent significantly more time with a novel object (object C) than chance levels ($t_7 = 0.125$, p=.904 and $t_7 = 1.162$, p=.283, respectively). Ryanodine-treated subjects did spend significantly more time with object C than chance ($t_7 = 5.333$, $p<.01$), indicating the lack of a LTM impairment.

Morris Water Maze Testing

Subjects underwent six days of MWM hidden platform training before criterion latency was reached in the vehicle group. For latency to reach the platform, there was a significant main effect of days ($F_{5,425} = 16.955$, $p<.01$), indicating subjects significantly improved across days. There was also a significant main effect of treatment for latency ($F_{2,85} = 4.281$, $p<.05$; Tukey post-hocs revealed that thapsigargin-treated rats had significantly longer latency versus vehicle, $p<.05$; figure 4A), indicating that thapsigargin impaired ability to locate the hidden platform. There were no differences in speed of swimming among groups during training ($F_{2,85} = 0.795$, p=.455; figure 4B), suggesting

neither ryanodine nor thapsigargin impaired swimming ability. There was a significant main effect on thigmotaxis, the amount of time spent in the perimeter of the maze, but no differences were observed among groups ($F_{2,85} = 4.408$, $p<.05$; Tukey post-hocs revealed no significant differences among groups; figure 4C), suggesting the drugs did not increase anxiety-like behavior.

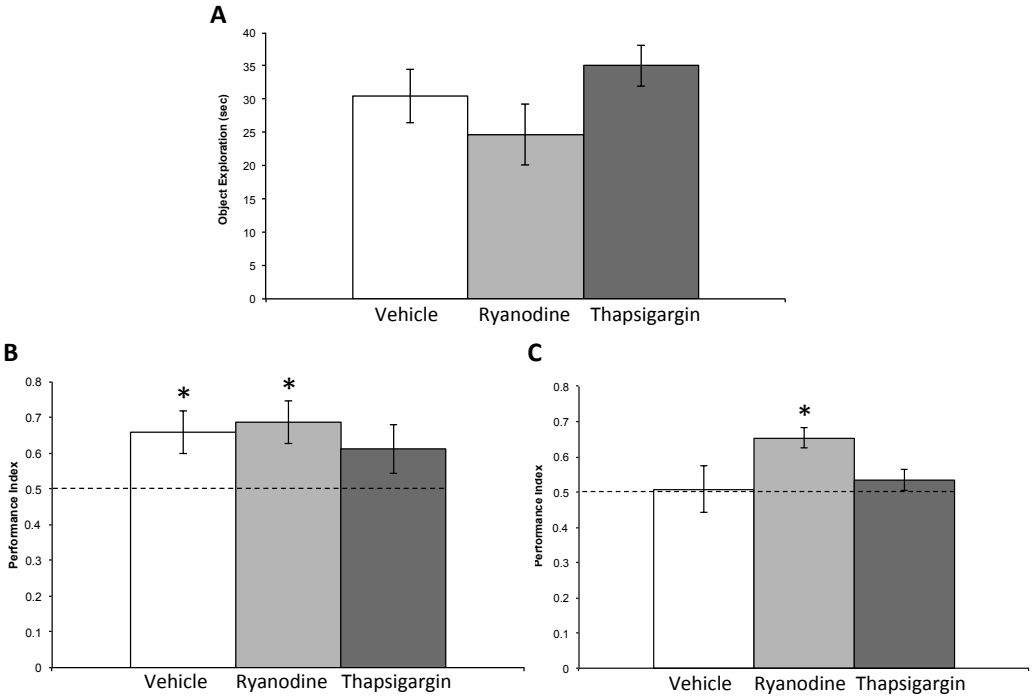

Figure 3. NOR testing in experiment 1 (n=8). (A) No significant differences among groups were found in the total time spent investigating the original objects (object A). (B) Thapsigargin produced a short-term memory deficit when presented with a novel object (object B) fifteen minutes following object A. (C) Only ryanodine-treated rats spent significantly more time with a novel object (object C) than chance levels twenty-four hours later. Data are expressed as the mean ± SEM. * indicates $p<.05$ in (B) and $p<.01$ in (C).

Five hours later a probe trial was conducted to assess discrete spatial learning of the platform location (see figure 5). Within group analyses of the percent time spent in

each quadrant were performed to evaluate if subjects spent significantly more time in the target quadrant than each of the other three quadrants (figure 5A). The vehicle group demonstrated a selective probe trial ($F_{3,24} = 14.470$, $p<.01$; Tukey post-hocs revealed subjects spent significantly more time in the target quadrant versus each of the other quadrants, $p<.01$) but ryanodine-administered rats did not show a preference for the target ($F_{3,24} = 9.632$, $p<.01$; Tukey post-hocs revealed that animals spent significantly more time in target versus the opposite and adjacent right quadrants ($p<.01$) but not the adjacent left quadrant, $p=.144$). Surprisingly, thapsigargin did not produce a probe trial impairment despite the deficits observed in hidden training ($F_{3,28} = 5.056$, $p<.01$; Tukey post-hocs revealed subjects spent significantly more time in the target quadrant versus each of the other quadrants, $p<.05$).

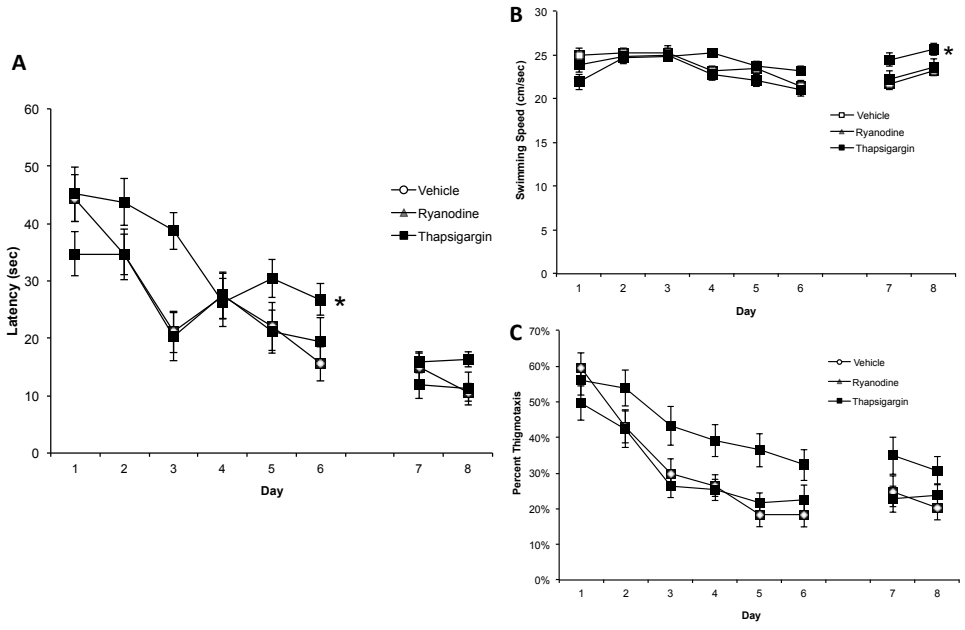

Figure 4. MWM testing in experiment 1. (A) Thapsigargin produced a significant deficit in latency to locate the hidden platform. (B) No differences were observed in speed of swimming or (C) thigmotaxis among groups. Data are expressed as the mean ± SEM. * indicates $p<.05$. Vehicle: n=7; ryanodine: n=7; thapsigargin: n=8.

Another approach to measure probe trial performance is to record annulus crossings, the number of times subjects crossed the target platform location and the analogous platform locations in the other three quadrants (see figure 5B). Vehicle-treated animals displayed a significant probe trial when annulus crossings were analyzed ($F_{3,24}$ = 6.571, $p<.01$; Tukey post-hocs revealed subjects crossed the target platform location significantly more times than the other three quadrants, $p<.05$). Both ryanodine and thapsigargin impaired probe trial annulus crossings (ryanodine: $F_{3,24} = 3.119$, $p<.05$; Tukey post-hocs showed that animals did not cross the target significantly more often than any other quadrant, $p>.05$; thapsigargin: $F_{3,28} = 1.721$, $p=.185$).

The day following the probe trial, visible platform training was conducted to assess general sensory and motor function. No significant differences were observed among groups in latency to locate the visible platform ($F_{2,85} = 1.670$, $p=.194$; figure 4A) or thigmotaxis ($F_{2,85} = 2.295$, $p=.107$; figure 4C). There were differences in speed of swimming ($F_{2,85} = 4.157$, $p<.05$; Tukey post-hocs revealed that thapsigargin produced a significant increase in swim speed during visible training versus vehicle, $p<.05$; figure 4B), but it is unlikely this difference altered performance due to the lack of difference in latency.

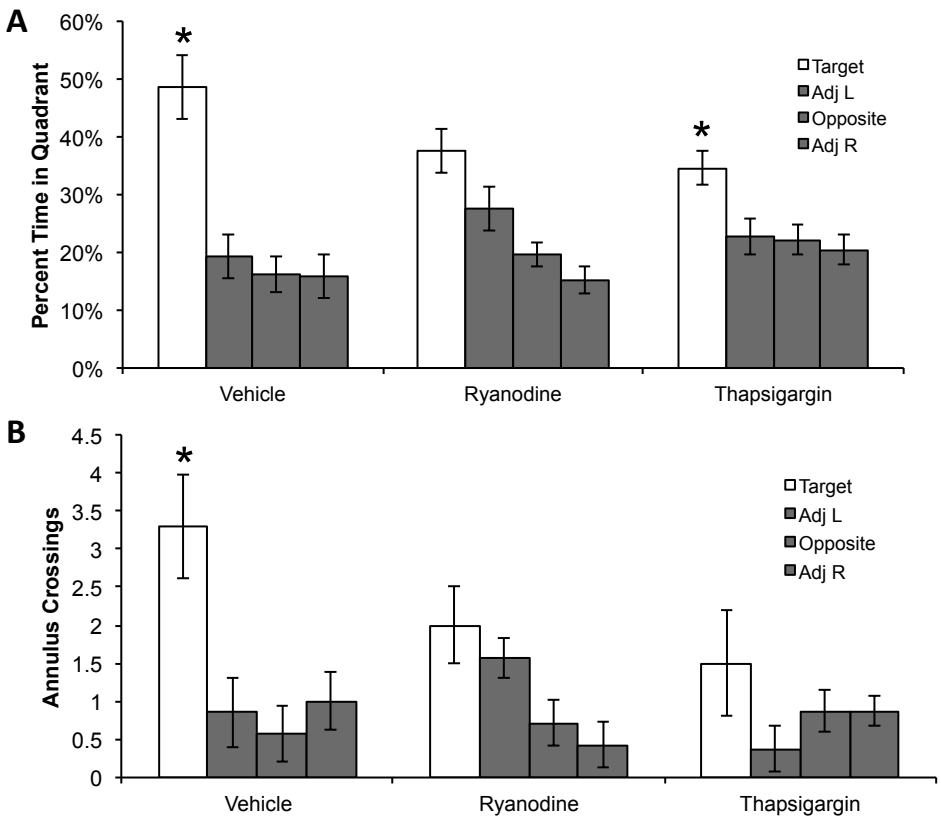

Figure 5. MWM probe trial performance in experiment 1. (A) Ryanodine-treated animals did not spend significantly more time in the target quadrant than other quadrants. (B) Only the vehicle group displayed a significant probe trial as measured by annulus crossings. Data are expressed as the mean ± SEM. * indicates $p<.05$. Vehicle: n=7; ryanodine: n=7; thapsigargin: n=8.

Protein Level Analyses

The most pathologically relevant proteins to AD are Aβ and tau, especially oAβ and ptau. To determine if inducing calcium dysregulation in the brain produced any change in AD-related proteins, we performed SDS/PAGE to examine levels of oAβ and ptau. When hippocampal tissue was examined for oAβ, it was discovered that thapsigargin produced a significant increase in the protein levels of the 18mer (18 Aβ monomers) versus vehicle ($F_{2,22} = 4.303$, $p<.05$; Tukey post-hocs revealed that

thapsigargin significantly increased 18mer levels compared to vehicle, p<.05; see figure 6).

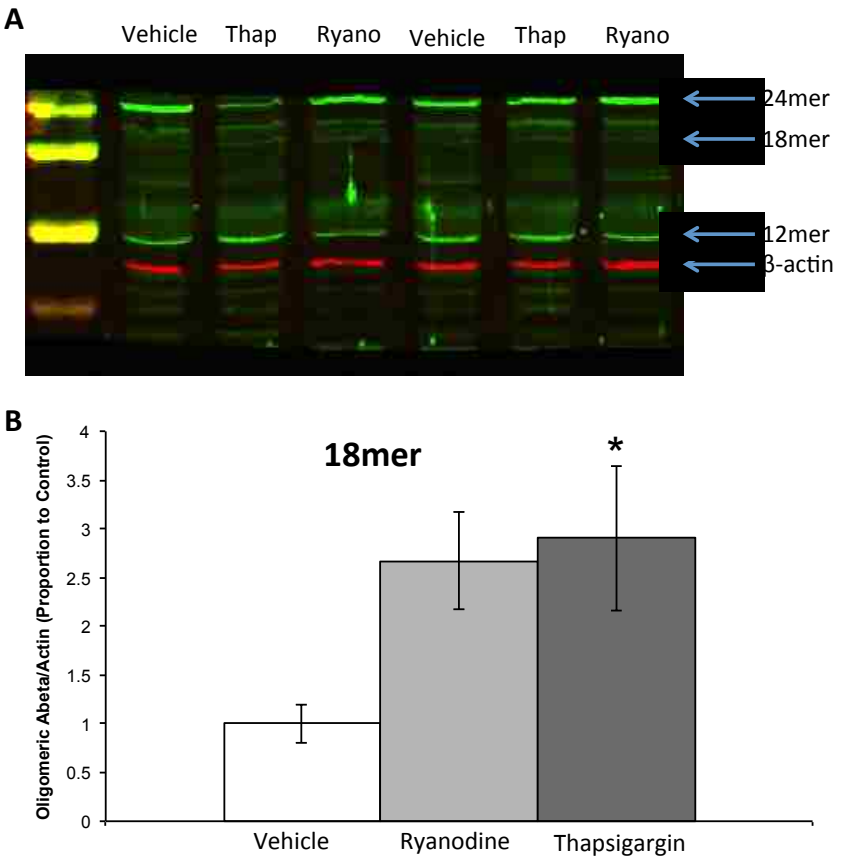

Figure 6. Oligomeric Aβ protein levels in hippocampus from experiment 1 (n=4). (A) Representative image of a membrane probed for oAβ (green) and β-actin (red). Arrows indicate specific oligomers or β-actin. (B) Thapsigargin significantly increased 18mer levels in the hippocampus compared to vehicle. Data are expressed as the mean ± SEM. * indicates p<.05.

Although thapsigargin produced an overall increase in several species of oAβ, the small group size (n=4) and large variability prohibited any other significant findings. Table 2 summarizes the non-significant findings with the other oligomers from the hippocampus.

Table 2.

*Western blot data from hippocampus in experiment 1 of Aβ oligomers with β-actin as a loading control (n=4). Specific oligomers are listed with mean ± SEM levels for ryanodine and thapsigargin, valued as proportion of control, which was set at 1. F and p values are also listed for the one-way between groups ANOVAs performed to analyzed the protein level differences among groups. Degrees of freedom were 2,22 for each ANOVA. * indicates significant ANOVA (no between group differences).*

Oligomer	Ryanodine	Thapsigargin	F value	p value
24mer	0.68 ± 0.17	0.58 ± 0.12	1.179	.326
20mer	0.84 ± 0.17	2.08 ± 0.77	2.178	.137
16mer	0.83 ± 0.43	1.51 ± 0.82	0.456	.639
12mer	0.84 ± 0.06	1.33 ± 0.21	3.129	.064
11mer	0.90 ± 0.14	1.13 ± 0.16	0.656	.529
10mer	0.65 ± 0.09	1.35 ± 0.30	3.462	.049*
9mer	0.64 ± 0.12	2.15 ± 0.80	2.887	.077
8mer	1.20 ± 0.31	1.61 ± 0.37	1.157	.333

Exploratory analyses were performed to assess if correlations existed between individual subject MWM probe trial performance and levels of specific proteins. Although there were no significant correlations for any specific oligomer when all groups were examined, there was a strong negative correlation in the thapsigargin group between probe trial performance and 24mer levels, indicating increased oAβ levels correlated with poorer performance ($F_{1,2} = 20.696$, $p<.05$; see figure 7).

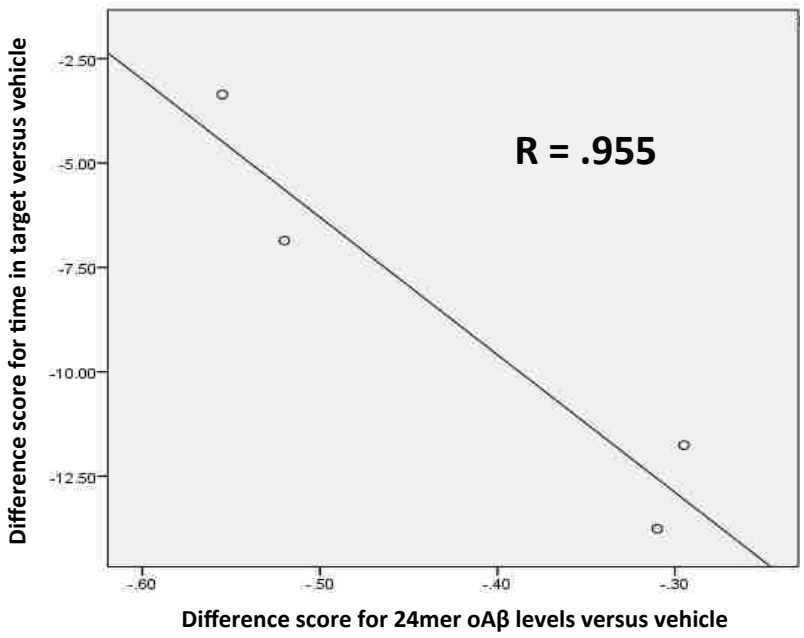

Figure 7. Correlations between probe trial performance and hippocampal oAβ levels from experiment 1 (n=4). The thapsigargin group's probe trial time in target quadrant difference score significantly correlated with 24mer oAβ levels, $p<.05$.

Tau phosphorylation was also investigated in the hippocampus following chronic calcium dysregulation, specifically at the Serine 396 phosphorylation site. Both ryanodine and thapsigargin produced a non-significant increase in tau phosphorylation compared to vehicle ($F_{2,22} = 0.764$, $p=.478$; see figure 8). Similar to many of the oAβ analyses, small group size (n=4) contributed to the lack of significant differences in this pilot study. No correlations were found between ptau levels and probe performance.

CB-D28k levels in the hippocampus were not significantly different among groups despite a large decrease following ryanodine or thapsigargin ($F_{2,22} = 2.381$, $p=.119$; see figure 9). No correlations were discovered between probe trial performance and CB-D28k levels in the hippocampus.

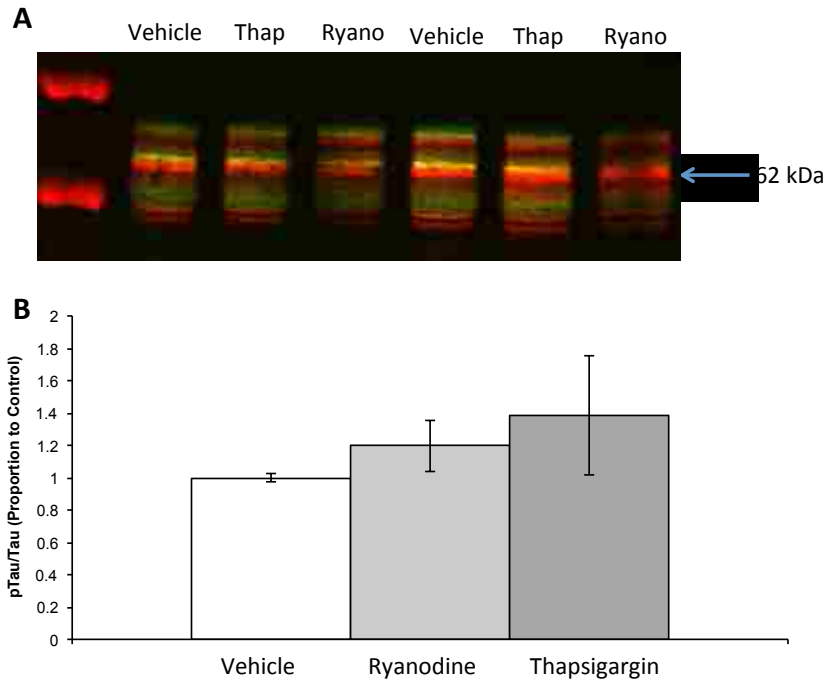

Figure 8. Ptau protein levels in hippocampus from experiment 1 (n=4). (A) Representative image of a membrane probed for tau phosphorylated at serine 396 (green) and tau (red). Arrow indicates molecular weight of one of the tau bands. (B) No significant differences were observed in ptau/tau levels despite modest increases following chronic ryanodine or thapsigargin treatment. Data are expressed as the mean ± SEM.

In the cortex, no significant differences were found in any of the oAβ species among groups (see figure 10 for representative image and table 3 for a summary of the data). Despite the lack of between-group differences in oAβ levels, strong negative correlations were observed when individual groups were examined. In the ryanodine group, a significant correlation was observed for the 24mer, similar to the hippocampus for thapsigargin ($F_{1,2} = 61.387$, $p<.05$; see figure 11). Although non-significant, strong negative correlations were observed in the thapsigargin group as well (10mer: R = .837, p=.163; 9mer: R = .717, p=.283; 7mer: R = .813, p=.187).

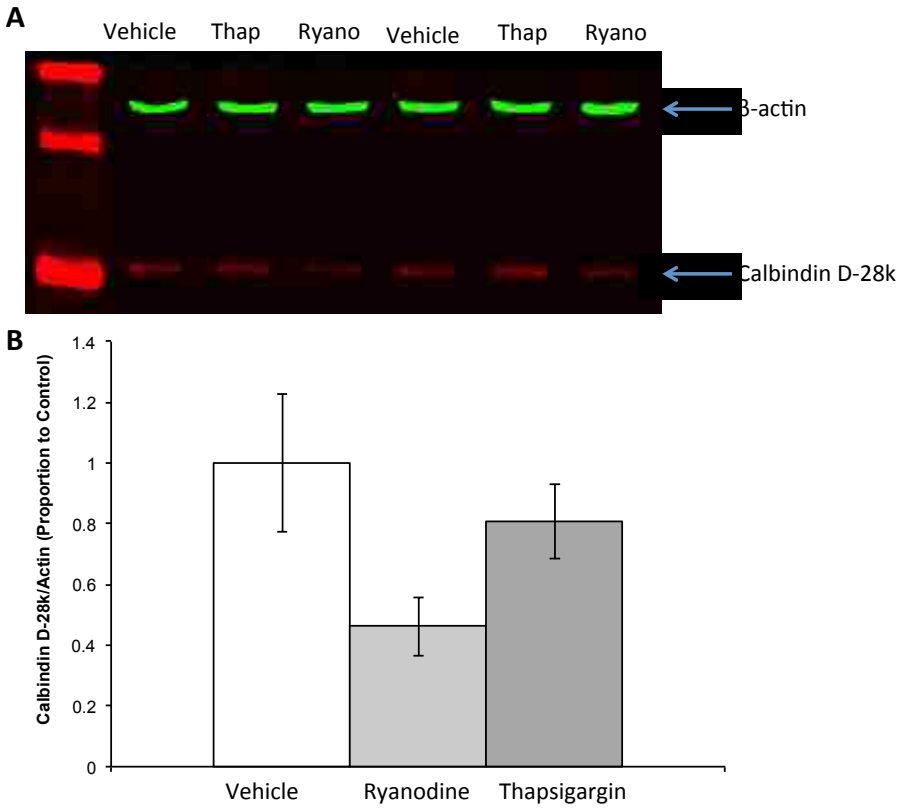

Figure 9. CB-D28k protein levels in hippocampus from experiment 1 (n=4). (A) Representative image of a membrane probed for CB-D28k (red) and β-actin (green). (B) No significant differences were observed in CB-D28k levels despite robust decreases following chronic ryanodine or thapsigargin treatment. Data are expressed as the mean ± SEM.

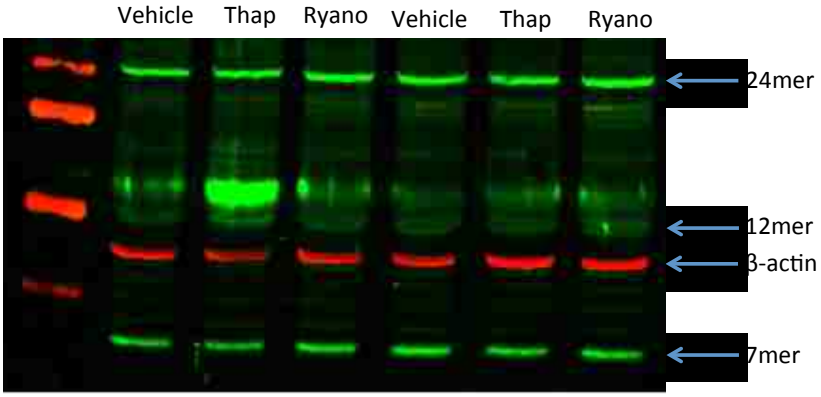

Figure 10. Oligomeric Aβ protein levels in cortex from experiment 1 (n=4). Representative image of a membrane probed for oAβ (green) and β-actin (red). Arrows indicate specific oligomers or β-actin.

Table 3.

Western blot data from cortex in experiment 1 of Aβ oligomers with β-actin as a loading control (n=4). Specific oligomers are listed with mean ± SEM levels for ryanodine and thapsigargin, valued as proportion of control, which was set at 1. F and p values are also listed for the one-way between groups ANOVAs performed to analyzed the protein level differences among groups. Degrees of freedom were 2,22 for each ANOVA.

Oligomer	Ryanodine	Thapsigargin	F value	p value
24mer	0.97 ± 0.09	0.93 ± 0.10	0.098	.907
20mer	1.06 ± 0.16	0.82 ± 0.16	0.432	.655
16mer	2.08 ± 0.79	2.92 ± 1.23	1.430	.261
12mer	1.08 ± 0.24	1.04 ± 0.14	0.044	.957
11mer	0.89 ± 0.11	0.85 ± 0.17	0.393	.680
10mer	0.81 ± 0.20	0.70 ± 0.15	0.970	.415
9mer	1.04 ± 0.17	1.06 ± 0.15	0.031	.970
8mer	1.17 ± 0.16	1.24 ± 0.22	0.549	.638
7mer	0.95 ± 0.13	0.92 ± 0.11	0.166	.848

Cortical ptau levels were also examined and similar to the hippocampus, a non-significant increase was observed following chronic ryanodine or thapsigargin administration ($F_{2,22} = 0.754$, p=.482; see figure 12). No robust correlations were found between probe trial performance and ptau levels in the cortex.

When membranes were probed for CB-D28k from the cortex, a similar but less pronounced trend to the hippocampal levels emerged with no significant differences among groups ($F_{2,22} = 1.473$, p=.251; see figure 13). No strong correlations were found between probe performance and CB-D28k levels.

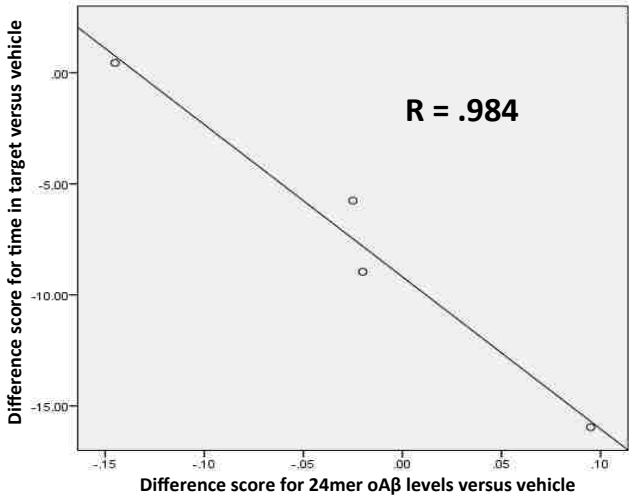

Figure 11. Correlations between probe trial performance and cortical oAβ levels from experiment 1 (n=4). The ryanodine group's probe trial time in target quadrant score significantly correlated with 24mer oAβ levels, $p<.05$.

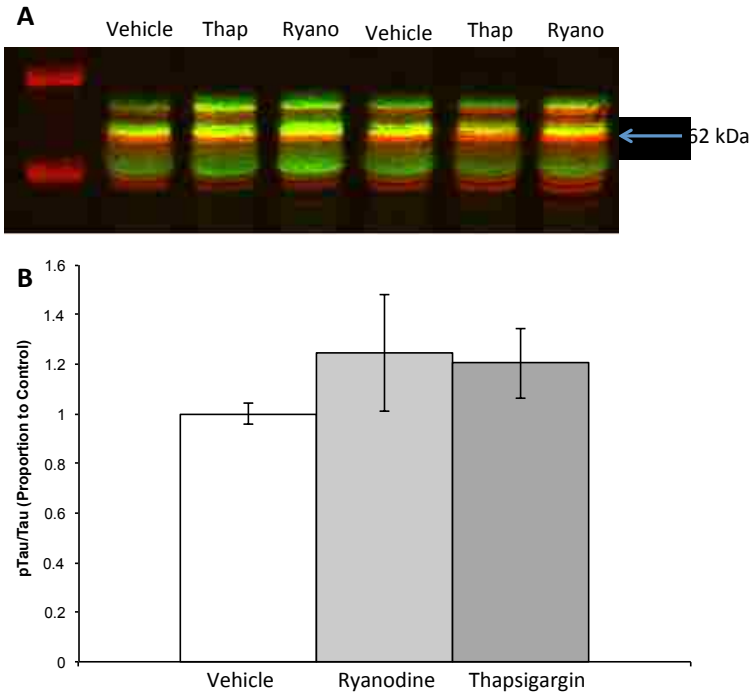

Figure 12. Ptau protein levels in cortex from experiment 1 (n=4). (A) Representative image of a membrane probed for tau phosphorylated at serine 396 (green) and tau (red). Arrow indicates molecular weight of one of the tau bands. (B) No significant differences were observed in ptau/tau levels following chronic ryanodine or thapsigargin treatment. Data are expressed as the mean ± SEM.

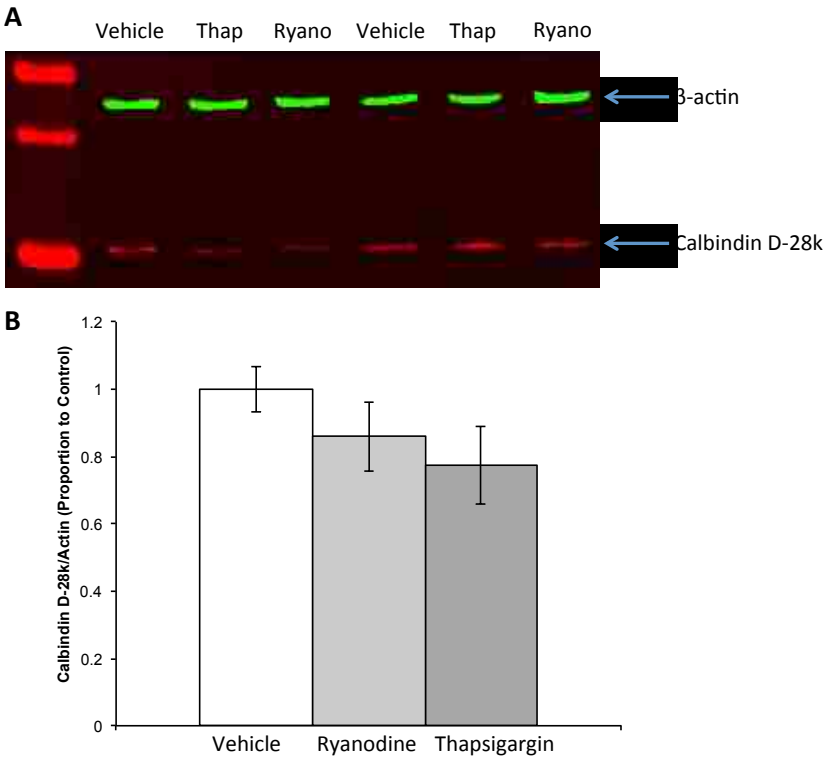

Figure 13. CB-D28k protein levels in cortex from experiment 1 (n=4). (A) Representative image of a membrane probed for CB-D28k (red) and β-actin (green). (B) No significant differences were observed in CB-D28k levels among groups. Data are expressed as the mean ± SEM.

Experiment 2

Open Field Testing

When multiple dosages of ryanodine and thapsigargin were compared, there were still no significant differences in the percent time subjects spent in the perimeter among groups ($F_{4,52} = 0.416$, p=.797; see figure 14A). There were no treatment-induced effects on locomotor activity as measured by total distance travelled ($F_{4,52} = 1.138$, p=.349; see figure 14B).

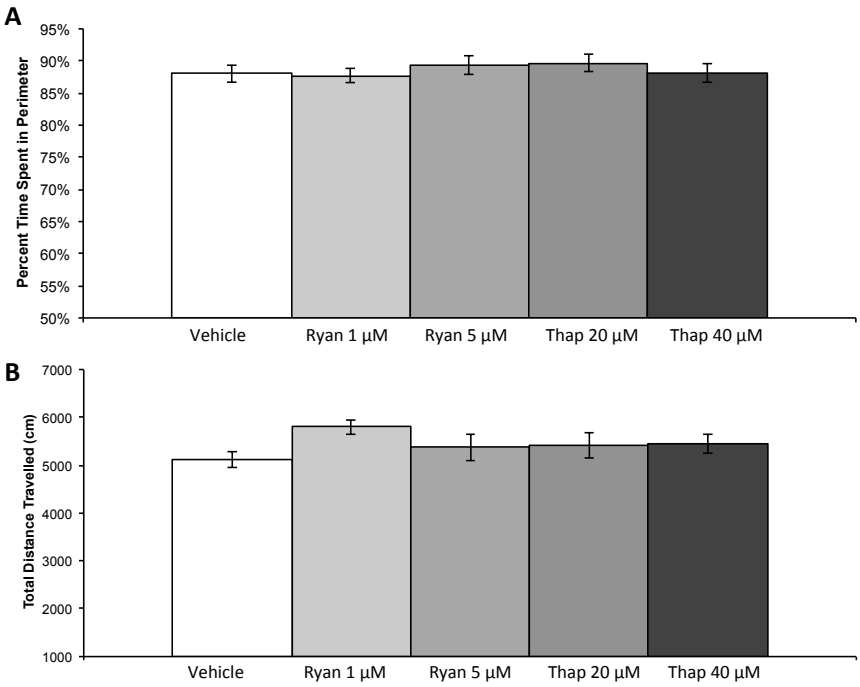

Figure 14. Open field testing in experiment 2. (A) No significant differences were found among groups in the percent time spent in the perimeter or (B) the total distance travelled. Data are expressed as the mean ± SEM. Vehicle: n=12; ryanodine at 1 µM: n=11; ryanodine at 5 µM: n=10; thapsigargin at 20 µM: n=12; thapsigargin at 40 µM: n=12.

Novel Object Recognition Testing

On the first day of NOR testing, there were no significant differences in the amount of time spent with identical objects (object A) among groups ($F_{4,52} = 1.278$, p=.291; see figure 15A). Because of the large N, no STM test could be performed in experiment 2 within the 12 hour light cycle on day 1. On day 2, LTM was assessed with a novel object (object B) being paired with object A (see figure 15B). Only the vehicle group spent significantly more time with the novel object than chance ($t_{11} = 2.256$, p<.05). Ryanodine at 1 or 5 µM and thapsigargin at 20 or 40 µM produced a learning and

memory impairment (t_{10} = 0.357, p=728, t_9 = 0.760, p=.467, t_{11} = 1.563, p=.146, and t_{11} = -0.233, p=0.820, respectively).

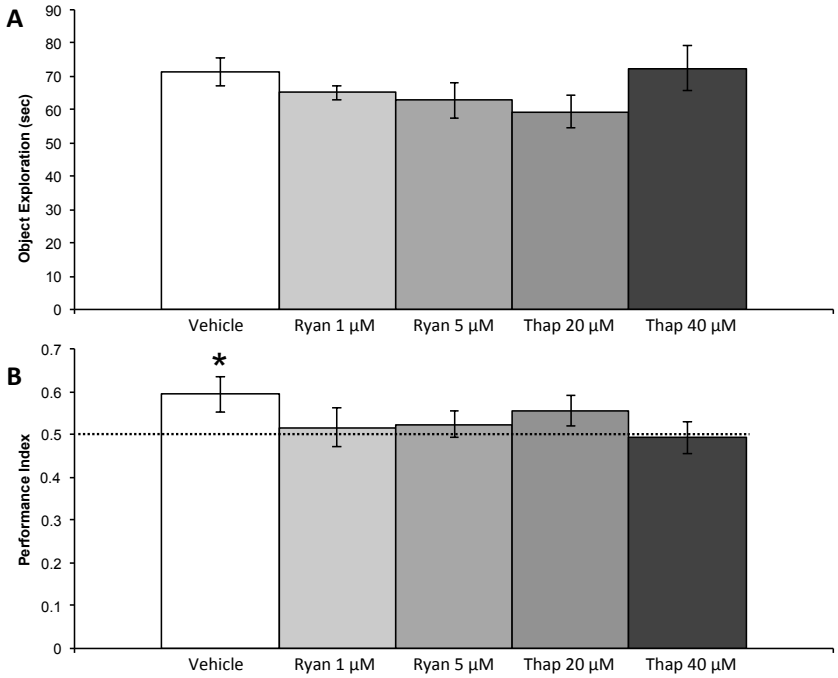

Figure 15. NOR testing in experiment 2. (A) No significant differences among groups were found in the total time spent investigating the original objects (object A). (B) Only vehicle animals displayed a significant preference for the novel object. Both doses of ryanodine and thapsigargin produced a deficit, p>.05. Data are expressed as the mean ± SEM. * indicates p<.05. Vehicle: n=12; ryanodine at 1 µM: n=11; ryanodine at 5 µM: n=10; thapsigargin at 20 µM: n=12; thapsigargin at 40 µM: n=12.

Morris Water Maze Testing

Vehicle-treated subjects only required four days to reach the criterion latency in experiment 2, for which there was a significant main effect of days ($F_{3,633}$ = 139.686, p<.01). There was no significant main effect of treatment for latency ($F_{4,211}$ = 0.368, p=.831; see figure 16A), speed of swimming ($F_{4,210}$ = 1.033, p=.391; see figure 16B), or thigmotaxis ($F_{4,210}$ = 1.370, p=.246; see figure 16C).

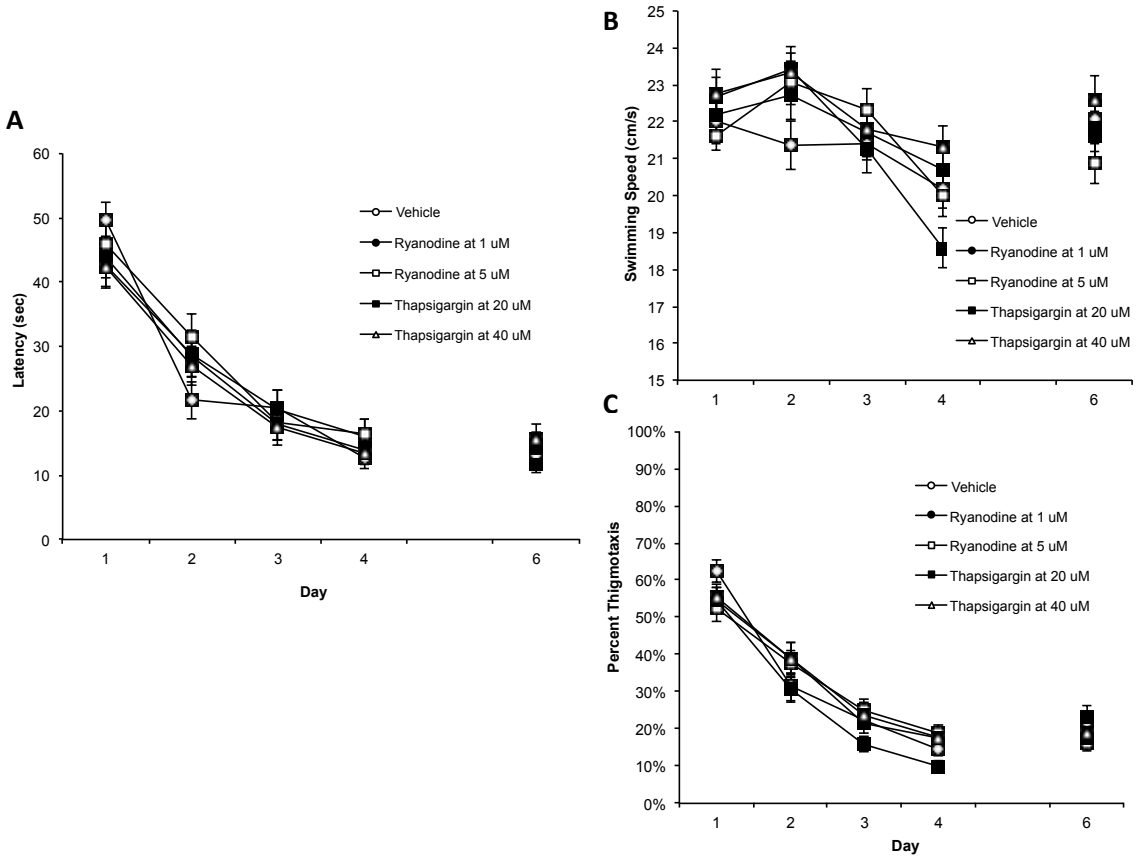

Figure 16. MWM testing in experiment 2. No differences were observed in latency to reach the hidden platform (A), speed of swimming (B), or thigmotaxis (C) among groups. Data are expressed as the mean ± SEM. Vehicle: n=11; ryanodine at 1 μM: n=10; ryanodine at 5 μM: n=10; thapsigargin at 20 μM: n=12; thapsigargin at 40 μM: n=11.

A probe trial was conducted twenty-four hours later to assess spatial learning and memory and no deficits were observed within any group in the percent time spent in the target quadrant versus non-target quadrants (vehicle: $F_{3,40} = 19.697$, $p<.01$; Tukey post-hocs target vs. non-target, $p<.01$ for all; ryanodine at 1 μM: $F_{3,36} = 9.698$, $p<.01$; Tukey post-hocs target vs. adjacent left and adjacent right, $p<.01$, and target vs. opposite, $p<.05$; ryanodine at 5 μM: $F_{3,36} = 14.783$, $p<.01$; Tukey post-hocs target vs. non-target, $p<.01$ for all; thapsigargin at 20 μM: $F_{3,44} = 5.654$, $p<.01$; Tukey post-hocs target vs. adjacent left

and opposite, p<.01, and target vs. adjacent right, p<.05; thapsigargin at 40 μM: $F_{3,40}$ = 15.972, p<.01; Tukey post-hocs target vs. non-target, p<.01 for all; see figure 17A).

When annulus crossings were examined, deficits were observed in the 5 μM ryanodine group and the 20 μM thapsigargin group (ryanodine at 5 μM: $F_{3,36}$ = 4.898, p<.01; Tukey post-hocs target vs. adjacent right and opposite, p<.05, but target vs. adjacent left, p=.198; thapsigargin at 20 μM: $F_{3,44}$ = 4.272, p<.05; Tukey post-hocs target vs. adjacent left, p<.01, but target vs. opposite and adjacent right, p=.108; see figure 17B). The other three groups each displayed significant annulus crossings during the probe trial (vehicle: $F_{3,40}$ = 4.821, p<.01; Tukey post-hocs target vs. non-target, p<.05 for all; ryanodine at 1 μM: $F_{3,36}$ = 11.242, p<.01; Tukey post-hocs target vs. non-target, p<.01 for all; thapsigargin at 40 μM: $F_{3,40}$ = 12.293, p<.01; Tukey post-hocs target vs. non-target, p<.01 for all; see figure 17B).

Following the probe trial, animals underwent one day of visible training to investigate any sensory or motor dysfunction. Similar to hidden training, no significant differences were observed among groups in latency to find the visible platform ($F_{4,207}$ = 0.528, p=.716; figure 16A), speed of swimming ($F_{4,207}$ = 1.031, p=.392; figure 16B), or thigmotaxis ($F_{4,207}$ = 1.292, p=.274; figure 16C).

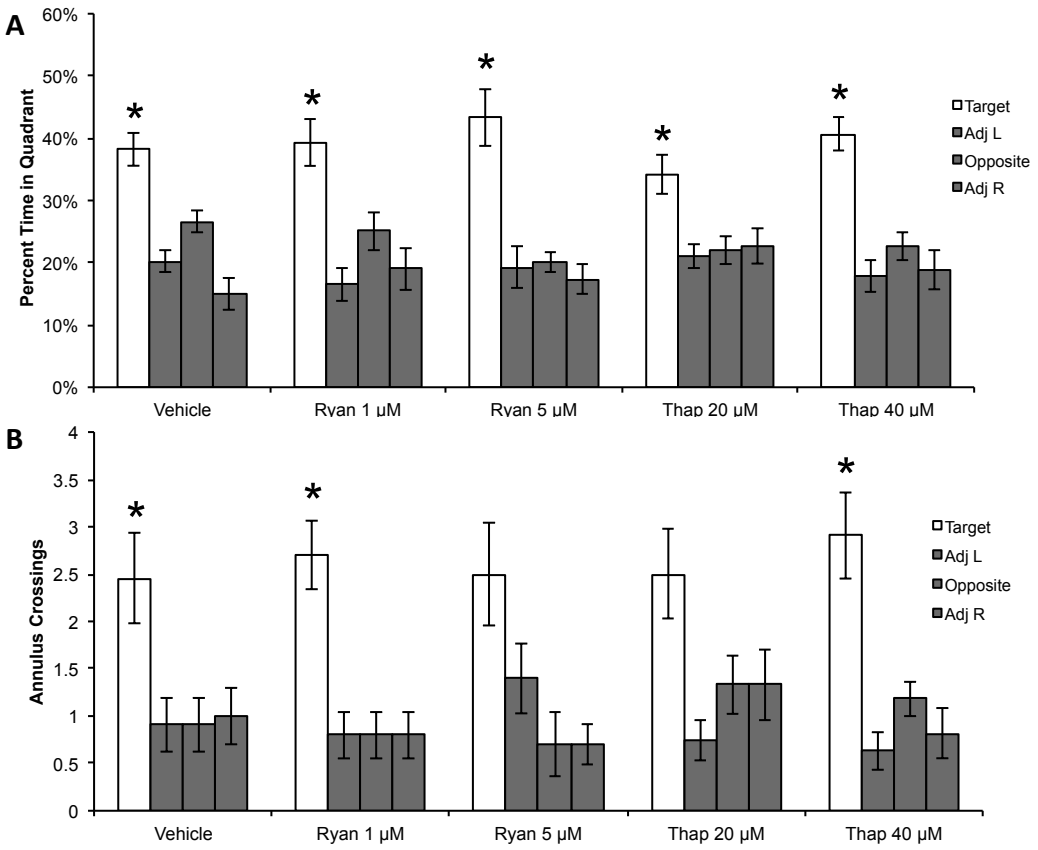

Figure 17. MWM probe trial performance in experiment 2. (A) All groups spent significantly more time in the target quadrant than the other three quadrants. (B) Ryanodine at 5 µM and thapsigargin at 20 µM each impaired probe trial performance as measured by annulus crossings. Data are expressed as the mean ± SEM. * indicates $p<.05$. Vehicle: n=11; ryanodine at 1 µM: n=10; ryanodine at 5 µM: n=10; thapsigargin at 20 µM: n=12; thapsigargin at 40 µM: n=11.

Protein Level Analyses

Hippocampal tissue from rats in experiment 2 was probed for oAβ or ptau, consistent with experiment 1. No significant differences were found in any of the oAβ species among groups following chronic ryanodine or thapsigargin, contrary to experiment 1 (see figure 18 and table 4 for representative images and comprehensive results, respectively). Correlational analyses were performed for all subjects as well as for

individual groups to investigate the relationship between probe trial performance and oAβ levels. The only strong correlations were discovered in the 40 μM thapsigargin group, suggesting poor probe trial performance in this group was related to increased oAβ levels, although none reached significance (10mer: R = .752, p=.143; 9mer: R = .724, p=.167; 8mer: R = .765, p=.132; 7mer: R = .652, p=.233).

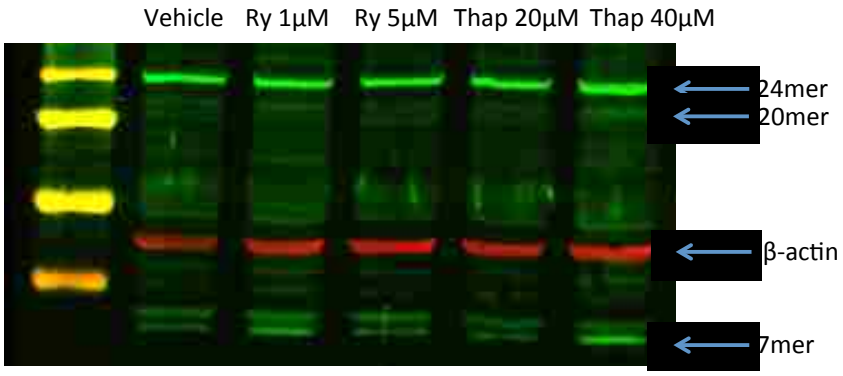

Figure 18. Oligomeric Aβ protein levels in hippocampus from experiment 2 (n=5). Representative image of a membrane probed for oAβ (green) and β-actin (red). Arrows indicate specific oligomers or β-actin. No significant differences were observed in any oAβ species among groups.

Tau phosphorylation was also examined in the hippocampus in experiment 2. Although the lower dosage of ryanodine produced an increase in ptau, no significant differences were observed among groups ($F_{4,48}$ = 1.809, p=.142; see figure 19). Interestingly, a strong negative correlation was observed in the 40 μM thapsigargin group between probe performance and ptau levels, but it did not reach significance (R = .704, p=.185).

Similar to the other proteins, no significant differences were observed among groups in CB-D28k levels in the hippocampus ($F_{4,47}$ = 3.041, p<.05; Tukey post-hocs did

not reveal any significant differences among groups, p>.05; see figure 20). Based on the lack of MWM deficits and the minimal differences observed in protein levels, no further assays were conducted in experiment 2 to conserve resources.

Table 4.

Western blot data from experiment 2 of Aβ oligomers with β-actin as a loading control (n=5). Specific oligomers are listed with mean ± SEM levels for each group, valued as proportion of control, which was set at 1. F and p values are also listed for the one-way between groups ANOVAs performed to analyzed the protein level differences among groups. Degrees of freedom were 4,47 for each ANOVA.

Oligomer	Ryan 1μM	Ryan 5μM	Thap 20μM	Thap 40μM	F value	p value
24mer	1.08 ± 0.09	0.99 ± 0.08	1.04 ± 0.10	1.00 ± 0.05	0.265	.899
20mer	1.42 ± 0.17	1.13 ± 0.09	1.43 ± 0.23	1.24 ± 0.17	1.583	.194
16mer	1.17 ± 0.21	0.89 ± 0.11	1.01 ± 0.15	1.08 ± 0.12	0.348	.844
12mer	1.33 ± 0.30	1.04 ± 0.21	1.27 ± 0.31	1.23 ± 0.34	0.328	.858
10mer	1.08 ± 0.13	1.01 ± 0.16	1.07 ± 0.12	1.06 ± 0.10	0.108	.979
9mer	1.09 ± 0.21	0.78 ± 0.10	1.22 ± 0.29	1.22 ± 0.23	0.877	.485
8mer	1.07 ± 0.16	1.07 ± 0.10	1.21 ± 0.14	1.02 ± 0.12	0.511	.728
7mer	1.28 ± 0.19	1.05 ± 0.20	1.06 ± 0.19	1.57 ± 0.15	1.880	.130

Experiment 3

Effects of LPS on Temperature and Weight

Temperatures and weights were recorded immediately prior to and for three days after the one-time administration of LPS. These measures were analyzed by group and by LPS versus saline treatments. At baseline, no significant differences were observed in

temperature by treatment (LPS vs. saline; $F_{1,35} = 0.758$, p=.390) or by group (vehicle, LPS, thapsigargin, and Thap+LPS; $F_{3,33} = 0.245$, p=.865). Temperature was then recorded at 24, 48, and 72 hours post-injection to assess whether LPS produced fever. As figure 21A indicates, repeated measures ANOVA revealed that LPS produced a robust increase in temperature across days ($F_{2,70} = 7.348$, p<.01) and versus saline ($F_{1,35} =$ 24.675, p<.01). When examined by group, the data were similar across days ($F_{2,70} =$ 7.172, p<.01) and by group ($F_{3,33} = 8.542$, p<.05; Tukey post-hocs revealed that both the LPS and Thap+LPS groups displayed significantly increased temperatures compared to vehicle, p<.01 for LPS and p<.05 for Thap+LPS; see figure 21B).

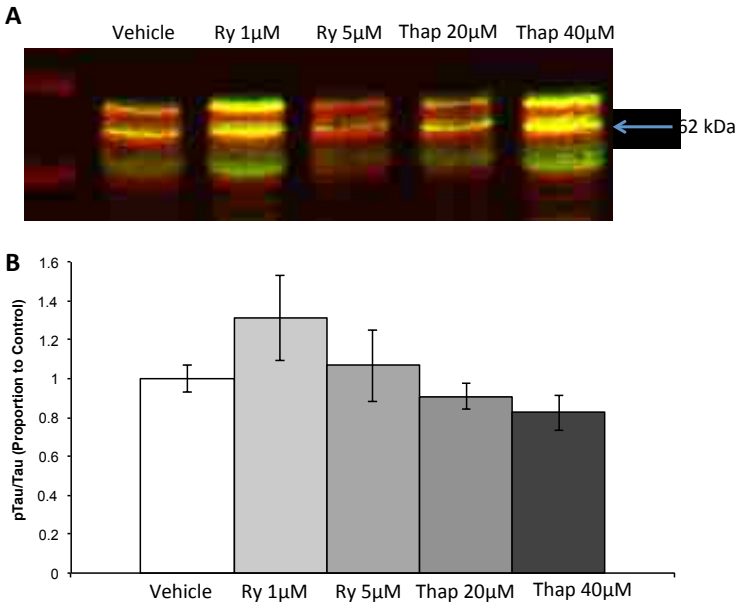

Figure 19. Ptau protein levels in hippocampus from experiment 2 (n=5). (A) Representative image of a membrane probed for tau phosphorylated at serine 396 (green) and tau (red). Yellow indicates overlapping molecular weights. Arrow indicates molecular weight of one of the tau bands. (B) No significant differences were observed in ptau/tau levels. Data are expressed as the mean ± SEM.

At baseline, no differences in weight were found by treatment ($F_{1,35}$ = 1.145, p=.292) or by group ($F_{3,33}$ = 1.319, p=.285). However, when weights were examined at the same time points as temperature, LPS produced a significant decrease in weight across days ($F_{2,70}$ = 9.440, p<.01) and versus saline ($F_{1,35}$ = 6.567, p<.05; see figure 22A). When analyzed by group, data were similar across days ($F_{2,70}$ = 9.001, p<.01) but no differences were observed among groups ($F_{3,33}$ = 2.976, p<.05; Tukey post-hocs did not show any differences among groups; figure 22B).

These data demonstrated that LPS did induce an acute immune response as indicated by the significant increase in body temperature and significant reduction in weight. These effects were temporary as both temperature and weight levels were no longer significant versus controls 72 hours following injection.

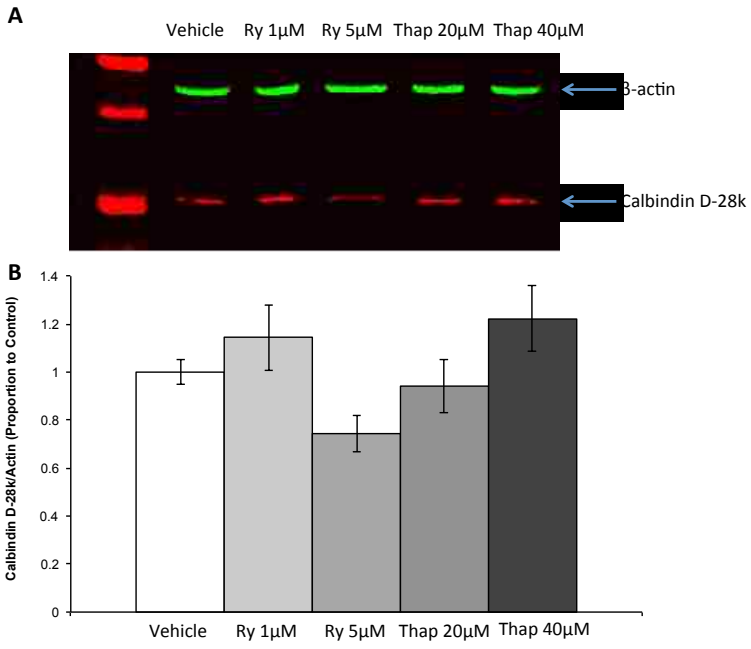

Figure 20. CB-D28k protein levels in hippocampus from experiment 2 (n=5). (A) Representative image of a membrane probed for CB-D28k (red) and β-actin (green). (B) No significant differences were observed in CB-D28k levels among groups. Data are expressed as the mean ± SEM.

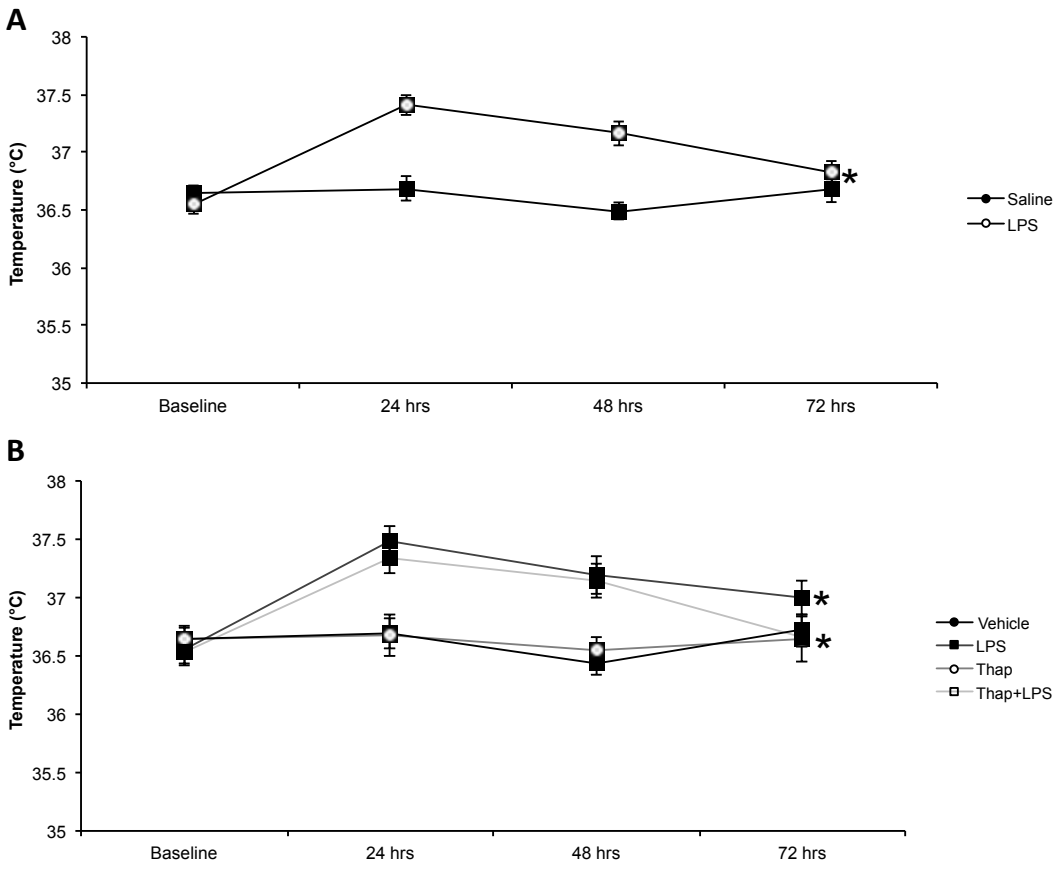

Figure 21. Temperature data at baseline and at multiple time points following LPS or saline injections. (A) LPS injection significantly increased body temperature regardless of group when compared to animals injected with saline, $p<.01$. (B) When compared to vehicle, the LPS alone and Thap+LPS groups displayed significantly elevated temperatures following LPS injection, $p<.01$ for LPS and $p<.05$ for Thap+LPS. Data are expressed as the mean ± standard error of the mean (SEM). Vehicle: n=10; LPS: n=9; thapsigargin: n=9; thap+LPS: n=9.

Open Field Testing

Neither LPS nor the combination of thapsigargin and LPS altered open field performance from experiments 1 and 2. No differences were observed in the percent time spent in the perimeter among groups ($F_{3,32} = 0.278$, $p=.841$; see figure 23A) nor in the total distance travelled ($F_{3,32} = 1.216$, $p=.320$; see figure 23B). Collectively, these studies suggest that none of the individual ligands administered, nor the combination of

thapsigargin and LPS, produced anxiogenic effects or impaired gross locomotor abilities. Therefore, any deficits observed in NOR or MWM tasks can be attributed to hippocampally-mediated learning and memory impairments.

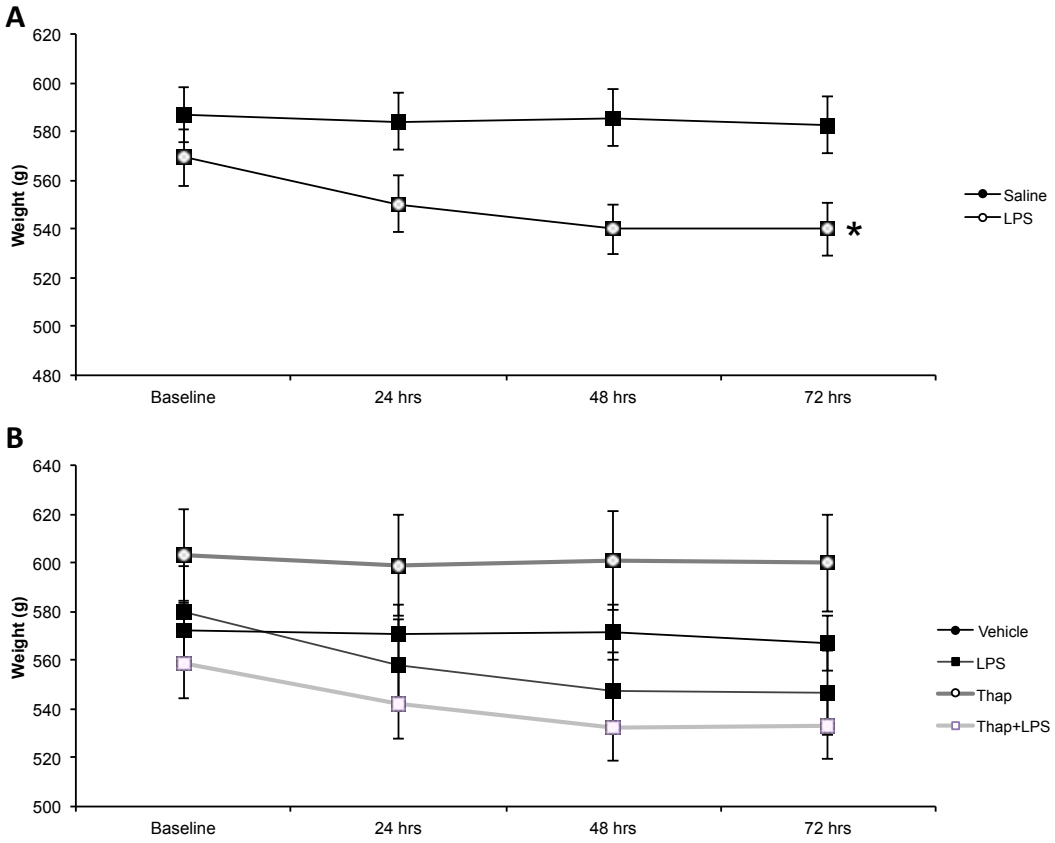

Figure 22. Analysis of weights at baseline and at multiple time points following LPS or saline injections. (A) LPS injection significantly decreased body weight regardless of group when compared to animals injected with saline, $p<.05$. (B) No significant differences were observed in weight across days when all groups were compared. Data are expressed as the mean ± SEM. Vehicle: n=10; LPS: n=9; thapsigargin: n=9; thap+LPS: n=9.

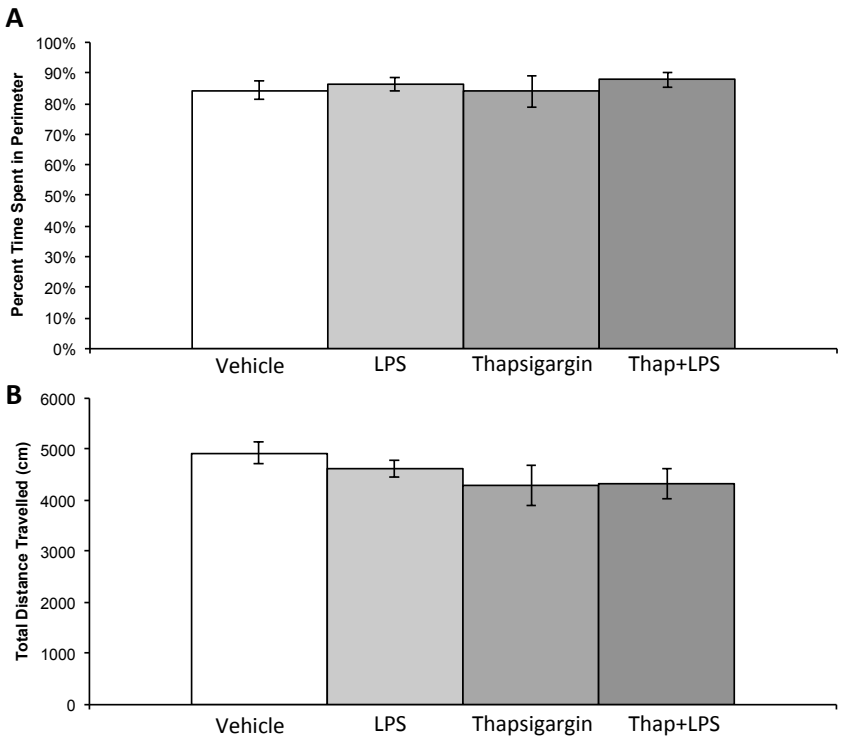

Figure 23. Open field testing in experiment 3. (A) No significant differences were found among groups in the percent time spent in the perimeter or (B) the total distance travelled. Data are expressed as the mean ± SEM. Vehicle: n=10; LPS: n=9; thapsigargin: n=8; thap+LPS: n=9.

Novel Object Recognition Testing

Similar to experiments 1 and 2, no differences in object exploration were observed on day 1 among groups ($F_{3,32} = 0.559$, p=.646; see figure 24A). In the LTM test on day 2 when a novel object was presented (see figure 24B), none of the groups exhibited a significant preference for the novel object (vehicle: $t_9 = -0.815$, p=.436; LPS: $t_8 = 1.084$, p=.310; thapsigargin: $t_7 = 2.036$, p=.081; thap+LPS: $t_8 = 0.232$, p=.822). The lack of any group displaying preference for the novel object may be due to the advanced age of the rats.

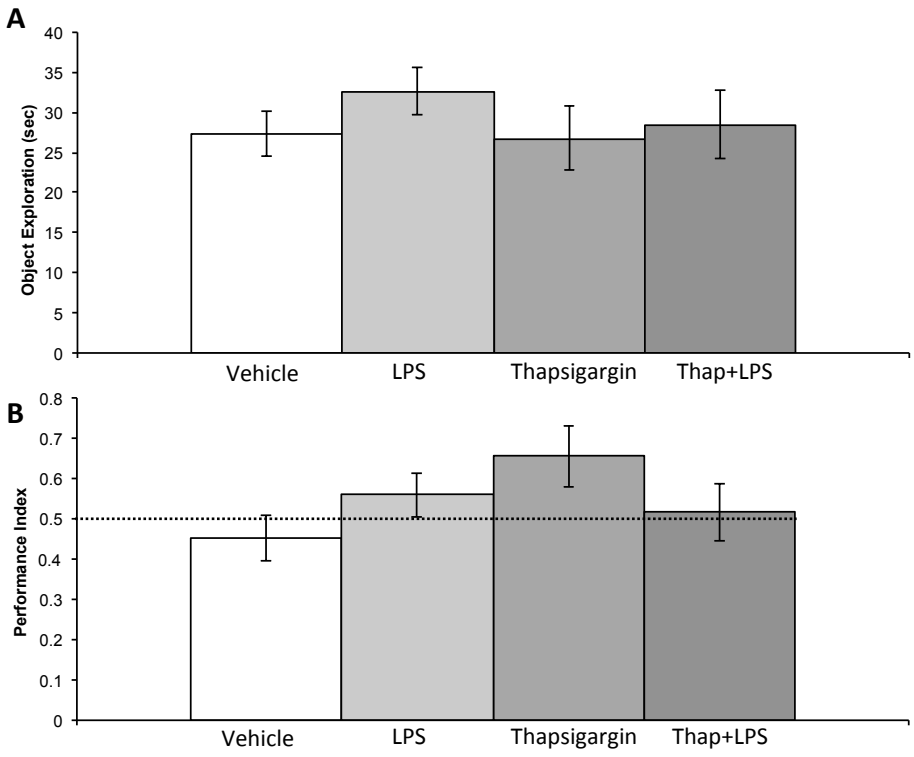

Figure 24. NOR testing in experiment 3. (A) No significant differences among groups were found in the total time spent investigating the original objects. (B) None of the groups displayed a significant preference for the novel object compared to chance levels, $p>.05$. Data are expressed as the mean ± SEM. Vehicle: n=10; LPS: n=9; thapsigargin: n=8; thap+LPS: n=9.

Morris Water Maze Testing

In experiment 3, vehicle-treated animals needed six days to achieve the criterion latency. There was a significant main effect of days ($F_{5,700} = 83.882$, $p<.01$) but no significant main effect of treatment ($F_{3,140} = 0.760$, $p=.518$; see figure 25A). Similarly, no differences among groups were observed in speed of swimming ($F_{3,139} = 0.290$, $p=.832$; see figure 25B) or thigmotaxis ($F_{3,139} = 0.305$, $p=.822$; see figure 25C).

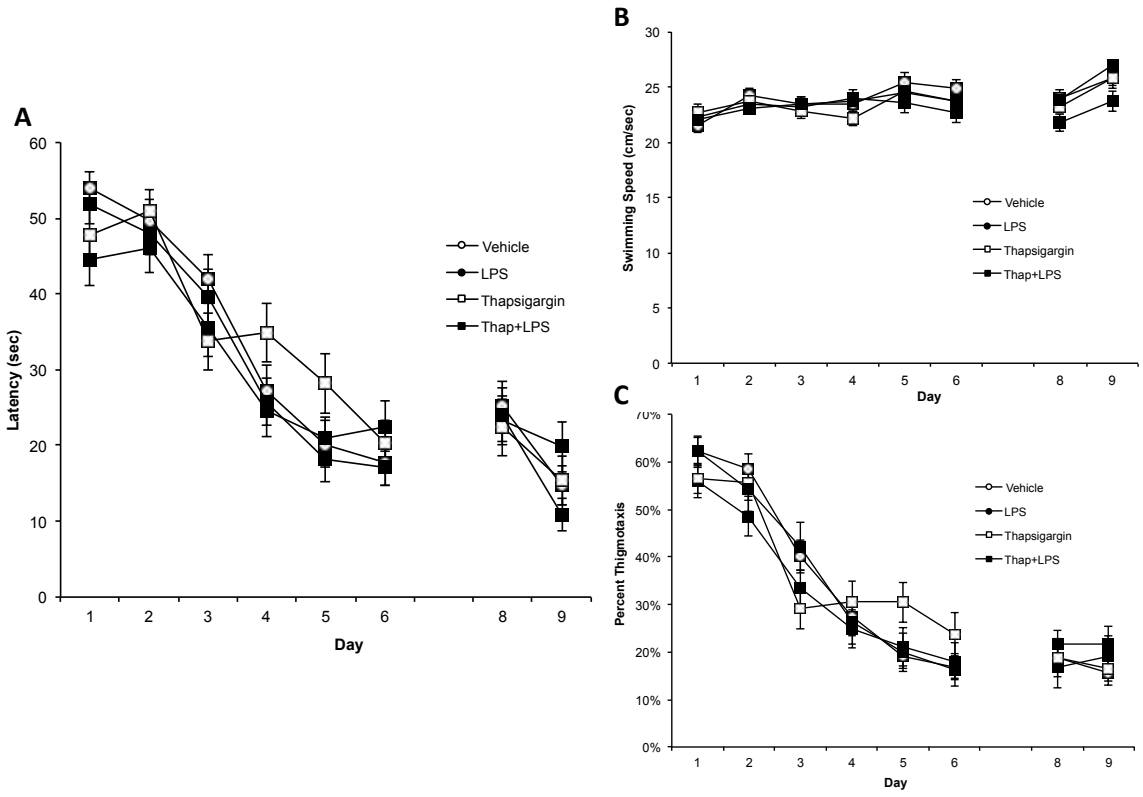

Figure 25. MWM testing in experiment 3. No differences were observed in latency to reach the hidden platform (A), speed of swimming (B), or thigmotaxis (C) among groups. Data are expressed as the mean ± SEM. Vehicle: n=10; LPS: n=9; thapsigargin: n=8; thap+LPS: n=9.

A probe trial was conducted twenty-four hours following achievement of latency criterion (see figure 26). The combination of thapsigargin and LPS produced a subtle, but significant impairment in probe trial performance as measured by percent time spent in each quadrant ($F_{3,32} = 5.679$, $p<.01$; Tukey post-hocs target vs. opposite, $p<.01$, and target vs. adjacent left, $p<.05$, but target vs. adjacent right, $p=.053$; figure 26A). The other three groups displayed a selective search based on time spent in target compared to other quadrants (vehicle: $F_{3,36} = 20.580$, $p<.01$; Tukey post-hocs target $p<.01$ vs. all other quadrants; LPS: $F_{3,32} = 7.010$, $p<.01$; Tukey post-hocs target vs. adjacent left and right,

p<.05, target vs. opposite, p<.01; thapsigargin: $F_{3,28}$ = 11.113, p<.01; Tukey post-hocs target p<.01 vs. all other quadrants; see figure 26A).

Annulus crossings data revealed that the LPS and thapsigargin groups each displayed deficits (LPS: $F_{3,32}$ = 2.629, p=.067; thapsigargin: $F_{3,28}$ = 5.194, p<.01; Tukey post-hocs target vs. adjacent left, p=.059, target vs. opposite, p<.05, and target vs. adjacent right, p<.01; see figure 26B). Vehicle-treated rats crossed the previous platform location significantly more often than non-target quadrants ($F_{3,36}$ = 11.760, p<.01; Tukey post-hocs target p<.01 vs. all other quadrants; figure 26B). Despite not displaying a selective search based on percent time in quadrant, the group administered thapsigargin and LPS did show significance based on annulus crossings ($F_{3,32}$ = 7.435, p<.01; Tukey post-hocs target vs. adjacent left and right, p<.05, target vs. opposite, p<.01; figure 26B).

Following the probe trial, two days of visible platform training were performed to assess visuomotor abilities. Similar to hidden platform training, no significant differences were found among groups in latency ($F_{3,140}$ = 0.456, p=713; see figure 25A), speed of swimming ($F_{3,140}$ = 2.835, p<.05; Tukey post-hocs showed that p>.05 for each group vs. vehicle; see figure 25B), or thigmotaxis ($F_{3,140}$ = 0.423, p=.737; see figure 25C).

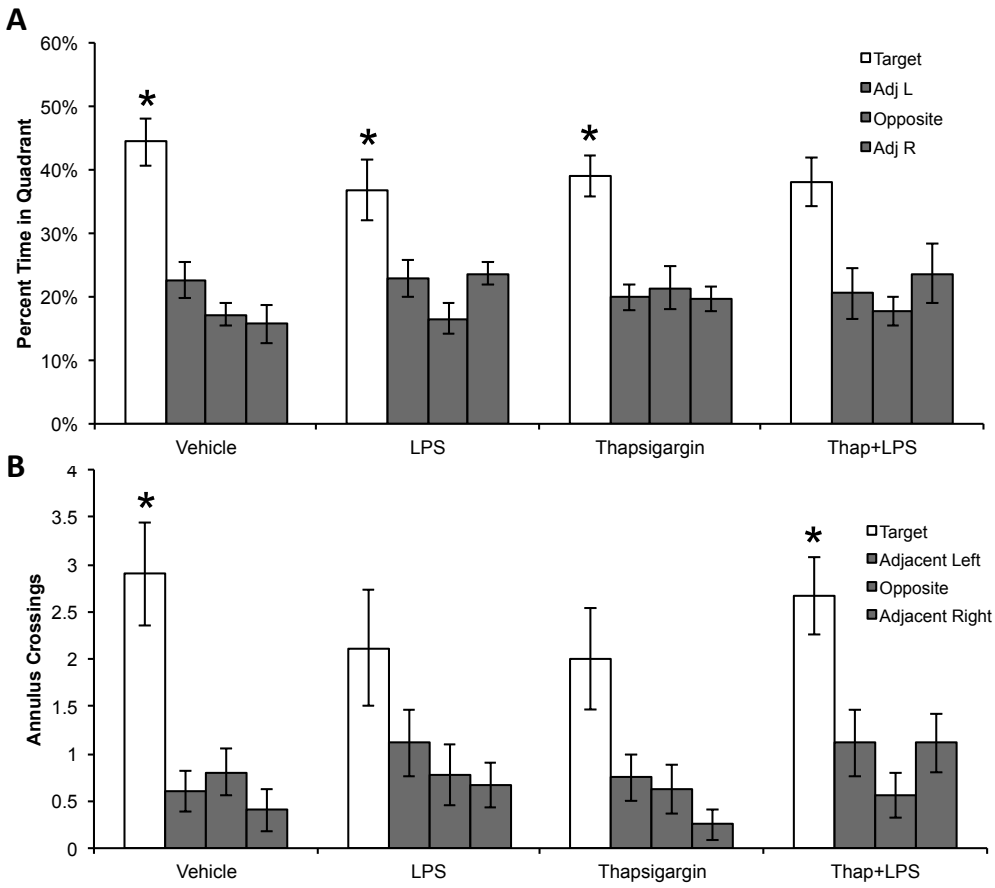

Figure 26. MWM probe trial performance in experiment 3. (A) The combination of thapsigargin and LPS produced a deficit in probe trial percent time in target versus non-target quadrants. (B) LPS and thapsigargin each impaired probe trial performance as measured by annulus crossings. Data are expressed as the mean ± SEM. * indicates $p<.05$. Vehicle: n=10; LPS: n=9; thapsigargin: n=8; thap+LPS: n=9.

Protein Level Analyses

Hippocampal tissue from rats in experiment 3 was probed for oAβ, similar to the previous studies. Following the administration of LPS and/or thapsigargin, there was a significant reduction in the 18mer in the thap+LPS group ($F_{3,47} = 3.879$, $p<.05$; Tukey post-hocs revealed that the combination of thapsigargin and LPS significantly reduced 18mer Aβ levels compared to vehicle, $p<.05$; see figure 27). No significant differences were observed in any other oligomeric species; these data are summarized in table 5.

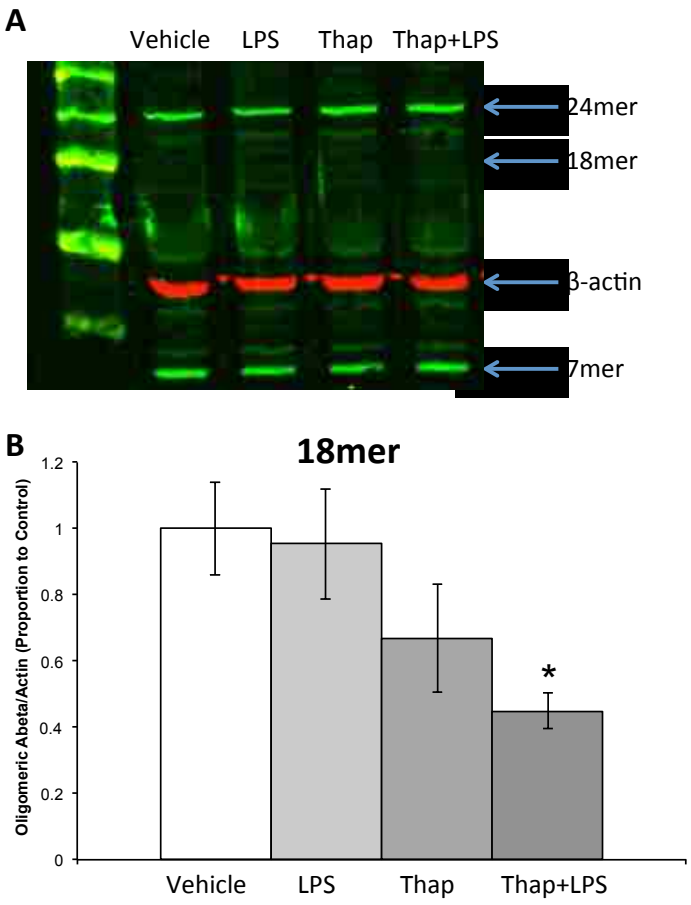

Figure 27. Oligomeric Aβ protein levels in hippocampus from experiment 3 (n=6). (A) Representative image of a membrane probed for oAβ (green) and β-actin (red). Arrows indicate specific oligomers or β-actin. (B) Thapsigargin plus LPS significantly decreased 18mer levels in the hippocampus compared to vehicle. Data are expressed as the mean ± SEM. * indicates $p<.05$.

Correlational analyses were performed with hippocampal oAβ levels and probe trial performance. Significant negative correlations were discovered when all groups were examined versus vehicle at the 10mer ($F_{1,16} = 4.565$, $p<.05$; see figure 28A) and 8mer ($F_{1,16} = 6.567$, $p<.05$; see figure 28B) oligomers while non-significant correlations were found in others (16mer: R = .451, p=.060; 11mer: R = .346, p=.159; 9mer: R = .324, p=.190; 7mer: R = .389, p=.111). When individual groups were examined, significant

correlations were observed in the thap+LPS group in 11mer levels ($F_{1,4}$ = 16.182, p<.05; see figure 29A) and 7mer levels ($F_{1,4}$ = 8,526, p<.05; see figure 29B). Strong, but non-significant negative correlations were also found in this group (10mer: R = .737, p=.094; 9mer: R = .770, p=.073; 8mer: R = .749, p=.086) and the thapsigargin group (16mer: R = .648, p=.164; 8mer: R = .644; p=.168).

Table 5.

Western blot data from hippocampus in experiment 3 of Aβ oligomers with β-actin as a loading control (n=6). Specific oligomers are listed with mean ± SEM levels for each group, valued as proportion of control, which was set at 1. F and p values are also listed for the one-way between groups ANOVAs performed to analyzed the protein level differences among groups. Degrees of freedom were 3,47 for each ANOVA.

Oligomer	LPS	Thapsigargin	Thap+LPS	F value	p value
24mer	0.90 ± 0.08	0.78 ± 0.09	0.87 ± 0.10	1.111	.354
20mer	0.99 ± 0.12	0.87 ± 0.14	0.93 ± 0.10	0.340	.796
19mer	1.82 ± 0.67	1.14 ± 0.24	1.39 ± 0.58	0.547	.652
16mer	1.11 ± 0.20	1.01 ± 0.18	1.14 ± 0.18	0.162	.921
12mer	1.19 ± 0.16	1.12 ± 0.23	0.71 ± 0.08	2.227	.098
11mer	0.89 ± 0.05	0.80 ± 0.08	0.70 ± 0.10	2.668	.058
10mer	0.93 ± 0.11	0.88 ± 0.10	0.94 ± 0.18	0.161	.922
9mer	0.93 ± 0.10	0.81 ± 0.18	0.67 ± 0.11	1.207	.318
8mer	0.90 ± 0.10	0.91 ± 0.09	0.92 ± 0.09	0.280	.839
7mer	0.96 ± 0.09	0.89 ± 0.09	0.91 ± 0.08	0.366	.778

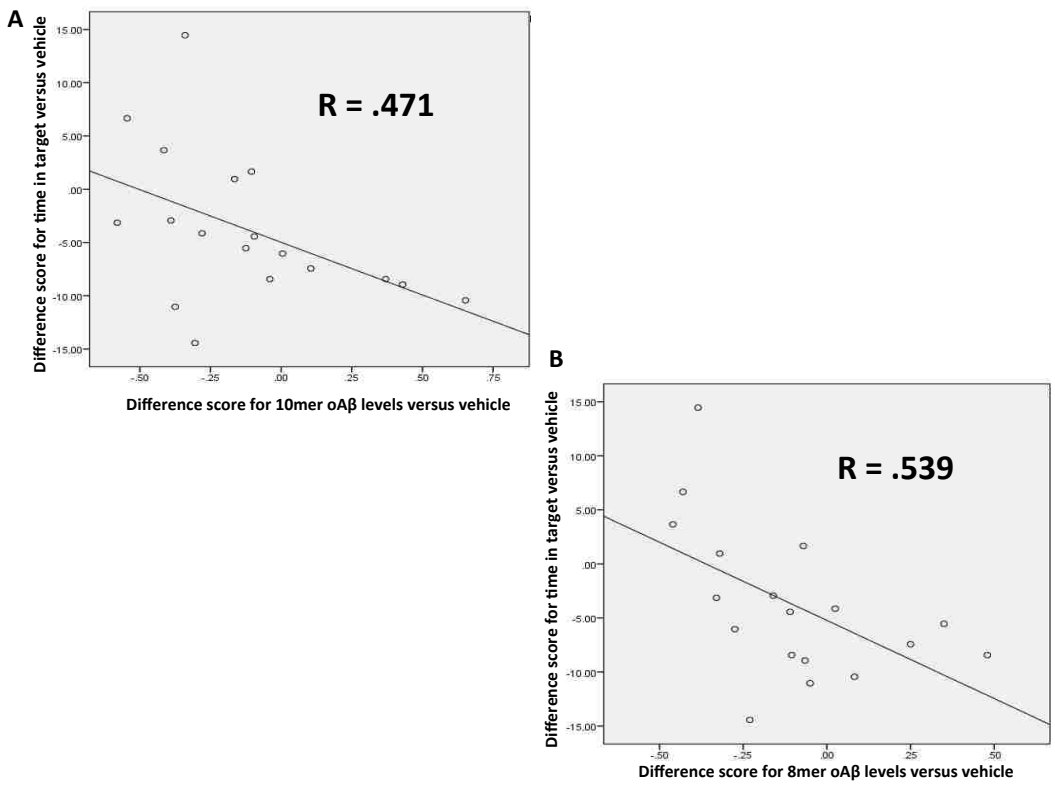

Figure 28. Correlations between probe trial performance and hippocampal oAβ levels from experiment 3 (n=6). When all subjects were examined, significant correlations were found between probe trial time in target quadrant and 10mer oAβ levels (A) and 8mer levels (B), $p<.05$.

When ptau levels were examined in the hippocampus, no significant differences were found among groups despite a modest increase in the thap+LPS group ($F_{3,44}$ = 1.144, p=.342; see figure 30). No correlations were found between probe trial performance and levels of ptau in the hippocampus.

To confirm any differences in ptau were not due altered levels of endogenous tau proteins, levels of tau were also examined in the hippocampus. As expected, no differences were observed among the groups in tau levels ($F_{3,44}$ = 0.297, p=.827; see figure 31).

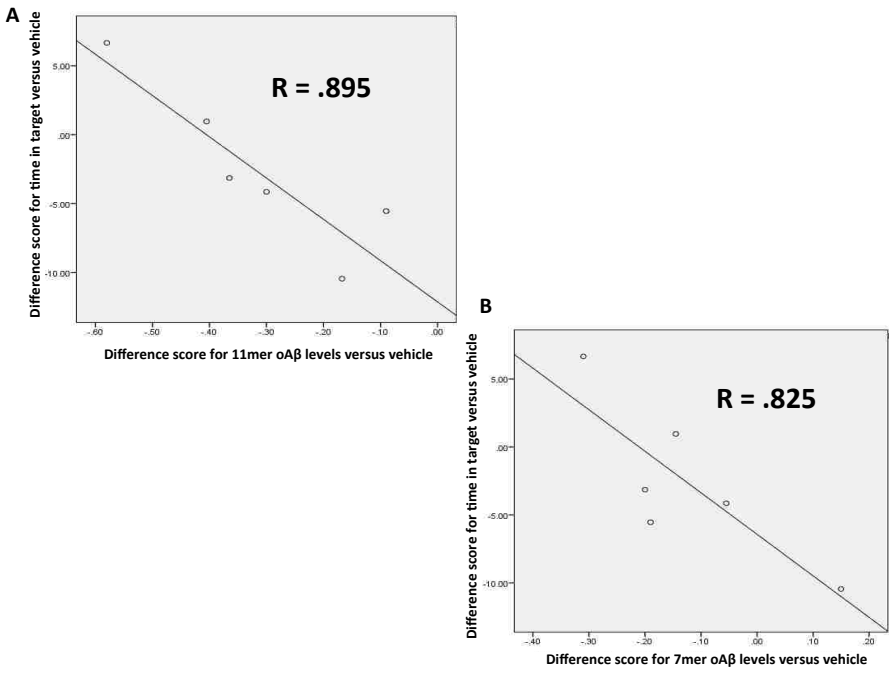

Figure 29. Correlations between thap+LPS group probe trial performance and hippocampal oAβ levels from experiment 3 (n=6). In the thap+LPS group, significant correlations were found between probe trial time in target quadrant and 11mer oAβ levels (A) and 7mer levels (B), $p<.05$.

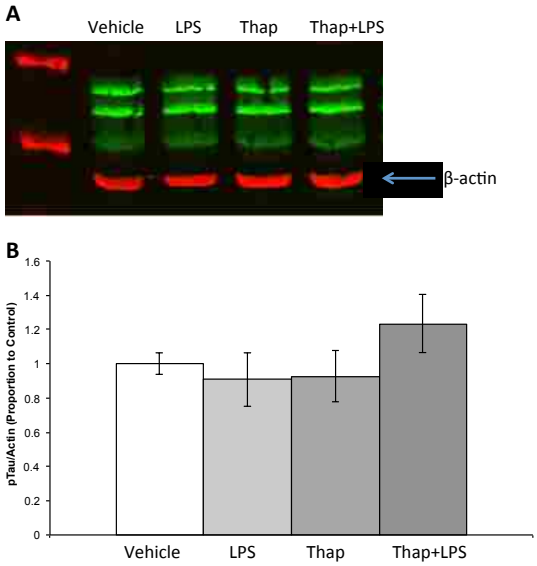

Figure 30. Ptau protein levels in hippocampus from experiment 3 (n=6). (A) Representative image of a membrane probed for tau phosphorylated at serine 396 (green) and β-actin (red). (B) No significant differences were observed in ptau levels among groups. Data are expressed as the mean ± SEM.

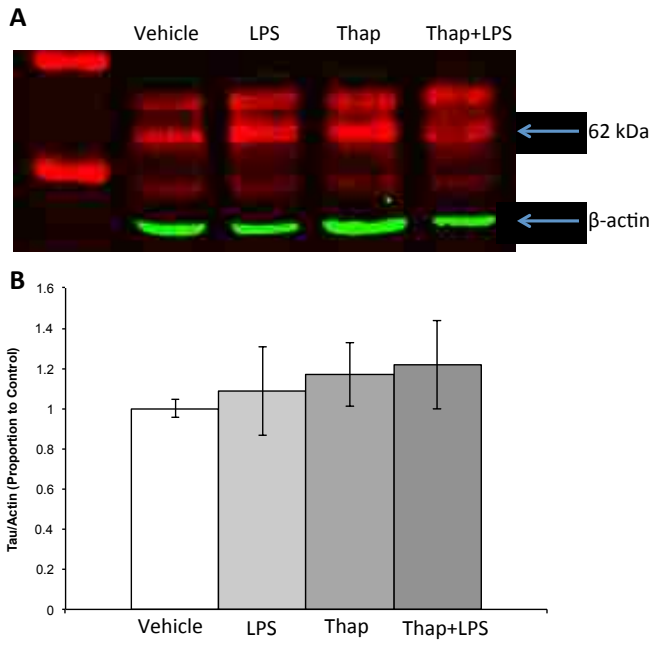

Figure 31. Tau protein levels in hippocampus from experiment 3 (n=6). (A) Representative image of a membrane probed for tau (red) and β-actin (green). Arrow indicates molecular weight of one of the tau bands. (B) No significant differences were observed in tau levels among groups. Data are expressed as the mean ± SEM.

Although no significant differences were observed among groups in CB-D28k levels in the hippocampus ($F_{3,44} = 2.452$, p=.076; see figure 32), there was likely a meaningful reduction in the LPS and thapsigargin groups. No correlations were found in the hippocampus between probe performance and CB-D28k levels.

When protein levels of oAβ were examined in the cortex, a significant increase was observed in 8mer levels following chronic thapsigargin treatment ($F_{3,44} = 4.506$, p<.01; Tukey post-hocs revealed that thapsigargin produced a significant increase versus vehicle, p<.01; see figure 33). No differences were found in the other oligomeric species; these data are summarized in table 6. No strong correlations were discovered between probe trial performance and oAβ protein levels in the cortex.

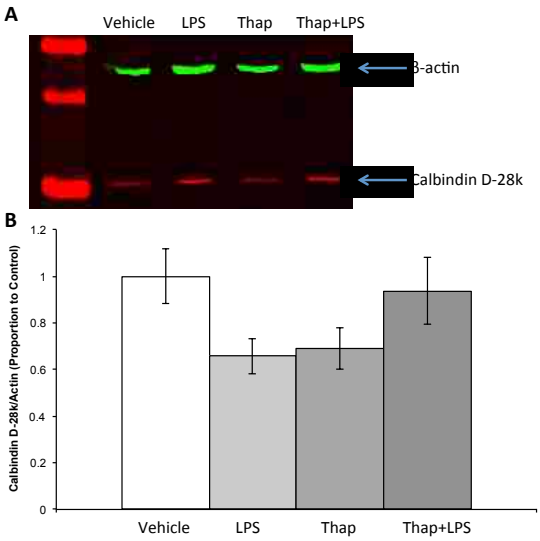

Figure 32. CB-D28k protein levels in hippocampus from experiment 3 (n=6). (A) Representative image of a membrane probed for CB-D28k (red) and β-actin (green). (B) No significant differences were observed in CB-D28k levels among groups. Data are expressed as the mean ± SEM.

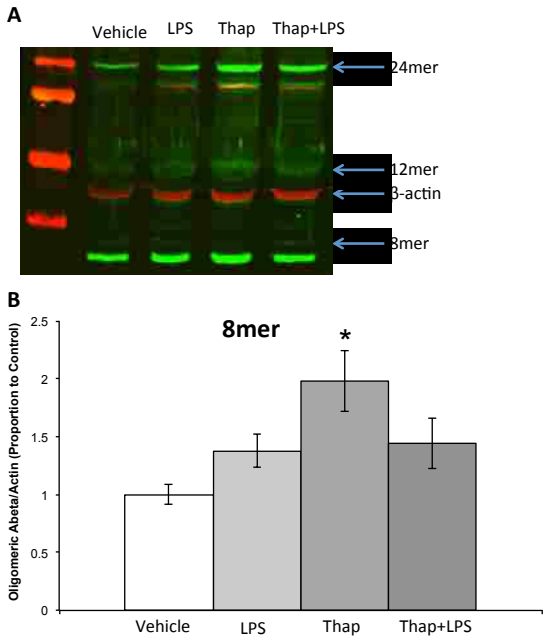

Figure 33. Oligomeric Aβ protein levels in cortex from experiment 3 (n=6). (A) Representative image of a membrane probed for oAβ (green) and β-actin (red). Arrows indicate specific oligomers or β-actin. (B) Thapsigargin significantly increased 8mer levels in the cortex compared to vehicle. Data are expressed as the mean ± SEM. * indicates p<.01.

Table 6.

Western blot data from cortex in experiment 3 of Aβ oligomers with β-actin as a loading control (n=6). Specific oligomers are listed with mean ± SEM levels for each group, valued as proportion of control, which was set at 1. F and p values are also listed for the one-way between groups ANOVAs performed to analyzed the protein level differences among groups. Degrees of freedom were 3,44 for each ANOVA.

Oligomer	LPS	Thapsigargin	Thap+LPS	F value	p value
24mer	1.18 ± 0.13	0.95 ± 0.09	1.06 ± 0.09	1.139	.344
20mer	1.08 ± 0.08	0.82 ± 0.09	1.00 ± 0.14	0.762	.521
18mer	1.49 ± 0.25	1.26 ± 0.25	1.31 ± 0.32	0.701	.557
12mer	1.37 ± 0.33	1.20 ± 0.22	0.99 ± 0.17	0.711	.551
11mer	1.15 ± 0.09	0.96 ± 0.05	0.94 ± 0.06	2.156	.107
7mer	1.03 ± 0.11	0.86 ± 0.03	0.92 ± 0.06	1.393	.258

Tau phosphorylation was investigated in the cortex as well and a robust increase was observed in the thap+LPS group, although it failed to reach significance, p=.057 ($F_{3,44}$ = 5.527, p<.01; Tukey post-hocs did not reveal any significant differences among groups; see figure 34). A moderate negative correlation was found in the thap+LPS group between probe trial performance and ptau levels (R = .596) but it was not significant (p=.212).

CB-D28k levels in the cortex did not significantly differ among groups but there was a slight reduction in the thapsigargin group ($F_{3,44}$ = 0.547, p=.653; see figure 35). There was however a significant positive correlation in the thap+LPS group between CB-D28k levels and probe trial performance ($F_{1,4}$ = 27.021, p<.01; see figure 36).

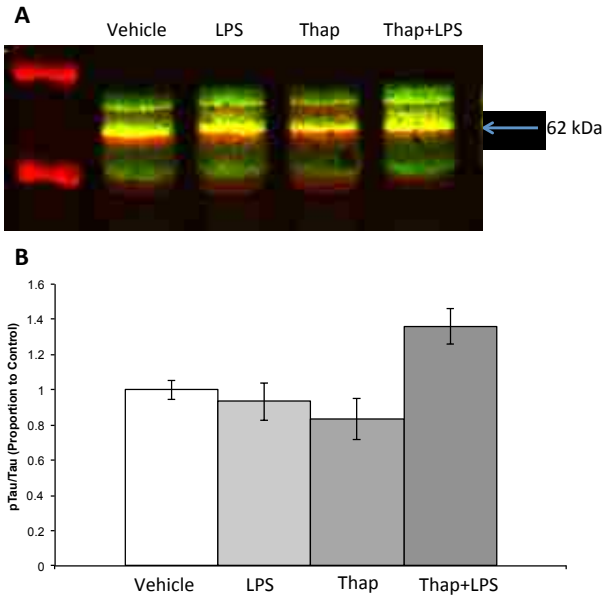

Figure 34. Ptau protein levels in cortex from experiment 3 (n=6). (A) Representative image of a membrane probed for tau phosphorylated at serine 396 (green) and β-actin (red). (B) No significant differences were observed in ptau levels among groups despite a large increase in the thap+LPS group (p=.057). Data are expressed as the mean ± SEM.

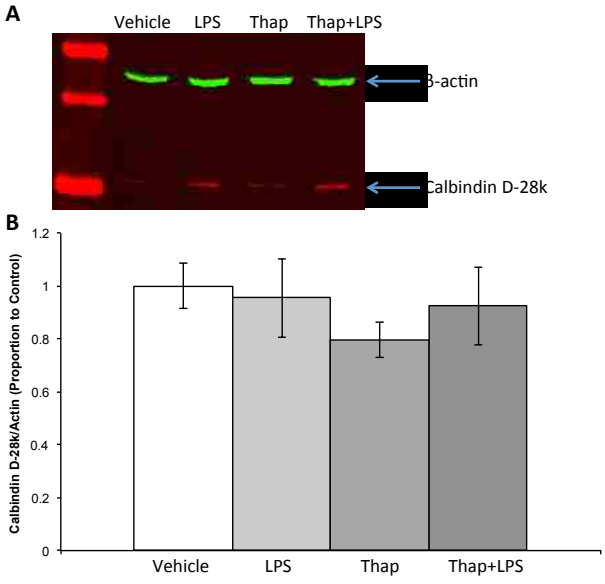

Figure 35. CB-D28k protein levels in cortex from experiment 3 (n=6). (A) Representative image of a membrane probed for CB-D28k (red) and β-actin (green). (B) No significant differences were observed in CB-D28k levels among groups. Data are expressed as the mean ± SEM.

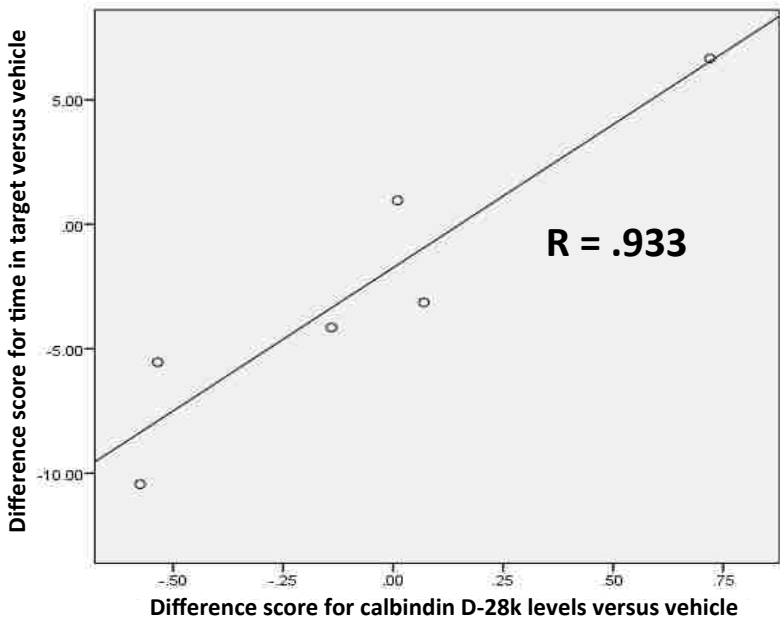

Figure 36. Correlations between thap+LPS group probe trial performance and cortical CB-D28k levels from experiment 3 (n=6). In the thap+LPS group, a significant correlation was found between probe trial time in target quadrant and CB-D28k levels in the cortex, $p<.01$.

CHAPTER 5

DISCUSSION

The above series of experiments was designed to evaluate the hypothesis that disrupting intracellular calcium homeostasis would be sufficient to elicit behavioral and neurological manifestations of AD. In order to investigate this hypothesis, compounds that perturb ER calcium regulation were chronically administered to rats, which were tested in multiple learning and memory paradigms. Brain neurochemistry was then examined in the hippocampus and cortex for protein markers consistently altered in AD. The data from these studies suggest calcium dysregulation disrupts aspects of hippocampal-dependent learning and memory, while producing variable changes in AD-related proteins in the brain.

Experiment 1

A pilot study was initially conducted with a relatively small group size (n=8) to assess if chronically altering intracellular calcium regulation produced AD-like changes in behavior or neurochemistry. The open field, NOR, and MWM tasks were conducted four weeks following implantation of osmotic min-pumps, which steadily released either vehicle, ryanodine (250 nM) or thapsigargin (10 μM) into the right lateral ventricle. Open field data indicated that neither ryanodine nor thapsigargin produced anxiogenic effects or affected locomotor activity. Learning and memory was first examined in NOR testing, which included a STM and LTM component. Deficits were observed in the thapsigargin group in both STM and LTM for novel object preference, indicating a learning impairment in this group. No deficits were found in the ryanodine group. Surprisingly,

vehicle animals also displayed an impairment in the LTM test, data which could reflect the inconsistency sometimes observed in rodent novelty-seeking behavior.

Thapsigargin impaired MWM acquisition, as measured by latency to the hidden platform, and probe trial annulus crossings. These data reveal a robust cognitive deficit in this group, which is consistent with the deficits observed in NOR. Ryanodine also produced a probe trial impairment, both in percent time spent in the target quadrant and annulus crossings, indicating a spatial learning and memory deficit. Overall, these data suggest that altering ER calcium regulation with ryanodine or thapsigargin is sufficient to disrupt hippocampal-dependent learning and memory, similar to the deficits observed in AD patients.

Following the completion of behavioral testing, brains were dissected out and specific brain regions were homogenized to examine protein levels. Levels of oAβ, a pathogenic contributor in AD (Lesné et al., 2006; Walsh et al., 2002), were significantly increased in the hippocampus following thapsigargin treatment at the 72 kDa band, which likely corresponds to an 18mer. Ryanodine produced a similar elevation in 18mer levels but it did not reach significance. Although thapsigargin increased levels of several other oligomers in the hippocampus, the small group size and large variability may have influenced the lack of significant results. Interestingly, a significant negative correlation was observed in the thapsigargin group between probe trial performance and 24mer oAβ levels. This correlation indicates that larger levels of 24mers were related to poorer probe performance, findings that reflect the correlations observed in AD mouse models (Lesné et al., 2006) and AD patients (Santos et al., 2012) between cognitive deficits and oAβ. In the cortex, no significant differences were observed in any of the oAβs suggesting the

thapsigargin-induced increase is region-specific. There was however a significant negative correlation in the ryanodine group between probe performance and 24mer levels, similar to that observed in the hippocampus in the thapsigargin group. Collectively, these data suggest that perturbing calcium regulation does alter levels of oAβ, but not in a manner entirely consistent with AD or mutant mouse models of the disease.

When the degree of tau phosphorylated at Serine 396 was examined in the hippocampus and cortex, no significant changes were observed following chronic ryanodine or thapsigargin treatment. Although small increases were found in each brain region, these did not mirror the large tau phosphorylation seen in AD or other studies that altered calcium regulation (Fu et al., 2010).

CB-D28k levels were not significantly changed following chronic ryanodine or thapsigargin infusion, despite the large reduction observed in the ryanodine group in the hippocampus (~60% reduction). Although the lack of significance limits the interpretations that can be made, it is interesting to note that CB-D28k levels are consistently reduced in AD brains (Iacopino & Christakos, 1990; Riascos et al., 2011) and mouse models of AD (Palop et al., 2003). It is difficult to extrapolate the findings from the current study to AD, but the alterations observed in CB-D28k levels are likely physiologically relevant despite their lack of significance. Furthermore, these findings suggest that the compounds administered did have a direct effect on calcium signaling as evidenced by the changes in CB-D28k, an important calcium-binding protein.

Because the results of the pilot study (experiment 1) indicated this approach may have promise to investigate mechanisms of AD, experiment 2 was designed to examine the effects of calcium dysregulation on a larger scale. The group size was increased to an n of 12 and dosages of ryanodine or thapsigargin were increased in order to produce more robust and uniform effects. An identical timeline as experiment 1 was performed for surgery, behavioral studies, and tissue collection and all methods conducted were identical to experiment 1. Open field data were similar to experiment 1, with no differences among groups, indicating that increasing the dose of these ligands did not alter locomotion or produce an anxiety phenotype. When NOR testing was performed, no differences were observed among groups in total time spent exploring the identical objects on Day 1, suggesting none of the drugs induced any neophobic effects. On Day 2, only vehicle subjects displayed a significant preference for the novel object compared to chance levels, indicating each of the treatments administered impaired NOR learning.

MWM testing commenced the following week and no differences were observed among groups in the acquisition phase of the task. Surprisingly, none of the groups displayed impairment on the probe trial as measured by percent time in quadrant. Subtle deficits were observed following chronic ryanodine at 5 μM or thapsigargin at 20 μM in the number of annulus crossings; however, these differences were neither as robust as anticipated nor reflective of AD-like impairments.

To assess if the drugs altered protein levels of AD-related markers, SDS/PAGE was initially performed on hippocampal samples. Interestingly, no significant differences were found in any of the targets examined (oAβ, ptau, or CB-D28k) among groups,

suggesting that the increased dosages did not enlarge nor even replicate the changes in experiment 1. Despite the lack of any significant differences among groups, CB-D28k levels displayed significant positive correlations with several oAβ species, including 7mers ($R = .546$, $p<.05$), 9mers ($R = .516$, $p<.05$), 10mers ($R = .514$, $p<.05$), and 16mers ($R = .784$, $p<.01$) (data not shown). It is unclear why there would be a positive relationship between CB-D28k and oAβ, as most studies imply a neuroprotective role for CB-D28k (Iacopino et al., 1992). It is also plausible that the correlation does not represent a direct causal relationship between the expression of these proteins.

The possibility exists that increasing the dose of each ligand forced neurons to compensate for the alterations in either RyR or SERCA function within the ER. For example, changes in the physiological functioning of the ER can produce ER stress as mentioned above (Unterberger et al., 2006). In an attempt to counteract the stress, cells may initiate the UPR to increase protein folding capacity and restore functioning to a homeostatic level (Kaufman, 1999).

Alternatively, if the increased dosages of these drugs resulted in cytotoxic levels of intracellular calcium, direct changes in calcium-related physiology may have occurred, such as an upregulation of SERCA pumps, downregulation of RYRs, or a change in any of the other numerous proteins that regulate calcium levels (Wernyj et al., 1999). Future studies may be able to illuminate the mechanisms responsible for the lack of cognitive deficits and protein-level differences in experiment 2. However, because no robust behavioral or neurological changes were found in this experiment, no further assays were conducted in order to conserve resources.

Because increasing the drug dose and group size in experiment 2 did not produce the AD phenotype desired, an alternative approach was employed in an attempt to more accurately model what may be occurring in AD. Specifically, we administered LPS coupled with chronic calcium dysregulation via thapsigargin to evaluate if inducing an acute neuroimmune response would be sufficient to produce AD-like behavior and pathology. Additionally, we employed aged rats (10-12 months old) because they likely have less capacity to compensate for any neurotoxic insults and more closely match an at-risk AD population. As mentioned above (see page 35), because it could not be determined exactly what concentration of thapsigargin was in the osmotic pumps, the results from this experiment are difficult to generalize and must be interpreted with care.

Immediately following the acute LPS injection, which was administered two weeks after surgery, temperatures and weights were recorded to determine if LPS produced an immune response. As expected, LPS significantly increased body temperature and significantly decreased weight for up to 48 hours following the injection. Levels returned to baseline by 72 hours post-injection. Based on these data, it was evident an immune response was mounted which previous work has shown leads to prolonged neuroinflammation, cytokine release, and microglial activation (Qin et al., 2007). Behavioral testing commenced three weeks later with open field and NOR.

No anxiety phenotype or changes in locomotion were observed during open field testing in experiment 3, consistent with the previous studies. During NOR testing, no differences were observed among groups in the time spent exploring objects on Day 1. Surprisingly, no groups displayed a significant preference for the novel object the

following day when it was presented with the familiar object. The vehicle group performed especially poorly, suggesting aged rats may encounter more difficulty with the task (de Lima et al., 2005) or perhaps exhibit less motivation for novelty-seeking behavior than younger animals. Unfortunately, the meaningfulness of the deficits observed in the other groups is diminished by the lack of significance in the control group. Therefore, the impairment in the vehicle group limits the interpretations that can be made about the drug-induced deficits.

During the MWM acquisition phase, no significant differences were observed among groups, suggesting all groups were able to similarly locate the platform. The thap+LPS group did display a deficit in the probe trial as measured by percent time in target quadrant, but not annulus crossings. Interestingly, although neither LPS nor thapsigargin impaired percent time in quadrant, each group showed a deficit in annulus crossings. Therefore, each treatment did manifest a learning and memory impairment in one aspect of the probe trial. However, the cognitive deficits exhibited by these groups did not come close to mirroring those observed in AD, suggesting the combination of thapsigargin and LPS was not sufficient to produce AD-like behavioral changes. If the dosage of thapsigargin had been 25 μM, as intended, it is possible more pronounced impairments would have been observed in these aged rats, similar to experiment 1 which employed a lower dose of 10 μM.

When protein levels were examined in the hippocampus, the thap+LPS group was found to have significantly decreased 18mer oAβ levels compared to vehicle. This result is in contrast to the data from experiment 1 showing that thapsigargin significantly increased 18mer levels in the hippocampus. In experiment 3, thapsigargin did not

produce any significant difference, whereas the combination of thap+LPS did significantly decrease 18mer levels. These data collectively may suggest that inducing an acute inflammatory response could reduce oAβ levels and potentially be beneficial. However, because thapsigargin in experiment 3 did not replicate the effects observed in experiment 1, further experiments would be necessary to make any definitive conclusions. If the thapsigargin dose had been 25 μM, a change in oAβ levels more similar to experiment 1 may have been observed and the thap+LPS group reduction may not have been seen.

Although no other significant differences were observed in oAβ levels, interesting correlations emerged between probe trial performance and smaller size oligomers. When all groups were examined, significant negative correlations were found between probe trial time in quadrant scores and either 10mer or 8mer levels. These data indicate that more impaired probe performance was related to larger levels of oAβ. Whether there is a direct causal relationship between cognitive performance and oAβ is unclear from the current data, although previous studies have shown oAβ can directly induce learning and memory deficits (Cleary et al., 2005; Lesné et al., 2006). Significant negative correlations were further observed in the thap+LPS group between probe performance and either 11mer or 7mer levels. These findings reinforce the notion that oAβ may contribute to cognitive deficits.

In the cortex, thapsigargin produced a significant increase in 8mer oAβ levels compared to vehicle, a change that was not observed when LPS was administered during chronic thapsigargin treatment (thap+LPS group). LPS binds to CD14 proteins and activates the toll-like receptor 4 (TLR4), which initiates an important signaling cascade

for the immune response (Kurt-Jones et al., 2000; Xia et al., 2006). In a transgenic mouse model of AD with the TLR4 gene knocked out, amyloid pathology was aggravated (Tahada et al., 2006), suggesting the immune response may be beneficial in AD. In the current study, it is possible that the administration of LPS mitigated the increase in oAβ levels observed in the thapsigargin group. This interpretation is supported by previous work demonstrating that LPS enhances the phagocytosis of exogenous Aβ (Liu et al., 2005).

Tau phosphorylation was quantified in two different ways in experiment 3. In the hippocampus, ptau levels were compared to β-actin while tau levels were separately compared to β-actin; no significant differences were observed among groups in either comparison. This alternative approach to quantify ptau and tau was performed to be consistent with the majority of the literature, which reports levels of ptau and tau independent of each other. However, it is likely the lack of direct ptau/tau comparisons is a byproduct of technique limitations rather than a methodological consideration. The Odyssey fluorescent imaging system used in the current experiments permitted the detection of proteins of similar molecular weights; other imaging approaches typically have more difficulty with this type of detection. Regardless of the approach, none of the ligands administered altered tau phosphorylation in the hippocampus. Furthermore, it is unlikely the thapsigargin dosage affected ptau levels; none of the experiments indicated any change in the levels of this protein following any dose of thapsigargin.

In the cortex, there were once again no significant differences among groups in ptau/tau levels, despite a likely meaningful 40% increase in the thap+LPS group ($p=.057$). Thapsigargin has been previously demonstrated to significantly enhance tau

phosphorylation following acute intracerebral infusion into the lateral ventricle (Fu et al., 2010). LPS has been shown to exacerbate tau pathology in a transgenic model of AD (Lee et al., 2010), suggesting the LPS injection may have potentiated any thapsigargin-induced effects on tau phosphorylation in the current study.

Consistent with experiment 1, thapsigargin produced a non-significant decrease in CB-D28k levels in the hippocampus (~40%), suggesting that the drug likely altered calcium regulation. Interestingly, LPS produced a similar decrease in the hippocampus, a finding consistent with previous research showing decreased CB-D28k expression following administration of tumor necrosis factor-α (TNF-α) (Parkash et al., 2005), a proinflammatory cytokine whose production is increased by LPS (Nadeau & Rivest, 1999). Surprisingly, the combination of thapsigargin and LPS did not alter CB-D28k levels in a similar fashion to either LPS or thapsigargin alone. Without performing further assays to parse out the potential mechanism(s) responsible for these differences, it is unclear why the CB-D28k levels may differ among these groups. Although these differences are consistent with experiment 1, the possibility exists that a lower dosage of thapsigargin in aged animals would have produced a more robust reduction in CB-D28k levels.

Interestingly, there was a strong positive correlation between hippocampal CB-D28k levels and 18mer oAβ levels in the thap+LPS group ($R = .807$, $p=.052$; data not shown). This correlation raises the possibility that the significant decrease observed in 18mer levels in the thap+LPS group could be related to its levels of CB-D28k. Why the increased presence of CB-D28k would be related to increased oAβ levels is unclear; however it is interesting to note that this relationship between increased CB-D28k and

oAβ was observed in the hippocampus in experiment 2 as well. Of course this possibility can merely be speculated at this point without further data to support it.

Although no changes were observed in the cortex in CB-D28k levels among groups, a significant positive correlation was found between probe performance and CB-D28k levels in the thap+LPS group, indicating a greater degree of CB-D28k was related to better performance. A significant negative correlation was found between CB-D28k levels and ptau levels in the cortex when all groups were examined ($R = .580$, $p<.05$; data not shown), suggesting the increased presence of CB-D28k reduced the amount of tau phosphorylation. Once again these conclusions cannot be confirmed without the inclusion of further testing and data collection. Furthermore, similar to the data from the hippocampus and from experiment 2, significant positive correlations were found between CB-D28k levels and oAβ levels among all groups for 7mers ($R = .725$, $p<.01$), 11mers ($R = .556$, $p<.05$), and 24mers ($R = .590$, $p<.05$). As mentioned above however, the importance of these relationships is unclear, especially with minimal significant differences observed in the between group protein level analyses.

Conclusions

The goal of the current series of experiments was to directly examine the hypothesis that prolonged intracellular calcium dysregulation could lead to Alzheimer's-like changes in the brain and behavior. It is evident from the data reported above that at least in a wild-type rodent model, this approach does not produce the robust cognitive deficits or biochemical changes normally associated with AD. However, interesting and novel information has still been obtained from these experiments. The data demonstrate

that chronic ryanodine or thapsigargin infusion into the lateral ventricle impairs learning and memory in multiple behavioral paradigms at multiple dosages and ages. These studies also show that thapsigargin treatment is sufficient to elevate oAβ levels in multiple brain regions at multiple dosages (see experiments 1 and 3). The considerable amount of tau phosphorylation typically observed in AD patients and models of AD was not observed in the current experiments, despite modest increases in various groups. Furthermore, the decreased expression of CB-D28k observed, although consistent with AD, never reached a level of statistical significance.

It is interesting to consider potential explanations for the alterations in CB-D28k levels in these experiments. Intuitively, elevated cytosolic calcium concentration, as is hypothesized to occur following chronic ryanodine or thapsigargin treatment, should lead to increased levels of a calcium buffering protein in an effort to reduce any calcium-induced excitotoxicity or synaptic dysfunction. However, the opposite effect was observed in the above studies. Interestingly, it has been shown that CB-D28k expression is decreased following a calcium overload induced by either glutamate (Mao et al., 2010) or status epilepticus in rats (Carter et al., 2008). CB-D28k levels may be reduced to enhance calcium-dependent inactivation (CDI) of voltage-gated calcium entry, an important mechanism to reduce net calcium influx following depolarization (Köhr & Mody, 1991). In support of this hypothesis, low or absent CB-D28k expression from Ammon's horn sclerosis (AHS; Nagerl & Mody, 1998) or CB-D28k gene knockout (Klapstein et al., 1998) leads to increased CDI and a corresponding decrease in calcium load. It is possible the decreased CB-D28k levels observed following chronic ryanodine, or to a lesser extent thapsigargin, serve a compensatory mechanism to enhance CDI and

reduce intracellular calcium overload. Future experiments employing calcium imaging or electrophysiological techniques may be able to test these hypotheses.

Overall, these experiments demonstrated that chronic calcium dysregulation is likely related to AD pathophysiology; however, it is likely not the sole etiologic factor that initiates AD pathology and symptoms. These data also indicated that although our manipulations did affect behavior and neurochemistry to a certain extent, the deficits observed in our studies were not consistent with other animal models of AD (Cleary et al., 2005; Hsiao et al., 1996). It may be interesting to perform these experiments in existing transgenic mouse models of AD, as they already exhibit robust AD pathology. This approach would elucidate how calcium dysregulation interacts with amyloid and/or tau pathology and perhaps advance our understanding of AD.

BIBLIOGRAPHY

Akiyama H, Barger S, Barnum S, Bradt B, Bauer J, Cole GM, et al. Inflammation and Alzheimer's disease. Neurobiol Aging 2000; 21(30: 383-421.

Alonso Adel C, Li B, Grundke-Iqbal I, Iqbal K. Polymerization of hyperphosphorylated tau into filaments eliminates its inhibitory activity. Proc Natl Acad Sci USA 2006; 103: 8864-9.

Amniai L, Lippens G, Landrieu I. Characterization of the AT180 epitope of phosphorylated Tau protein by a combined nuclear magnetic resonance and fluorescence spectroscopy approach. Biochem Biophys Res Commun 2011; 412: 743-6.

Anagnostaras SG, Murphy GG, Hamilton SE, Mitchell SL, Rahnama NP, Nathanson NM, et al. Selective cognitive dysfunction in acetylcholine M1 muscarinic receptor mutant mice. Nat Neurosci 2003; 6: 51-8.

Arriagada PV, Growdon JH, Hedley-Whyte ET, Hyman BT. Neurofibrillary tangles but not senile plaques parallel duration and severity of Alzheimer's disease. Neurology 1992; 42: 631-639.

Atwood CS, Perry G, Zeng H, Kato Y, Jones WD, Ling KQ, et al. Copper mediates dityrosine cross-linking of Alzheimer's amyloid-beta. Biochemistry 2004; 43: 560-8.

Bading H, Ginty DD, Greenberg ME. Regulation of gene expression in hippocampal neurons by distinct calcium signaling pathways. Science 1993; 260: 181-6.

Bartsch D, Casadio A, Karl KA, Serodio P, Kandel ER. CREB1 encodes a nuclear activator, a repressor, and a cytoplasmic modulator that form a regulatory unit critical for long-term facilitation. Cell 1998; 95: 211-23.

Bartus RT. Physostigmine and recent memory: effects in young and aged nonhuman primates. Science 1979; 206: 1087-9.

Bartus RT, Dean RL III, Beer B, Lippa AS. The Cholinergic Hypothesis of Geriatric Memory Dysfunction. Science 1982; 217: 408-17.

Bateman RJ, Munsell LY, Morris JC, Swarm R, Yarasheski KE, Holtzman DM. Human amyloid-beta synthesis and clearance rates as measured in cerebrospinal fluid in vivo. Nat Med 2006; 12: 856-61.

Beach TG, Hughes LH, Honer WG. Cholinergic fibre loss associated with diffuse plaques in the non-demented elderly: the preclinical stage of Alzheimer's disease? Acta Neuropathol 1997; 93: 146-53.

Beach TG, Sue LI, Scott S, Sparks DL. Neurofibrillary tangles are constant in aging human nucleus basalis. Alzheimer's Reports 1998; 1: 375-80.

Beach TG, Kuo YM, Spiegel K, Emmerling MR, Sue LI, Kokjohn K, et al. The cholinergic deficit coincides with Abeta deposition at the earliest histopathologic stages of Alzheimer disease. J Neuropathol Exp Neurol 2000; 59(4): 308-13.

Beal MF. Excitotoxicity and nitric oxide in Parkinson's disease pathogenesis. Ann Neurol 1998; 44(3 Suppl 1): S110-4.

Beecham GW, Schnetz-Boutaud N, Haines JL, Pericak-Vance MA. CALHM1 polymorphism is not associated with late-onset Alzheimer disease. Ann Hum Genet 2009; 73(Pt 3): 379-81.

Bertaina-Anglade V, Drieu-La-Rochelle C, Mocaër E, Seguin L. Memory facilitating effects of agomelatine in the novel object recognition memory paradigm in the rat. Pharmacol Biochem Behav 2011; 98: 511-7.
Bertram L, Schjeide BM, Hooli B, Mullin K, Hiltunen M, Soininen H, et al. No association between CALHM1 and Alzheimer's disease risk. Cell 2008; 135(6): 993-4.
Beutner G, Sharma VK, Lin L, Ryu SY, Dirksen RT, Sheu SS. Type 1 ryanodine receptor in cardiac mitochondria: transducer of excitation-metabolism coupling. Biochim Biophys Acta 2005; 1717(1): 1-10.
Bezprozvanny I, Mattson MP. Neuronal calcium mishandling and the pathogenesis of Alzheimer's disease. Trends Neurosci 2008; 31: 454-463.
Blaustein MP, Lederer WJ. Sodium/calcium exchange: its physiological implications. Physiol Rev 1999; 79: 763-854.
Blurton-Jones M, LaFerla FM. Pathways by which Aβ facilitates tau pathology. Curr Alzheimer Res 2006; 3(5): 437-448.
Bojarski L, Herms J, Kuznicki J. Calcium dysregulation in Alzheimer's disease. Neurochem Int 2008; 52: 621-633.
Borchelt DR, Thinakaran G, Eckman CB, Lee MK, Davenport F, Ratovitsky T, et al. Familial Alzheimer's disease-linked presenilin 1 variants elevate Abeta1-42/1-40 ratio in vitro and in vivo. Neuron 1996; 17: 1005-13.
Borst JG, Sakmann B. Calcium influx and transmitter release in a fast CNS synapse. Nature 1996; 383: 431-4.
Bowen DM, Benton JS, Spillane JA, Smith CC, Allen SJ. Choline acetyltransferase activity and histopathology of frontal neocortex from biopsies of demented patients. J Neurol Sci 1982; 57: 191-202.
Braak H, Braak E. Neuropathological staging of Alzheimer-related changes. Acta Neuropathol (Berl) 1991; 82: 239-259.
Bramblett GT, Goedert M, Jakes R, Merrick SE, Trojanowski JQ, Lee VM. Abnormal tau phosphorylation at Ser396 in Alzheimer's disease recapitulates development and contributes to reduced microtubule binding. Neuron 1993; 10: 1089-99.
Braun AP, Schulman H. The multifunctional calcium/calmodulin-dependent protein kinase: from form to function. Annu Rev Physiol 1995; 57: 417-45.
Brenner DE, Kukull WA, van Belle G, Bowen JD, McCormick WC, Teri L, Larson EB. Relationship between cigarette smoking and Alzheimer's disease in a population-based case-control study. Neurology 1993; 43(2): 293-300.
Brustovetsky N, Brustovetsky T, Purl KJ, Capano M, Crompton M, Dubinsky JM. Increased susceptibility of striatal mitochondria to calcium-induced permeability transition. J Neurosci 2003; 23(12): 4858-67.
Butler M, Shelanski ML. Microheterogeneity of microtubule-associated tau proteins is due to differences in phosphorylation. J Neurochem 1986; 47: 1517-22.
Buxbaum JD, Oishi M, Chen HI, Pinkas-Kramarski R, Jaffe EA, Gandy SE, et al. Cholinergic agonists and interleukin 1 regulate processing and secretion of the Alzheimer beta/A4 amyloid protein precursor. Proc Natl Acad Sci USA 1992; 89: 10075-8.

Buxbaum JD, Ruefli AA, Parker CA, Cypess AM, Greengard P. Calcium regulates processing of the Alzheimer amyloid protein precursor in a protein kinase C-independent manner. Proc Natl Acad Sci USA 1994; 91(10): 4489-93.
Caccamo A, Oddo S, Billings LM, Green KN, Martinez-Coria H, Fisher A, et al. M1 receptors play a central role in modulating AD-like pathology in transgenic mice. Neuron 2006; 49: 671-82.
Camandola S, Mattson MP. Aberrant subcellular neuronal calcium regulation in aging and Alzheimer's disease. Biochim Biophys Acta 2011; 1813: 965-73.
Canzoniero LMT, Snider BJ. Calcium in Alzheimer's disease pathogenesis: Too much, too little or in the wrong place? J Alz Disease 2005; 8: 147-54.
Carter DS, Harrison AJ, Falenski KW, Blair RE, DeLorenzo RJ. Long-term decrease in calbindin-D28K expression in the hippocampus of epileptic rats following pilocarpine-induced status epilepticus. Epilepsy Res 2008; 79(2-3): 213-23.
Castellani RJ, Nunomura A, Lee HG, Perry G, Smith MA. Phosphorylated tau: toxic, protective, or none of the above. J Alzheimers Dis 2008; 14: 377-83.
Cataldo JK, Prochaska JJ, Glantz SA. Cigarette smoking is a risk factor for Alzheimer's Disease: an analysis controlling for tobacco industry affiliation. J Alzheimers Dis 2010; 19(2): 465-80.
Catterall WA. Voltage-gated calcium channels. Cold Spring Harb Perspect Biol 2011; 3: a003947.
Chafekar SM, Zwart R, Veerhuis R, Vanderstichele H, Baas F, Scheper W. Increased Abeta1-42 production sensitizes neuroblastoma cells for ER stress toxicity. Curr Alzheimer Res 2008; 5: 469-74.
Chai CK. The genetics of Alzheimer's disease. Am J Alzheimers Dis Other Demen 2007; 22(1): 37-41.
Chakroborty S, Goussakov I, Miller MB, Stutzmann GE. Deviant ryanodine receptor-mediated calcium release resets synaptic homeostasis in presymptomatic 3xTg-AD mice. J Neurosci 2009; 29(30): 9458-70.
Cheung KH, Shineman D, Müller M, Cárdenas C, Mei L, Yang J, et al. Mechanism of Ca2+ disruption in Alzheimer's disease by presenilin regulation of InsP3 receptor channel gating. Neuron 2008; 58(6): 871-83.
Choi DW. Glutamate neurotoxicity in cortical cell culture is calcium dependent. Neurosci Lett 1985; 58: 293-7.
Citron M, Oltersdorf T, Haass C, McConlogue L, Hung AY, Seubert P, et al. Mutation of the beta-amyloid precursor protein in familial Alzheimer's disease increases beta-protein production. Nature 1992; 360: 372-4.
Citron M, Diehl TS, Gordon G, Biere AL, Seubert P, Selkoe DJ. Evidence that the 42- and 40-amino acid forms of amyloid beta protein are generated from the beta-amyloid precursor protein by different protease activities. Proc Natl Acad Sci USA 1996; 93: 13170-5.
Citron M, Westaway D, Xia W, Carlson G, Diehl T, Levesque G, et al. Mutant presenilins of Alzheimer's disease increase production of 42-residue amyloid beta-protein in both transfected cells and transgenic mice. Nat Med 1997; 3: 67-72.

Cleary JP, Walsh DM, Hofmeister JJ, Shankar GM, Kuskowski MA, Selkoe DJ, et al. Natural oligomers of the amyloid-beta protein specifically disrupt cognitive function. Nat Neurosci 2005; 8: 79-84.
Cluskey S, Ramsden DB. Mechanisms of neurodegeneration in amyotrophic lateral sclerosis. Mol Pathol 2001; 54: 386-92.
Combs CK, Karlo JC, Kao SC, Landreth GE. beta-Amyloid stimulation of microglia and monocytes results in TNFalpha-dependent expression of inducible nitric oxide synthase and neuronal apoptosis. J Neurosci 2001; 21: 1179-88.
Corder EH, Saunders AM, Strittmatter WJ, Schmechel DE, Gaskell PC, Small GW, et al. Gene dose of apolipoprotein E type 4 allele and the risk of Alzheimer's disease in late onset families. Science 1993; 261(5123): 921-3
Cox T, Tye N. Effects of physotigmine on the acquisition of a position discrimination in rats. Neuropharmacology 1973; 12: 477-84.
Crestini A, Piscopo P, Iazeolla M, Albani D, Rivabene R, Forloni G, et al. Rosuvastatin and thapsigargin modulate γ-secretase gene expression and APP processing in a human neuroglioma model. J Mol Neurosci 2011; 43: 461-9.
Cruts M, van Duijn CM, Backhovens H, Van den Broeck M, Wehnert A, Serneels S, et al. Estimation of the genetic contribution of presenilin-1 and -2 mutations in a population-based study of presenile Alzheimer disease. Hum Mol Genet 1998; 7(1): 43-51.
Crystal H, Dickson D, Fuld P, Masur D, Scott R, Mehler M, et al. Clinico-pathologic studies in dementia: nondemented subjects with pathologically confirmed Alzheimer's disease. Neurology 1988; 38: 1682-7.
Cummings J. What can be inferred from the interruption of the semagacestat trial for treatment of Alzheimer's disease? Biol Psychiatry 2010; 68(10): 876-8.
Davies P, Maloney AJ. Selective loss of central cholinergic neurons in Alzheimer's disease. Lancet 1976; 2: 1403.
Davies P. Neurotransmitter-related enzymes in senile dementia of the Alzheimer type. Brain Res 1979; 171: 319-27.
Davis KL, Mohs RC, Tinklenberg JR, Pfefferbaum A, Hollister LE, Kopell BS. Physostigmine: improvement of long-term memory processes in normal humans. Science 1978; 201: 272-4.
Dawson GR, Seabrook GR, Zheng H, Smith DW, Graham S, O'Dowd G, et al. Age-related cognitive deficits, impaired long-term potentiation and reduction in synaptic marker density in mice lacking the beta-amyloid precursor protein. Neuroscience 1999; 90(1): 1-13.
de Lima MN, Laranja DC, Caldana F, Bromberg E, Roesler R, Schröder N. Reversal of age-related deficits in object recognition memory in rats with l-deprenyl. Exp Gerontol 2005; 40(6): 506-11.
De Strooper B, Saftig P, Craessaerts K, Vanderstichele H, Guhde G, Annaert W, et al. Deficiency of presenilin-1 inhibits the normal cleavage of amyloid precursor protein. Nature 1998; 391: 387-90.
DeLuca HF, Engstrom GW. Calcium uptake by rat kidney mitochondria. Proc Natl Acad Sci USA 1961; 47: 1744-50.
Deutsch JA. The Cholinergic Synapse and the Site of Memory. Science 1971; 174: 788-94.

Dolev I, Michaelson DM. A nontransgenic mouse model shows inducible amyloid-beta (Abeta) peptide deposition and elucidates the role of apolipoprotein E in the amyloid cascade. Proc Natl Acad Sci USA 2004; 101: 13909-14.
Douglas RM, Goddard GV. Long-term potentiation of the perforant path-granule cell synapse in the rat hippocampus. Brain Res 1975; 86: 205-215.
Dovey HF, John V, Anderson JP, Chen LZ, de Saint Andrieu P, Fang LY, et al. Functional gamma-secretase inhibitors reduce beta-amyloid peptide levels in brain. J Neurochem 2001; 76(1): 173-81.
Dreses-Werringloer U, Lambert JC, Vingtdeux V, Zhao H, Vais H, Siebert A, et al. A polymorphism in CALHM1 influences Ca2+ homeostasis, Abeta levels, and Alzheimer's disease risk. Cell 2008; 133(7): 1149-61.
Duff K, Eckman C, Zehr C, Yu X, Prada CM, Perez-tur J, et al. Increased amyloid-beta42(43) in brains of mice expressing mutant presenilin 1. Nature 1996; 383: 710-13.
Ennaceur A, Delacour J. A new one-trial test for neurobiological studies of memory in rats. 1: Behavioral data. Behav Brain Res 1988; 31: 47-59.
Feuillette S, Miguel L, Frébourg T, Campion D, Lecourtois M. Drosophila models of human tauopathies indicate that Tau protein toxicity in vivo is mediated by soluble cytosolic phosphorylated forms of the protein. J Neurochem 2010; 113: 895-903.
Flynn DD, Mash DC. Characterization of L-[3H]nicotine binding in human cerebral cortex: comparison between Alzheimer's disease and the normal. J Neurochem 1986; 47: 1948-54.
Forlenza OV, Spink JM, Dayanandan R, Anderton BH, Olesen OF, Lovestone S. Muscarinic agonists reduce tau phosphorylation in non-neuronal cells via GSK-3beta inhibition and in neurons. J Neural Transm 2000; 107: 1201-12.
Fu ZQ, Yang Y, Song J, Jiang Q, Lin ZC, Wang Q, et al. LiCl attenuates thapsigargin-induced tau hyperphosphorylation by inhibiting GSK-3β in vivo and in vitro. J Alzheimers Dis 2010; 21: 1107-17.
Furukawa K, Wang Y, Yao PJ, Fu W, Mattson MP, Itoyama Y, et al. Alteration in calcium channel properties is responsible for the neurotoxic action of a familial frontotemporal dementia tau mutation. J Neurochem 2003; 87(2): 427-36.
Gallego-Sandín S, Alonso MT, García-Sancho J. Calcium homoeostasis modulator 1 (CALHM1) reduces the calcium content of the endoplasmic reticulum (ER) and triggers ER stress. Biochem J 2011; 437: 469-75.
Gibson GE, Peterson C. Calcium and the aging nervous system. Neurobiol Aging 1987; 8: 329-43.
Glenner GG, Wong CW. Alzheimer’s disease: initial report of the purification and characterization of a novel cerebrovascular amyloid protein. Biochem Biophys Res Commun 1984; 120: 885-890.
Goate A, Chartier-Harlin MC, Mullan M, Brown J, Crawford F, Fidani L, et al. Segregation of a missense mutation in the amyloid precursor protein gene with familial Alzheimer's disease. Nature 1991; 349: 704-706.
Goedert M, Wischik CM, Crowther RA, Walker JE, Klug A. Cloning and sequencing of the cDNA encoding a core protein of the paired helical filament of Alzheimer

disease: identification as the microtubule-associated protein tau. Proc Natl Acad Sci USA 1988; 85: 4051-5.
Goedert M, Spillantini MG, Jakes R, Rutherford D, Crowther RA. Multiple isoforms of human microtubule-associated protein tau: sequences and localization in neurofibrillary tangles of Alzheimer's disease. Neuron 1989; 3: 519-26.
Goedert M, Spillantini MG, Crowther RA. Cloning of a big tau microtubule-associated protein characteristic of the peripheral nervous system. Proc Natl Acad Sci USA 1992; 89: 1983-87.
Goedert M. Tau protein and the neurofibrillary pathology of Alzheimer's disease. Ann NY Acad Sci 1996; 777: 121-31.
Golde TE, Estus S, Younkin LH, Selkoe DJ, Younkin SG. Processing of the amyloid protein precursor to potentially amyloidogenic derivatives. Science 1992; 255: 728-30.
Gómez-Isla T, Hollister R, West H, Mui S, Growdon JH, Petersen RC, et al. Neuronal loss correlates with but exceeds neurofibrillary tangles in Alzheimer's disease. Ann Neurol 1997; 41(1): 17-24.
Gotz J, Chen F, van Dorpe J, Nitsch RM. Formation of neurofibrillary tangles in P301L tau transgenic mice induced by Abeta 42 fibrils. Science 2001; 293(5534): 1491-5.
Green KN, LaFerla FM. Linking calcium to Abeta and Alzheimer's disease. Neuron 2008; 59: 190-194.
Greenberg ME, Ziff EB, Greene LA. Stimulation of neuronal acetylcholine receptors induces rapid gene transcription. Science 1986; 234: 80-3.
Greer PL, Greenberg ME. From synapse to nucleus: calcium-dependent gene transcription in the control of synapse development and function. Neuron 2008; 59: 846-60.
Grundke-Iqbal I, Iqbal K, Tung YC, Quinlan M, Wisniewski HM, Binder LI. Abnormal phosphorylation of the microtubule-associated protein tau (tau) in Alzheimer cytoskeletal pathology. Proc Natl Acad Sci USA 1986; 83: 4913-17.
Guerreiro R, Wojtas A, Bras J, Carrasquillo M, Rogaeva E, Majounie E, et al. TREM2 variants in Alzheimer's disease. N Engl J Med 2013; 368(2): 117-27.
Gunteski-Hamblin AM, Greeb J, Shull GE. A novel Ca2+ pump expressed in brain, kidney, and stomach is encoded by an alternative transcript of the slow-twitch muscle sarcoplasmic reticulum Ca-ATPase gene. Identification of cDNAs encoding Ca2+ and other cation-transporting ATPases using an oligonucleotide probe derived from the ATP-binding site. J Biol Chem 1988; 263: 15032-40.
Guo JP, Arai T, Miklossy J, McGeer PL. Abeta and tau form soluble complexes that may promote self aggregation of both the insoluble forms observed in Alzheimer's disease. Proc Natl Acad Sci USA 2006; 103: 1953-8.
Hardingham GE, Chawla S, Johnson CM, Bading H. Distinct functions of nuclear and cytoplasmic calcium in the control of gene expression. Nature 1997; 385: 260-5.
Hardy JA, Higgins GA. Alzheimer's disease: the amyloid cascade hypothesis. Science 1992; 256(5054): 184-5.
Harvey AL, Rowan EG. Effects of tacrine, aminopyridines, and physostigmine on acetylcholinesterase, acetylcholine release, and potassium currents. Adv Neurol 1990; 51: 227-33.

Hasegawa M. β-amyloid and tau protein. Psychogeriatrics 2004; 4: S62-69.
Hayes A, Thaker U, Iwatsubo T, Pickering-Brown SM, Mann DM. Pathological relationships between microglial cell activity and tau and amyloid beta protein in patients with Alzheimer's disease. Neurosci Lett 2002; 331: 171-4.
Heese K, Akatsu H. Alzheimer's Disease – An Interactive Perspective. Current Alzheimer Research 2006; 3: 109-121.
Hellström-Lindahl E, Moore H, Nordberg A. Increased levels of tau protein in SH-SY5Y cells after treatment with cholinesterase inhibitors and nicotinic agonists. J Neurochem 2000; 74: 777-84.
Hensley K. Neuroinflammation in Alzheimer's disease: mechanisms, pathologic consequences, and potential for therapeutic manipulation. J Alzheimers Dis 2010; 21(1): 1-14.
Herber DL, Maloney JL, Roth LM, Freeman MJ, Morgan D, Gordon MN. Diverse microglial responses after intrahippocampal administration of lipopolysaccharide. Glia 2006; 53(4): 382-91.
Herms J, Schneider I, Dewachter I, Caluwaerts N, Kretzschmar H, Van Leuven F. Capacitive calcium entry is directly attenuated by mutant presenilin-1, independent of the expression of the amyloid precursor protein. J Biol Chem 2003; 278(4): 2484-9.
Ho YS, Yang X, Lau JC, Hung CH, Wuwongse S, Zhang Q, et al. Endoplasmic reticulum stress induces tau pathology and forms a vicious cycle: implication in Alzheimer's disease pathogenesis. J Alzheimers Dis 2012; 28: 839-54.
Holmes C. Genotype and phenotype in Alzheimer's disease. Br J Psychiatry 2002; 180: 131-134.
Holtzman DM, Santucci D, Kilbridge J, Chua-Couzens J, Fontana DJ, Daniels SE, et al. Developmental abnormalities and age-related neurodegeneration in a mouse model of Down syndrome. Proc Natl Acad Sci USA 1996; 93: 13333-8.
Holtzman DM. Role of apoe/Abeta interactions in the pathogenesis of Alzheimer's disease and cerebral amyloid angiopathy. J Mol Neurosci 2001; 17: 147-55.
Holtzman DM. In vivo effects of ApoE and clusterin on amyloid-beta metabolism and neuropathology. J Mol Neurosci 2004; 23: 247-254.
Hong M, Zhukareva V, Vogelsberg-Ragaglia V, Wszolek Z, Reed L, Miller BI, et al. Mutation-specific functional impairments in distinct tau isoforms of hereditary FTDP-17. Science 1998; 282: 1914-17.
Hsiao K, Chapman P, Nilsen S, Eckman C, Harigaya Y, Younkin S, et al. Correlative memory deficits, Abeta elevation, and amyloid plaques in transgenic mice. Science 1996; 274: 99-102.
Hussain I, Hawkins J, Harrison D, Hille C, Wayne G, Cutler L, et al. Oral administration of a potent and selective non-peptidic BACE-1 inhibitor decreases beta-cleavage of amyloid precursor protein and amyloid-beta production in vivo. J Neurochem 2007; 100(3): 802-09.
Hutton M, Lendon CL, Rizzu P, Baker M, Froelich S, Houlden H, et al. Association of missense and 5'-splice-site mutations in tau with the inherited dementia FTDP-17. Nature 1998; 393: 702-5.

Iacopino AM, Christakos S. Specific reduction of calcium-binding protein (28-kilodalton calbindin-D) gene expression in aging and neurodegenerative diseases. Proc Natl Acad Sci U S A 1990; 87(11): 4078-82.
Iacopino A, Christakos S, German D, Sonsalla PK, Altar CA. Calbindin-D28K-containing neurons in animal models of neurodegeneration: possible protection from excitotoxicity. Brain Res Mol Brain Res 1992; 13(3): 251-61.
Impey S, Obrietan K, Wong ST, Poser S, Yano S, Wayman G, et al. Cross talk between ERK and PKA is required for Ca2+ stimulation of CREB-dependent transcription and ERK nuclear translocation. Neuron 1998; 21: 869-83.
Inestrosa NC, Alvarez A, Pérez CA, Moreno RD, Vicente M, Linker C, et al. Acetylcholinesterase accelerates assembly of amyloid-beta-peptides into Alzheimer's fibrils: possible role of the peripheral site of the enzyme. Neuron 1996; 16: 881-91.
Ishii M, Kurachi Y. Muscarinic acetylcholine receptors. Curr Pharm Des 2006; 12: 3573-81.
Ito E, Oka K, Etcheberrigaray R, Nelson TJ, McPhie DL, Tofel-Grehl B, et al. Internal Ca2+ mobilization is altered in fibroblasts from patients with Alzheimer disease. Proc Natl Acad Sci USA 1994; 91(2): 534-8.
Iwata N, Tsubuki S, Takaki Y, Watanabe K, Sekiguchi M, Hosoki E, et al. Identification of the major Abeta1-42-degrading catabolic pathway in brain parenchyma: suppression leads to biochemical and pathological deposition. Nat Med 2000; 6: 143-50.
Iwatsubo T, Odaka A, Suzuki N, Mizusawa H, Nukina N, Ihara Y. Visualization of A beta 42(43) and A beta 40 in senile plaques with end-specific A beta monoclonals: evidence that an initially deposited species is A beta 42(43). Neuron 1994; 13: 45-53.
Jarrett JT, Berger EP, Lansbury PT Jr. The carboxy terminus of the beta amyloid protein is critical for the seeding of amyloid formation: implications for the pathogenesis of Alzheimer's disease. Biochemistry 1993; 32: 4693-7.
Jiang D, Sullivan PG, Sensi SL, Steward O, Weiss JH. Zn(2+) induces permeability transition pore opening and release of pro-apoptotic peptides from neuronal mitochondria. J Biol Chem 2001; 276(50): 47524-9.
Jiang Q, Lee CY, Mandrekar S, Wilkinson B, Cramer P, Zelcer N, et al. ApoE promotes the proteolytic degradation of Abeta. Neuron 2008; 58: 681-693.
Jonsson T, Stefansson H, Steinberg S, Jonsdottir I, Jonsson PV, Snaedal J, et al. Variant of TREM2 associated with the risk of Alzheimer's disease. N Engl J Med. 2013; 368(2): 107-16.
Kar S, Slowikowski S, Westaway D, Mount H. Interactions between β-amyloid and central cholinergic neurons: implications for Alzheimer’s disease. J Psychiatry Neurosci 2004; 29 (6): 427-441.
Katayama T, Imaizumi K, Manabe T, Hitomi J, Kudo T, Tohyama M. Induction of neuronal death by ER stress in Alzheimer's disease. J Chem Neuroanat 2004; 28(1-2): 67-78.
Katzman R, Terry R, DeTeresa R, Brown T, Davies P, Fuld P, et al. Clinical, pathological, and neurochemical changes in dementia: a subgroup with preserved mental status and numerous neocortical plaques. Ann Neurol 1988; 23: 138-44.

Kauer JA, Malenka RC, Nicoll RA. NMDA application potentiates synaptic transmission in the hippocampus. Nature 1988; 334: 250-52.
Kaufman RJ. Stress signaling from the lumen of the endoplasmic reticulum: coordination of gene transcriptional and translational controls. Genes Dev 1999; 13(10): 1211-33.
Kelliher M, Fastbom J, Cowburn RF, Bonkale W, Ohm TG, Ravid R, et al. Alterations in the ryanodine receptor calcium release channel correlate with Alzheimer's disease neurofibrillary and beta-amyloid pathologies. Neuroscience 1999; 92(2): 499-513.
Kelly PH, Bondolfi L, Hunziker D, Schlecht HP, Carver K, Maguire E, et al. Progressive age-related impairment of cognitive behavior in APP23 transgenic mice. Neurobiol Aging 2003; 24: 365-78.
Khachaturian ZS. Hypothesis on the regulation of cytosol calcium concentration and the aging brain. Neurobiol Aging 1987; 8: 345-6.
Kinney JW, Starosta G, Crawley JN. Central galanin administration blocks consolidation of spatial learning. Neurobiology of Learning and Memory 2003; 80: 42-54.
Kirichok Y, Krapivinsky G, Clapham DE. The mitochondrial calcium uniporter is a highly selective ion channel. Nature 2004; 427: 360-4.
Klapstein GJ, Vietla S, Lieberman DN, Gray PA, Airaksinen MS, Thoenen H, et al. Calbindin-D28k fails to protect hippocampal neurons against ischemia in spite of its cytoplasmic calcium buffering properties: evidence from calbindin-D28k knockout mice. Neuroscience 1998; 85(2): 361-73.
Kochubey O, Lou X, Schneggenburger R. Regulation of transmitter release by Ca(2+) and synaptotagmin: insights from a large CNS synapse. Trends Neurosci 2011; 34: 237-46.
Köhr G, Mody I. Endogenous intracellular calcium buffering and the activation/inactivation of HVA calcium currents in rat dentate gyrus granule cells. J Gen Physiol 1991; 98(5): 941-67.
Kosik KS, Joachim CL, Selkoe DJ. Microtubule-associated protein tau (tau) is a major antigenic component of paired helical filaments in Alzheimer disease. Proc Natl Acad Sci USA 1986; 83: 4044-48.
Kovacs DM, Fausett HJ, Page KJ, Kim TW, Moir RD, Merriam DE, et al. Alzheimer-associated presenilins 1 and 2: neuronal expression in brain and localization to intracellular membranes in mammalian cells. Nat Med 1996; 2(2): 224-9.
Kraemer BC, Zhang B, Leverenz JB, Thomas JH, Trojanowski JQ, Schellenberg GD. Neurodegeneration and defective neurotransmission in a Caenorhabditis elegans model of tauopathy. Proc Natl Acad Sci USA 2003; 100: 9980-85.
Kurochkin IV, Goto S. Alzheimer's beta-amyloid peptide specifically interacts with and is degraded by insulin degrading enzyme. FEBS Lett 1994; 345: 33-37.
Kurt-Jones EA, Popova L, Kwinn L, Haynes LM, Jones LP, Tripp RA, et al. Pattern recognition receptors TLR4 and CD14 mediate response to respiratory syncytial virus. Nat Immunol 2000; 1(5): 398-401.
Kuznetsov G, Brostrom MA, Brostrom CO. Demonstration of a calcium requirement for secretory protein processing and export. Differential effects of calcium and dithiothreitol. J Biol Chem 1992; 267(6): 3932-9.
LaDu MJ, Falduto MT, Manelli AM, Reardon CA, Getz GS, Frail DE. Isoform-specific binding of apolipoprotein E to beta-amyloid. J Biol Chem 1994; 269: 23403-6.

LaDu MJ, Pederson TM, Frail DE, Reardon CA, Getz GS, Falduto MT. Purification of apolipoprotein E attenuates isoform-specific binding to beta-amyloid. J Biol Chem 1995; 270: 9039-42.
Laemmli UK. Cleavage of structural proteins during the assembly of the head of bacteriophage T4. Nature 1970; 227: 680-5.
LaFerla FM. Calcium dyshomeostasis and intracellular signalling in Alzheimer's disease. Nat Rev Neurosci 2002; 3(11): 862-72.
Landfield PW. 'Increased calcium-current' hypothesis of brain aging. Neurobiol Aging 1987; 8: 346-7.
Landfield PW, Campbell LW, Hao SY, Kerr DS. Aging-related increases in voltage-sensitive, inactivating calcium currents in rat hippocampus. Implications for mechanisms of brain aging and Alzheimer's disease. Ann N Y Acad Sci 1989; 568: 95-105.
Lannfelt L, Basun H, Wahlund LO, Rowe BA, Wagner SL. Decreased alpha-secretase-cleaved amyloid precursor protein as a diagnostic marker for Alzheimer's disease. Nat Med 1995; 1: 829-32.
Lee DC, Rizer J, Selenica ML, Reid P, Kraft C, Johnson A, et al. LPS- induced inflammation exacerbates phospho-tau pathology in rTg4510 mice. J Neuroinflammation 2010; 7: 56.
Leissring MA, Paul BA, Parker I, Cotman CW, LaFerla FM. Alzheimer's presenilin-1 mutation potentiates inositol 1,4,5-trisphosphate-mediated calcium signaling in Xenopus oocytes. J Neurochem 1999; 72: 1061-8.
Leslie SW, Chandler LJ, Barr EM, Farrar RP. Reduced calcium uptake by rat brain mitochondria and synaptosomes in response to aging. Brain Res 1985; 329(1-2): 177-83.
Lesné S, Koh MT, Kotilinek L, Kayed R, Glabe CG, Yang A, et al. A specific amyloid-beta protein assembly in the brain impairs memory. Nature 2006; 440: 352-7.
Lewis J, McGowan E, Rockwood J, Melrose H, Nacharaju P, Van Slegtenhorst M, et al. Neurofibrillary tangles, amyotrophy and progressive motor disturbance in mice expressing mutant (P301L) tau protein. Nat Genet 2000; 25: 402-5.
Lewis J, Dickson DW, Lin WL, Chisholm L, Corral A, Jones G, et al. Enhanced neurofibrillary degeneration in transgenic mice expressing mutant tau and APP. Science 2001; 293(5534): 1487-1491.
Levy-Lahad E, Wasco W, Poorkaj P, Romano DM, Oshima J, Pettingell WH, et al. Candidate gene for the chromosome 1 familial Alzheimer's disease locus. Science 1995; 269: 970-973.
Liu Y, Walter S, Stagi M, Cherny D, Letiembre M, Schulz-Schaeffer W, et al. LPS receptor (CD14): a receptor for phagocytosis of Alzheimer's amyloid peptide. Brain 2005; 128(Pt 8): 1778-89.
Lopez JR, Lyckman A, Oddo S, Laferla FM, Querfurth HW, Shtifman A. Increased intraneuronal resting [Ca2+] in adult Alzheimer's disease mice. J Neurochem 2008; 105: 262-271.
Lovestone S, Hartley CL, Pearce J, Anderton BH. Phosphorylation of tau by glycogen synthase kinase-3 beta in intact mammalian cells: the effects on the organization and stability of microtubules. Neuroscience 1996; 73(4): 1145-57.

Lucas D, Newhouse J. The toxic effects of sodium L-glutamate on the inner layers of the retina. Arch Ophthalmol 1957; 58: 193-201.
Lytton J. Na+/Ca2+ exchangers: three mammalian gene families control Ca2+ transport. Biochem J 2007; 406: 365-82.
Lytton J, Westlin M, Hanley MR. Thapsigargin inhibits the sarcoplasmic or endoplasmic reticulum Ca-ATPase family of calcium pumps. J Biol Chem 1991; 266: 17067-71.
Mancuso M, Coppede F, Migliore L, Siciliano G, Murri L. Mitochondrial dysfunction, oxidative stress and neurodegeneration. J Alzheimers Dis 2006; 10(1): 59-73.
Mao QQ, Zhong XM, Feng CR, Pan AJ, Li ZY, Huang Z. Protective effects of paeoniflorin against glutamate-induced neurotoxicity in PC12 cells via antioxidant mechanisms and Ca(2+) antagonism. Cell Mol Neurobiol 2010; 30(7): 1059-66.
Masters CL, Simms G, Weinman NA, Multhaup G, McDonald BL, Beyreuther K. Amyloid plaque core protein in Alzheimer's disease and Down's syndrome. Proc Natl Acad Sci USA 1985; 82: 4245-49.
Mattson MP, Cheng B, Davis D, Bryant K, Lieberburg I, Rydel RE. beta-Amyloid peptides destabilize calcium homeostasis and render human cortical neurons vulnerable to excitotoxicity. J Neurosci 1992; 12: 376-89.
Mattson MP. Calcium and neuronal injury in Alzheimer's disease. Contributions of beta-amyloid precursor protein mismetabolism, free radicals, and metabolic compromise. Ann NY Acad Sci 1994; 747: 50-76.
Mattson MP, Zhu H, Yu J, Kindy MS. Presenilin-1 mutation increases neuronal vulnerability to focal ischemia in vivo and to hypoxia and glucose deprivation in cell culture: involvement of perturbed calcium homeostasis. J Neurosci 2000; 20: 1358-64.
McGehee DS, Heath MJ, Gelber S, Devay P, Role LW. Nicotine enhancement of fast excitatory synaptic transmission in CNS by presynaptic receptors. Science 1995; 269: 1692-6.
McKee AC, Kosik KS, Kennedy MB, Kowall NW. Hippocampal neurons predisposed to neurofibrillary tangle formation are enriched in type II calcium/calmodulin-dependent protein kinase. J Neuropathol Exp Neurol 1990; 49: 49-63.
McLean CA, Cherny RA, Fraser FW, Fuller SJ, Smith MJ, Beyreuther K, et al. Soluble pool of Abeta amyloid as a determinant of severity of neurodegeneration in Alzheimer's disease. Ann Neurol 1999; 46: 860-6.
McPherson PS, Campbell KP. Characterization of the major brain form of the ryanodine receptor/Ca2+ release channel. J Biol Chem 1993; 268: 19785-90.
Mignery GA, Südhof TC, Takei K, De Camilli P. Putative receptor for inositol 1,4,5-trisphosphate similar to ryanodine receptor. Nature 1989; 342: 192-5.
Miguel-Hidalgo JJ, Alvarez XA, Cacabelos R, Quack G. Neuroprotection by memantine against neurodegeneration induced by beta-amyloid(1-40). Brain Res 2002; 958: 210-21.
Miller KK, Verma A, Snyder SH, Ross CA. Localization of an endoplasmic reticulum calcium ATPase mRNA in rat brain by in situ hybridization. Neuroscience 1991; 43: 1-9.

Minster RL, Demirci FY, DeKosky ST, Kamboh MI. No association between CALHM1 variation and risk of Alzheimer disease. Hum Mutat 2009; 30(4): E566-9.
Morikawa M, Fryer JD, Sullivan PM, Christopher EA, Wahrle SE, DeMattos RB, et al. Production and characterization of astrocyte-derived human apolipoprotein E isoforms from immortalized astrocytes and their interactions with amyloid-beta. Neurobiol Dis 2005; 19: 66-76.
Mullan M, Crawford F, Axelman K, Houlden H, Lilius L, Winblad B, et al. A pathogenic mutation for probable Alzheimer's disease in the APP gene at the N-terminus of beta-amyloid. Nat Genet 1992; 1: 345-7.
Murray CL, Skelly DT, Cunningham C. Exacerbation of CNS inflammation and neurodegeneration by systemic LPS treatment is independent of circulating IL-1β and IL-6. J Neuroinflammation 2011; 8: 50.
Murray FE, Landsberg JP, Williams RJ, Esiri MM, Watt F. Elemental analysis of neurofibrillary tangles in Alzheimer's disease using proton-induced X-ray analysis. Ciba Found Symp 1992; 169: 201-10.
Murrell J, Farlow M, Ghetti B, Benson MD. A mutation in the amyloid precursor protein associated with hereditary Alzheimer's disease. Science 1991; 254: 97-99.
Nadeau S, Rivest S. Regulation of the gene encoding tumor necrosis factor alpha (TNF-alpha) in the rat brain and pituitary in response in different models of systemic immune challenge. J Neuropathol Exp Neurol 1999; 58(1): 61-77.
Nagerl UV, Mody I. Calcium-dependent inactivation of high-threshold calcium currents in human dentate gyrus granule cells. J Physiol 1998; 509 (Pt 1): 39-45.
Nelson O, Tu H, Lei T, Bentahir M, de Strooper B, Bezprozvanny I. Familial Alzheimer disease-linked mutations specifically disrupt Ca2+ leak function of presenilin 1. J Clin Invest 2007; 117(5): 1230-9.
Nicholls DG. Mitochondria and calcium signaling. Cell Calcium 2005; 38(3-4): 311-7.
Nitsch RM, Slack BE, Wurtman RJ, Growdon JH. Release of Alzheimer amyloid precursor derivatives stimulated by activation of muscarinic acetylcholine receptors. Science 1992; 258: 304-07.
Nordberg A, Hellström-Lindahl E, Lee M, Johnson M, Mousavi M, Hall R, et al. Chronic nicotine treatment reduces beta-amyloidosis in the brain of a mouse model of Alzheimer's disease (APPsw). J Neurochem 2002; 81: 655-8.
Oddo S, Caccamo A, Shepherd JD, Murphy MP, Golde TE, Kayed R, et al. Triple-transgenic model of Alzheimer's disease with plaques and tangles: intracellular Abeta and synaptic dysfunction. Neuron 2003a; 39(3): 409-21.
Oddo S, Caccamo A, Kitazawa M, Tseng BP, LaFerla FM. Amyloid deposition precedes tangle formation in a triple transgenic model of Alzheimer's disease. Neurobiol Aging 2003b; 24(8): 1063-70.
Oddo S, Caccamo A, Green KN, Liang K, Tran L, Chen Y,et al. Chronic nicotine administration exacerbates tau pathology in a transgenic model of Alzheimer's disease. Proc Natl Acad Sci USA 2005; 102: 3046-51.
Ono K, Hasegawa K, Yamada M, Naiki H. Nicotine breaks down preformed Alzheimer's beta-amyloid fibrils in vitro. Biol Psychiatry 2002; 52: 880-6.
Otvos L Jr, Szendrei GI, Lee VM, Mantsch HH. Human and rodent Alzheimer beta-amyloid peptides acquire distinct conformations in membrane-mimicking solvents. Eur J Biochem 1993; 211: 249-57.

Padua RA, Nagy JI, Geiger JD. Subcellular localization of ryanodine receptors in rat brain. Eur J Pharmacol 1996; 298: 185-9.
Palop JJ, Jones B, Kekonius L, Chin J, Yu GQ, Raber J, et al. Neuronal depletion of calcium-dependent proteins in the dentate gyrus is tightly linked to Alzheimer's disease-related cognitive deficits. Proc Natl Acad Sci U S A 2003; 100(16): 9572-7.
Parkash J, Chaudhry MA, Rhoten WB. Tumor necrosis factor-alpha-induced changes in insulin-producing beta-cells. Anat Rec A Discov Mol Cell Evol Biol 2005; 286(2): 982-93.
Paschen W, Mengesdorf T. Endoplasmic reticulum stress response and neurodegeneration. Cell Calcium 2005; 38(3-4): 409-15.
Paulson JC, McClure WO. Microtubules and axoplasmic transport. Brain Res 1974; 73: 333-37.
Paxinos G, Watson C. The Rat Brain in Stereotaxic Coordinates (2nd ed.). 1986; Orlando, FL: Academic Press.
Perry EK, Perry RH, Gibson PH, Blessed G, Tomlinson BE. A cholinergic connection between normal aging and senile dementia in the human hippocampus. Neurosci Lett 1977; 6: 85-89.
Perry EK, Blessed G, Tomlinson BE, Perry RH, Crow TJ, Cross AJ, et al. Neurochemical activities in human temporal lobe related to aging and Alzheimer-type changes. Neurobiol Aging 1981; 2(4): 251-6.
Perry EK, Morris CM, Court JA, Cheng A, Fairbairn AF, McKeith IG, et al. Alteration in nicotine binding sites in Parkinson's disease, Lewy body dementia and Alzheimer's disease: possible index of early neuropathology. Neuroscience 1995; 64: 385-95.
Peterson C, Gibson GE, Blass JP. Altered calcium uptake in cultured skin fibroblasts from patients with Alzheimer's disease. N Engl J Med 1985; 312: 1063-5.
Peterson C, Goldman JE. Alterations in calcium content and biochemical processes in cultured skin fibroblasts from aged and Alzheimer donors. Proc Natl Acad Sci USA 1986; 83: 2758-62.
Pierrot N, Ghisdal P, Caumont AS, Octave JN. Intraneuronal amyloid-beta1-42 production triggered by sustained increase of cytosolic calcium concentration induces neuronal death. J Neurochem 2004; 88: 1140-50.
Poorkaj P, Bird TD, Wijsman E, Nemens E, Garruto RM, Anderson L, et al. Tau is a candidate gene for chromosome 17 frontotemporal dementia. Ann Neurol 1998; 43: 815-25.
Pozzo-Miller LD, Pivovarova NB, Leapman RD, Buchanan RA, Reese TS, Andrews SB. Activity-dependent calcium sequestration in dendrites of hippocampal neurons in brain slices. J Neurosci 1997; 17(22): 8729-38.
Price JL, Davis PB, Morris JC, White DL. The distribution of tangles, plaques and related immunohistochemical markers in healthy aging and Alzheimer's disease. Neurobiol Aging 1991; 12: 295-312.
Qin L, Wu X, Block ML, Liu Y, Breese GR, Hong JS, et al. Systemic LPS causes chronic neuroinflammation and progressive neurodegeneration. Glia 2007; 55(5): 453-62.
Querfurth HW, Selkoe DJ. Calcium ionophore increases amyloid beta peptide production by cultured cells. Biochemistry 1994; 33: 4550-61.

Querfurth HW, Jiang J, Geiger JD, Selkoe DJ. Caffeine stimulates amyloid beta-peptide release from beta-amyloid precursor protein-transfected HEK293 cells. J Neurochem 1997; 69(4): 1580-91.
Quintanilla RA, Orellana DI, González-Billault C, Maccioni RB. Interleukin-6 induces Alzheimer-type phosphorylation of tau protein by deregulating the cdk5/p35 pathway. Exp Cell Res 2004; 295: 245-57.
Ramsden M, Kotilinek L, Forster C, Paulson J, McGowan E, SantaCruz K, et al. Age-dependent neurofibrillary tangle formation, neuron loss, and memory impairment in a mouse model of human tauopathy (P301L). J Neurosci 2005; 25(46): 10637-10647.
Raza M, Deshpande LS, Blair RE, Carter DS, Sombati S, DeLorenzo RJ. Aging is associated with elevated intracellular calcium levels and altered calcium homeostatic mechanisms in hippocampal neurons. Neurosci Lett 2007; 418: 77-81.
Riascos D, de Leon D, Baker-Nigh A, Nicholas A, Yukhananov R, Bu J, et al. Age-related loss of calcium buffering and selective neuronal vulnerability in Alzheimer's disease. Acta Neuropathol 2011; 122(5): 565-76.
Rintoul GL, Raymond LA, Baimbridge KG. Calcium buffering and protection from excitotoxic cell death by exogenous calbindin-D28k in HEK 293 cells. Cell Calcium 2001; 29: 277-87.
Rogers SL, Farlow MR, Doody RS, Mohs R, Friedhoff LT. A 24-week, double-blind, placebo-controlled trial of donepezil in patients with Alzheimer's disease. Donepezil Study Group. Neurology 1998; 50: 136-45.
Roher AE, Chaney MO, Kuo YM, Webster SD, Stine WB, Haverkamp LJ, et al. Morphology and toxicity of Abeta-(1-42) dimer derived from neuritic and vascular amyloid deposits of Alzheimer's disease. J Biol Chem 1996; 271: 20631-5.
Role LW, Berg DK. Nicotinic receptors in the development and modulation of CNS synapses. Neuron 1996; 16:1077–85.
Rosler M, Anand R, Cicin-Sain A, Gauthier S, Agid Y, Dal-Bianco P, et al. Efficacy and safety of rivastigmine in patients with Alzheimer's disease: international randomised controlled trial. BMJ 1999; 318: 633-8.
Sabbagh JJ, Heaney CF, Bolton MM, Murtishaw AS, Ure JA, Kinney JW. Administration of donepezil does not rescue galanin-induced spatial learning deficits. Int J Neurosci 2012; 122(12): 742-7.
Sadot E, Gurwitz D, Barg J, Behar L, Ginzburg I, Fisher A. Activation of m1 muscarinic acetylcholine receptor regulates tau phosphorylation in transfected PC12 cells. J Neurochem 1996; 66: 877-80.
Salomon AR, Marcinowski KJ, Friedland RP, Zagorski MG. Nicotine inhibits amyloid formation by the beta-peptide. Biochemistry 1996; 35: 13568-78.
Santacruz K, Lewis J, Spires T, Paulson J, Kotilinek L, Ingelsson M, et al. Tau suppression in a neurodegenerative mouse model improves memory function. Science 2005; 309: 476-81.
Santos AN, Ewers M, Minthon L, Simm A, Silber RE, Blennow K, et al. Amyloid-β oligomers in cerebrospinal fluid are associated with cognitive decline in patients with Alzheimer's disease. J Alzheimers Dis 2012; 29(1): 171-6.

Saunders AM, Strittmatter WJ, Schmechel D, George-Hyslop PH, Pericak-Vance MA, Joo SH, et al. Association of apolipoprotein E allele epsilon 4 with late-onset familial and sporadic Alzheimer's disease. Neurology 1993; 43: 1467-1472.
Schellenberg GD. Genetic dissection of Alzheimer disease, a heterogeneous disorder. Proc Natl Acad Sci USA 1995; 92: 8552-59.
Schwaller B. Cytosolic Ca2+ buffers. Cold Spring Harb Perspect Biol 2010; 2(11): a004051.
Seabrook GR, Smith DW, Bowery BJ, Easter A, Reynolds T, Fitzjohn SM, et al. Mechanisms contributing to the deficits in hippocampal synaptic plasticity in mice lacking amyloid precursor protein. Neuropharmacology 1999; 38(3): 349-359.
Selkoe DJ. Normal and abnormal biology of the beta-amyloid precursor protein. Annu Rev Neurosci 1994; 17: 489-517.
Selkoe DJ. Alzheimer's Disease: genes, proteins, and therapy. Physiol Rev 2001; 81(2): 741-766.
Senechal Y, Kelly PH, Dev KK. Amyloid precursor protein knockout mice show age-dependent deficits in passive avoidance learning. Behav Brain Res 2008; 186(1): 126-132.
Shankar GM, Bloodgood BL, Townsend M, Walsh DM, Selkoe DJ, Sabatini BL. Natural oligomers of the Alzheimer amyloid-beta protein induce reversible synapse loss by modulating an NMDA-type glutamate receptor-dependent signaling pathway. J Neurosci 2007; 27: 2866-75.
Sheehan JP, Swerdlow RH, Miller SW, Davis RE, Parks JK, Parker WD, et al. Calcium homeostasis and reactive oxygen species production in cells transformed by mitochondria from individuals with sporadic Alzheimer's disease. J Neurosci 1997; 17(12): 4612-22.
Sheng JG, Zhu SG, Jones RA, Griffin WS, Mrak RE. Interleukin-1 promotes expression and phosphorylation of neurofilament and tau proteins in vivo. Exp Neurol 2000; 163: 388-91.
Sherrington R, Rogaev EI, Liang Y, Rogaeva EA, Levesque G, Ikeda M, et al. Cloning of a gene bearing missense mutations in early-onset familial Alzheimer's disease. Nature 1995; 375: 754-760.
Shmigol A, Verkhratsky A, Isenberg G. Calcium-induced calcium release in rat sensory neurons. J Physiol 1995;489 (Pt 3):627-36.
Shoji M, Golde TE, Ghiso J, Cheung TT, Estus S, Shaffer LM, et al. Production of the Alzheimer amyloid beta protein by normal proteolytic processing. Science 1992; 258: 126-9.
Singaraja RR. TREM2 : A new risk factor for Alzheimer's Disease. Clin Genet 2013 Jan 25. doi: 10.1111/cge.12108. [Epub ahead of print]
Sisodia SS, Price DL. Role of the beta-amyloid protein in Alzheimer's disease. FASEB J 1995; 9: 366-70.
Skaper SD. The brain as a target for inflammatory processes and neuroprotective strategies. Ann N Y Acad Sci 2007; 1122: 23-34.
Sleegers K, Brouwers N, Bettens K, Engelborghs S, van Miegroet H, De Deyn PP, et al. No association between CALHM1 and risk for Alzheimer dementia in a Belgian population. Hum Mutat 2009; 30(4): E570-4.

Souren LE, Franssen EH, Reisberg B. Contractures and loss of function in patients with Alzheimer's disease. Journal of the American Geriatric Society 1995; 43(6): 650–655.
Smith IF, Hitt B, Green KN, Oddo S, LaFerla FM. Enhanced caffeine-induced Ca2+ release in the 3xTg-AD mouse model of Alzheimer's disease. J Neurochem 2005; 94(6): 1711-8.
Snowdon DA, Greiner LH, Mortimer JA, Riley KP, Greiner PA, Markesbery WR. Brain infarction and the clinical expression of Alzheimer disease. The Nun Study. JAMA 1997; 12: 813-7.
Sparagna GC, Gunter KK, Sheu SS, Gunter TE. Mitochondrial calcium uptake from physiological-type pulses of calcium. A description of the rapid uptake mode. J Biol Chem 1995; 270(46): 27510-5.
Spencer DG Jr, Lal H. Effects of anticholinergic drugs on learning and memory. Drug Dev Res 1983; 3: 489-502.
Spencer DG Jr, Pontecorvo MJ, Heise GA. Central cholinergic involvement in working memory: effects of scopolamine on continuous nonmatching and discrimination performance in the rat. Behav Neurosci 1985; 99: 1049-65.
Spillantini MG, Murrell JR, Goedert M, Farlow MR, Klug A, Ghetti B. Mutation in the tau gene in familial multiple system tauopathy with presenile dementia. Proc Natl Acad Sci USA 1998; 95: 7737-41.
Steiner H, Duff K, Capell A, Romig H, Grim MG, Lincoln S, et al. A loss of function mutation of presenilin-2 interferes with amyloid beta-peptide production and notch signaling. J Biol Chem 1999; 274: 28669-73.
Strehler EE, Filoteo AG, Penniston JT, Caride AJ. Plasma-membrane Ca(2+) pumps: structural diversity as the basis for functional versatility. Biochem Soc Trans 2007; 35: 919-22.
Sturchler-Pierrat C, Abramowski D, Duke M, Wiederhold KH, Mistl C, Rothacher S, et al. Two amyloid precursor protein transgenic mouse models with Alzheimer disease-like pathology. Proc Natl Acad Sci USA 1997; 94: 13287-92.
Stutzmann GE, Caccamo A, LaFerla FM, Parker I. Dysregulated IP3 signaling in cortical neurons of knock-in mice expressing an Alzheimer's-linked mutation in presenilin1 results in exaggerated Ca2+ signals and altered membrane excitability. J Neurosci 2004; 24(2): 508-13.
Stutzmann GE, Smith I, Caccamo A, Oddo S, Laferla FM, Parker I. Enhanced ryanodine receptor recruitment contributes to Ca2+ disruptions in young, adult, and aged Alzheimer's disease mice. J Neurosci 2006; 26(19): 5180-9.
Suzuki N, Cheung TT, Cai XD, Odaka A, Otvos L Jr, Eckman C, et al. An increased percentage of long amyloid beta protein secreted by familial amyloid beta protein precursor (beta APP717) mutants. Science 1994; 264: 1336-40.
Tahara K, Kim HD, Jin JJ, Maxwell JA, Li L, Fukuchi K. Role of toll-like receptor signalling in Abeta uptake and clearance. Brain 2006; 129(Pt 11): 3006-19.
Takasugi N, Tomita T, Hayashi I, Tsuruoka M, Niimura M, Takahashi Y, et al. The role of presenilin cofactors in the gamma-secretase complex. Nature 2003; 422: 438-441.
Takeuchi A, Irizarry MC, Duff K, Saido TC, Hsiao Ashe K, Hasegawa M, et al. Age-related amyloid beta deposition in transgenic mice overexpressing both Alzheimer

mutant presenilin 1 and amyloid beta precursor protein Swedish mutant is not associated with global neuronal loss. Am J Pathol 2000; 157: 331-9.
Tan EK, Ho P, Cheng SY, Yih Y, Li HH, Fook-Chong S, et al. CALHM1 variant is not associated with Alzheimer's disease among Asians. Neurobiol Aging 2011; 32: 546.e11-2.
Tan J, Town T, Paris D, Mori T, Suo Z, Crawford F, et al. Microglial activation resulting from CD40-CD40L interaction after beta-amyloid stimulation. Science 1999; 286: 2352-5.
Tariot PN, Solomon PR, Morris JC, Kershaw P, Lilienfeld S, Ding C. A 5-month, randomized, placebo-controlled trial of galantamine in AD. The Galantamine USA-10 Study Group. Neurology 2000; 54: 2269-76.
Taylor-Robinson SD, Weeks RA, Sargentoni J, Marcus CD, Bryant DJ, Harding AE, et al. Evidence for glutamate excitotoxicity in Huntington's disease with proton magnetic resonance spectroscopy. Lancet 1994; 343: 1170.
Terry RD, Katzman R. Senile dementia of the Alzheimer type. Ann Neurol 1983; 14: 497-506.
Terry RD, Masliah E, Salmon DP, Butters N, DeTeresa R, Hill R, et al. Physical basis of cognitive alterations in Alzheimer's disease: synapse loss is the major correlate of cognitive impairment. Ann Neurol 1991; 30: 572-580.
Thibault O, Landfield PW. Increase in single L-type calcium channels in hippocampal neurons during aging. Science 1996; 272: 1017-1020.
Thibault O, Gant JC, Landfield PW. Expansion of the calcium hypothesis of brain aging and Alzheimer's disease: minding the store. Aging Cell 2007; 6: 307-317.
Tokuda T, Calero M, Matsubara E, Vidal R, Kumar A, Permanne B, et al. Lipidation of apolipoprotein E influences its isoform-specific interaction with Alzheimer's amyloid beta peptides. Biochem J 2000; 348 Pt 2: 359-65.
Townsend M, Cleary JP, Mehta T, Hofmeister J, Lesne S, O'Hare E, et al. Orally available compound prevents deficits in memory caused by the Alzheimer amyloid-beta oligomers. Ann Neurol 2006; 60: 668-76.
Tu H, Nelson O, Bezprozvanny A, Wang Z, Lee SF, Hao YH, et al. Presenilins form ER Ca2+ leak channels, a function disrupted by familial Alzheimer's disease-linked mutations. Cell 2006; 126(5): 981-93.
Unterberger U, Höftberger R, Gelpi E, Flicker H, Budka H, Voigtländer T. Endoplasmic reticulum stress features are prominent in Alzheimer disease but not in prion diseases in vivo. J Neuropathol Exp Neurol 2006; 65(4): 348-57.
Vale C, Alonso E, Rubiolo JA, Vieytes MR, LaFerla FM, Gimenez-Llort L, et al. Profile for amyloid-beta and tau expression in primary cortical cultures from 3xTg-AD mice. Cell Mol Neurobiol 2010; 30: 577-590.
Valentino RJ, Dingledine R. Presynaptic inhibitory effect of acetylcholine in the hippocampus. J Neurosci 1981; 1: 784-92.
Vassar R, Bennett BD, Babu-Khan S, Kahn S, Mendiaz EA, Denis P, et al. Beta-secretase cleavage of Alzheimer's amyloid precursor protein by the transmembrane aspartic protease BACE. Science 1999; 286: 735-41.
Verkhratsky A. Physiology and pathophysiology of the calcium store in the endoplasmic reticulum of neurons. Physiol Rev 2005; 85(1): 201-79.

Waldemar G, Dubois B, Emre M, Georges J, McKeith IG, Rossor M, et al. Recommendations for the diagnosis and management of Alzheimer's disease and other disorders associated with dementia: EFNS guideline. European Journal of Neurology 2007; 14 (1): E1–26.

Walsh DM, Klyubin I, Fadeeva JV, Cullen WK, Anwyl R, Wolfe MS, et al. Naturally secreted oligomers of amyloid beta protein potently inhibit hippocampal long-term potentiation in vivo. Nature 2002; 416: 535-9.

Weingarten MD, Lockwood AH, Hwo SY, Kirschner MW. A protein factor essential for microtubule assembly. Proc Natl Acad Sci USA 1975; 72: 1858-62.

Wernyj RP, Mattson MP, Christakos S. Expression of calbindin-D28k in C6 glial cells stabilizes intracellular calcium levels and protects against apoptosis induced by calcium ionophore and amyloid beta-peptide. Brain Res Mol Brain Res 1999; 64(1): 69-79.

Wevers A, Schroder H. Nicotinic acetylcholine receptors in Alzheimer's disease. J Alzheimers Dis 1999; 1: 207-19.

Wevers A, Burghaus L, Moser N, Witter B, Steinlein OK, Schütz U, et al. Expression of nicotinic acetylcholine receptors in Alzheimer's disease: postmortem investigations and experimental approaches. Behav Brain Res 2000; 113: 207-15.

Whitehouse JM. Cholinergic mechanisms in discrimination learning as a function of stimuli. J Comp Physiol Psychol 1967; 63: 448-51.

Whitehouse PJ, Price DL, Struble RG, Clark AW, Coyle JT, Delon MR. Alzheimer's disease and senile dementia: loss of neurons in the basal forebrain. Science 1982; 215: 1237-9.

Wilson CA, Doms RW, Zheng H, Lee VM. Presenilins are not required for A beta 42 production in the early secretory pathway. Nat Neurosci 2002; 5(9): 849-55.

Wisniewski KE, Wisniewski HM, Wen GY. Occurrence of neuropathological changes and dementia of Alzheimer's disease in Down's syndrome. Ann Neurol 1985; 17: 278-82.

Wolfe MS, Xia W, Ostaszewski BL, Diehl TS, Kimberly WT, Selkoe DJ. Two transmembrane aspartates in presenilin-1 required for presenilin endoproteolysis and γ-secretase activity. Nature 1999; 398: 513-517.

Woolf NJ. The critical role of cholinergic basal forebrain neurons in morphological change and memory encoding: a hypothesis. Neurobiol Learn Mem 1996; 66: 258-66.

Wyss-Coray T, Mucke L. Inflammation in neurodegenerative disease--a double-edged sword. Neuron 2002; 35(3): 419-32.

Xia Y, Yamagata K, Krukoff TL. Differential expression of the CD14/TLR4 complex and inflammatory signaling molecules following i.c.v. administration of LPS. Brain Res 2006; 1095(1): 85-95.

Yoshida H, Ihara Y. Tau in paired helical filaments is functionally distinct from fetal tau: assembly incompetence of paired helical filament-tau. J Neurochem 1993; 61: 1183-6.

Yu H, Saura CA, Choi SY, Sun LD, Yang X, Handler M, et al. APP processing and synaptic plasticity in presenilin-1 conditional knockout mice. Neuron 2001; 31: 713-26.

Zeng H, Zhang Y, Peng L, Shao H, Menon NK, Yang J, et al. Nicotine and amyloid formation. Biol Psychiatry 2001; 49: 248-57.
Zheng WH, Bastianetto S, Mennicken F, Ma W, Kar S. Amyloid beta peptide induces tau phosphorylation and loss of cholinergic neurons in rat primary septal cultures. Neuroscience 2002; 115(1): 201-11.

Curriculum Vitae

Jonathan J. Sabbagh

(857) 636-9206
Email: sabbaghj@unlv.nevada.edu

Professional Information:

Work Address: University of Nevada, Las Vegas
4505 S Maryland Pkwy Box 455030
Las Vegas, NV 89154-5030
Phone (702) 895-5523

Education:

Ph.D. Candidate in Experimental Psychology with an emphasis in Neuroscience 2007 – present (expected date of graduation: May 2013). University of Nevada, Las Vegas, Las Vegas, NV 89154

M.A. Experimental Psychology – Emphasis in Behavioral Neuroscience (December 2010) University of Nevada, Las Vegas, Las Vegas, NV 89154
Thesis Title: "Donepezil and Galanin Interactions in an Animal Model of Alzheimer's Disease" Advisor: Dr. Jefferson W. Kinney

B.S. Neuroscience (May 2004)
Tulane University, New Orleans, LA 70118

Teaching Experience:

Undergraduate:
- Introductory Psychology (Fall 2009 – Spring 2012)
- Physiological Psychology (Fall 2011 – Spring 2012)

Research Skills/Techniques:

- Participated in the initial development and construction of the behavioral neuroscience lab at UNLV;
- Extensive experience with the appropriate care and use of animal subjects, including rats, mice, and ground squirrels;
- Skilled in research design, implementation, and data analysis in animal learning;
- Expertise in several behavioral tasks with rodents including the Morris water maze, Barnes maze, radial arm maze, cued and contextual fear conditioning, acoustic startle, pre-pulse inhibition, open field, novel object recognition, tail flick nociception task, and a general screen to examine basic sensory function and reflexes;
- Experienced in aseptic surgical techniques;

- Proficient in stereotaxic surgical procedures, including chronic cannula placement and osmotic mini-pump implantation in rats;
- Experienced in multiple wound closure techniques associated with stereotaxic surgery, including suture closure and dental acrylic application;
- Considerable expertise in neural tissue collection, including transcardiac perfusion and dissection of specific neural structures;
- Experienced in the frozen sectioning of neural tissue for histological analyses;
- Extensive experience utilizing immunohistochemistry techniques, including the use of DAB and immunofluorescence;
- Proficient in light and fluorescent microscopy;
- Expertise in tissue homogenization and protein concentration assays;
- Skilled in western blotting and gel electrophoresis techniques;
- Trained on multiple western blot imaging techniques, including the Typhoon variable mode imaging system, the Odyssey IR Imaging system, and the UVP imaging system;
- Experienced in programming of software for behavioral testing;
- Proficient with ELISA technique and interpretation;
- Expertise in annotative work, including detailed annotation of the central nervous system.

Research:

Grants Contributed to:

Years inclusive 3/2013 – 3/2015. "Chronic dysregulation of intracellular calcium as a novel model of Alzheimer's disease" submitted 7/2012 to the National Institute of Mental Health (NIMH), Chronic Dysfunction and Integrative Neurodegeneration Study Section (CDIN). PI – Jefferson Kinney.

Publications:

Monica M. Bolton, Chelcie F. Heaney, Jonathan J. Sabbagh, Andrew S. Murtishaw and Jefferson W. Kinney. Deficits in emotional learning and memory in an animal model of schizophrenia. Behavioral Brain Research 2012; 233(1):35-44.

Jonathan J. Sabbagh, Chelcie F. Heaney, Monica M. Bolton, Andrew S. Murtishaw, Jennifer A. Ure and Jefferson W. Kinney. Administration of donepezil does not rescue galanin-induced spatial learning deficits International Journal of Neuroscience 2012; 122(12):742-7.

Jonathan J. Sabbagh, Chelcie F. Heaney, Monica M. Bolton, Andrew S. Murtishaw and Jefferson W. Kinney. Examination of spatial learning deficits in an animal model of schizophrenia. Physiology and Behavior 2012; 107(3):355-63.

Chelcie F. Heaney, Monica M. Bolton, Andrew S. Murtishaw, Jonathan J. Sabbagh, Christy M. Magcalas, and Jefferson W. Kinney. Baclofen administration alters fear

extinction and GABAergic protein levels. Neurobiology of Learning and Memory 2012; 98(3):261-71.

Jonathan J. Sabbagh, Jefferson W. Kinney, and Jeffrey L. Cummings. Animal systems in the development of treatments for Alzheimer's disease: challenges, methods, and implications. Neurobiology of Aging 2013; 34(1):169-83.

Manuscripts in Preparation:

Jonathan J. Sabbagh, Andrew S. Murtishaw, Monica M. Bolton, Chelcie F. Heaney, and Jefferson W. Kinney. Chronic ketamine produces altered distribution of parvalbumin-positive cells in the hippocampus of adult rats. Submitted to Neuroscience Letters.

Jonathan J. Sabbagh, Jefferson W. Kinney, and Jeffrey L. Cummings. Alzheimer's disease biomarkers: correspondence between animal models and human studies. Re-Submitted to Neurobiology of Disease.

Monica M. Bolton, Chelcie F. Heaney, Andrew S. Murtishaw, Jonathan J. Sabbagh, Christy M. Magcalas, and Jefferson W. Kinney. Developmental alterations in GABAB perturb behavior and GABAergic protein levels.

Jonathan J. Sabbagh, Andrew S. Murtishaw, Monica M. Bolton, Chelcie F. Heaney, Michael A. Langhardt, and Jefferson W. Kinney. Chronic calcium dysregulation produces cognitive deficits and increased oligomeric Aβ levels.

Presentations:

Sabbagh, J.J., Heaney, C.F., Bolton, M.M., Kinney, J.W. Efficacy of acute versus chronic administration of an NMDA receptor antagonist to induce an animal model of schizophrenia. Poster presented at Society for Neuroscience annual meeting, Chicago, IL 2009.

Sabbagh, J.J. Donepezil and galanin interactions in an animal model of Alzheimer's disease. Experimental Psychology Professional Seminar, University of Nevada, Las Vegas 2009.

Sabbagh, J.J. Donepezil and galanin interactions in an animal model of Alzheimer's disease. Invited speaker to BIOS symposium for School of Life Sciences at University of Nevada, Las Vegas, 2010.

Sabbagh, J.J., Heaney, C.F., Bolton, M.M., Ure, J.A., Kinney, J.W. Donepezil and galanin interactions in learning and memory and a model of cholinergic loss. Poster presented at Society for Neuroscience annual meeting, San Diego, CA 2010.

Heaney, C.F., Sabbagh, J.J., Bolton, M.M., Murtishaw, A.S., Santa-Ana, I., Kinney, J.W. An investigation of alterations in GABAergic tone in an animal model of schizophrenia. Poster presented at Society for Neuroscience annual meeting San Diego, CA 2010.

Sabbagh, J.J., Bolton, M.M., Heaney, C.F., Murtishaw, A.S., Kinney, J.W. Deficits in emotional learning and memory in an animal model of schizophrenia. Poster presented at Society for Neuroscience annual meeting Washington, D.C. 2011.

Heaney, C.F., Bolton, M.M., Murtishaw, A.S., Sabbagh, J.J, Kinney, J.W. An investigation of the effects of alterations in GABAB receptor function on learning and memory. Poster presented at Society for Neuroscience annual meeting Washington, D.C. 2011.

Bolton, M.M., Heaney, C.F., Sabbagh, J.J., Murtishaw, A.S., Kinney, J.W. Comparison of an adult and developmental animal model of schizophrenia. Poster presented at Society for Neuroscience annual meeting Washington, D.C. 2011.

Magcalas, C.M., Heaney, C.F., Bolton, M.M., Murtishaw, A.S., Sabbagh, J.J., and Kinney, J.W. Alterations in GABAb in development produce behavioral and protein changes in adulthood. Poster presented at the Undergraduate Research Opportunity Program session, (Nevada InBRE), UNLV August 2012.

Sabbagh, J.J., Murtishaw, A.S., Heaney, C.F., Bolton, M.M., Magcalas, C.M., Kinney, J.W. Chronic calcium dysregulation produces cognitive deficits and biochemical changes relevant to Alzheimer's disease. Poster presented at Society for Neuroscience annual meeting New Orleans, LA 2012.

Heaney, C.F., Bolton, M.M., Murtishaw, A.S., Sabbagh, J.J, Magcalas, C.M., Kinney, J.W. Changes in GABAB receptor tone in development produce behavioral deficits in adulthood. Poster presented at Society for Neuroscience annual meeting New Orleans, LA 2012.

Bolton, M.M., Heaney, C.F., Sabbagh, J.J., Murtishaw, A.S., Magcalas, C.M., Kinney, J.W. Comparison of postnatal ketamine dosage on behavioral deficits in adulthood. Poster presented at Society for Neuroscience annual meeting New Orleans, LA 2012.

Murtishaw, A.S., Sabbagh, J.J., Heaney, C.F., Bolton, M.M., Magcalas, C.M., Langhardt, M.A., Kinney, J.W. Ketamine-induced behavioral impairments and alterations in hippocampal gabaergic neuron distribution. Poster presented at Society for Neuroscience annual meeting New Orleans, LA 2012.

Service:

- Ad-hoc reviewer – Hippocampus.

- Student representative of the Neuroscience emphasis committee for the experimental psychology program in the Department of Psychology at the University of Nevada, Las Vegas (2008 – 2011).
- Cohort representative to the Experimental Student Committee for the experimental psychology program in the Department of Psychology at the University of Nevada, Las Vegas (2008-09 and 2011-2012).
- Teaching and guidance of undergraduate students as a graduate student member of the University of Nevada, Las Vegas Neuroscience Journal Club (2009-2011).
- Founding member of the University of Nevada, Las Vegas Graduate Neuroscience Association (2011 – present).
- Supervision and training of undergraduate research assistants on several techniques, including the Morris water maze, cued and contextual fear conditioning, acoustic startle, neural tissue collection, cryostat sectioning, western blotting, and immunohistochemistry (2008-2013).
- Coordination and implementation of a Brain Awareness Week presentation to multiple classes of 4th grade students at Wallin Elementary School, Henderson, NV (2012).

Awards:

- Awarded the University of Nevada, Las Vegas College of Liberal Arts Dean's Graduate Student Stipend Award to conduct research for summer 2012.
- Awarded a travel grant from the University of Las, Vegas Graduate and Professional Student Association to attend the 2012 Society for Neuroscience conference in New Orleans, LA.

Memberships in Professional and Scientific Societies:

- Student member of the Society for Neuroscience (2008 – Current);
- Member of the Sierra Nevada chapter of the Society for Neuroscience (2009 – Current).